Histone acetylation and expression of corresponding histone acetyltransferases in human abdominal aortic aneurysm

Klinik und Poliklinik für Vaskuläre und Endovaskuläre Chirurgie
(Direktor: Univ.-Prof. Dr. H.-H. G. U. Eckstein)
Klinikum rechts der Isar

Yanshuo Han

Vollständiger Abdruck der von der Fakultät für Medizin der Technischen Universität München zur Erlangung des akademischen Grades eines
Doktors der Medizin
genehmigten Dissertation.

Vorsitzender: Univ.-Prof. Dr. E. J. Rummeny

Prüfer der Dissertation:

1. Univ.-Prof. Dr. H.-H. G. U. Eckstein
2. Priv.-Doz. Dr. M. G. F. Wildgruber

Die Dissertation wurde am 30.10.2014 bei der Technischen Universität München eingereicht und durch die Fakultät für Medizin am 14.10.2015 angenommen.

Histone acetylation and expression of corresponding histone acetyltransferases in human abdominal aortic aneurysm

A dissertation submitted in partial fulfillment of the
requirements for the degree of Medical Doctor (M.D.) in the
Klinikum Rechts der Isar
at the Technischen Universität München

By
Yanshuo Han

Munich, Germany

Department of Vascular and Endovascular Surgery
Supervisor: Univ.-Prof. Dr. H.-H. G. U. Eckstein

2015

TABLE OF CONTENTS

1. INTRODUCTION

1.1 Epidemiology

1.1.1 Definition of abdominal aortic aneurysms

The abdominal aortic aneurysm (AAA) is the most common aneurysm disease of the vascular surgery field. Abdominal aortic aneurysm is defined as the expansion or dilatation of the abdominal aorta. The most widely accepted definition is based on the abdominal aorta diameter, exceeding the normal diameter by more than 50% corresponding to more than 3.0 cm in either anterior-posterior or transverse planes, and is more than two standard deviations above the mean aortic diameter independent of the gender [1].

1.1.2 Prevalence

Through various factors such as age, geographical location and gender, prevalence rates demonstrated broad diversity. Base on UK population, a randomized study (between 65 to 80 years old, n=15,775) reported that the general prevalence rate is 4.0% and 7.6% in men and 1.3% in women, respectively [2]. Base on US veterans population, a cross-sectional screening study (between 50 and 79 years old, n=73,451) demonstrated that the prevalence of AAA (diameter > 3.0 cm) is 5.9% [3]. In addition, this study concluded that the highest prevalence were white male smokers by ethnic and environmental risk factors. There is little evidence of AAA prevalence for twenty-one century; however, a study reported that repair rate for AAA decreased from 2001 to 2006 within US population [4].

1.1.3 Positive risk factors

Male gender, advanced age and smoking were considered to be the most important risk factors [5,6,7,8]. Men are six times more frequently suffering from AAA than women [5,8]. Smoking is an independent risk factor for AAA with an odd radio of more than 3.0 in all studies. Furthermore, the increase in size of AAA is accelerated in smokers.

In addition, family history is another important positive risk factor for AAA. Precisely, it is vertically interconnected with the development of AAA between first-degree relatives and persons suffered from AAA was two times higher compared to persons with no family history [9]. Furthermore, it is also lateral interconnected with the fact that brothers of AAA patients are at higher risk to develop AAA. Nevertheless, genetic basis was found so far only in a few family-type AAAs [10].

Moreover, obesity, hypertension, hypercholesterolemia, atherosclerotic vascular disease, coronary artery disease (CAD) and history of aneurysms were considerable proportion of positive risk factors [3,11,12,13]. In addition, high levels of lipoprotein and homocysteinemia [14] are also considered being additional risk factors of AAA.

1.1.4 Negative risk factors

Ethnic origin may also be a risk factor of AAA. For example Asian race was deemed to be such a negative factor, however, the data involved screening from different ethnic backgrounds in a specific areas [15]. In contrast, Yii et al. suggested that AAA in Asian population is not uncommon and the incidence is comparable to the Western world [16]. Furthermore, the presence of diabetes mellitus (odd radio = 0.54) was also negatively associated with AAA [3].

1.2 Natural history

1.2.1 High growth rate

A study concluded that the expansion of AAA reached a range of 0.2 to 0.4 cm per year, 0.2 to 0.5 cm per year and 0.3 to 0.7 cm per year for the original diameter less than 4 cm, 4 to 5 cm and more than 5 cm, respectively [17]. The AAA growth rate in the expansion group is significantly faster than that in the non-expansion group in e.g. Japanese patients [18]. It is generally accepted that baseline diameter is strongly associated with growth rate, and larger diameter of AAA is associated with higher growth rate [19]. Simultaneously, smoking was significantly associated with expansion rate of AAA and smoking termination was considered to reduce the growth rate of AAA [20,21]. Recently, a strong correlation between growth rates of maximum diameter and intraluminal thrombus volumes has been confirmed [22].

1.2.2 Low growth rate

The most studies conclude that treatment with statins is generally associated with lower growth rates of AAA [23,24,25]. Although data on the predictive factor of beta-blockers and diabetes are controversial, several studies demonstrated that they might play a negative role in the growth rate of AAA [26,27].

1.2.3 Incidence of rupture

Similarly, as well as high growth rate of AAA, larger diameter of AAA was associated with AAA rupture. A study reported that the associated rupture risk at four years was 2%, 10% and 22% for the original diameter less than 4 cm, 4 to 5 cm and more than 5 cm, respectively [17]. The potential rupture rates were 2.1% and 4.5 % within one year for small AAA (3.0 to 4.4 cm) and 4.5 to 5.9 cm, respectively [28].

Meanwhile, expansion rate is a critical key factor related to the AAA rupture risk [29]. Besides, individual study has confirmed that intraluminal thrombus might be associated with an increased AAA rupture risk [30].

1.3 Clinic and morphology

1.3.1 Symptom

AAAs is often asymptomatic and symptomatic AAA leads to pulsating sensations in the abdomen or pain in the chest, lower back, or scrotum. AAAs was mainly discovered incidental or casual during a regular medical checkup (e.g. abdominal ultrasonography), or when the aneurysm rupture evoked emergency conditions. Symptomatic AAA is thought to be associated with a higher rupture risk than asymptomatic AAA. Usually, a palpable abdominal mass is a representative symptom under physical examination. The main risk of an untreated AAA is always significant expansion, rupture, hemorrhage, and death.

1.3.2 Rupture

Ruptured abdominal aortic aneurysm (rAAA) represents an emergent clinical condition with life-threatening implication. The symptom of rAAA usually includes grievous pain of the abdomen, lower back and groin. Losing a lot of blood quickly results in hemorrhagic shock, cyanosis or tachycardia and can be fatal for the person concerned. Despite the advances in surgical and non-invasive interventions, the overall mortality rate of rAAA is 80-90%, of which 66% die before reaching hospital [31].

1.3.3 Concomitant aneurysm

Abdominal aortic often occurs with iliac, femoral and popliteal aneurysms. The European society for vascular surgery guideline considers that 85% femoral artery aneurysms patients and 62% popliteal aneurysms patients have a concomitant AAA [1].

1.3.4 Morphometry and classification

While length, width and angulation of the aneurysm neck have all been previously assessed in endovascular abdominal aortic aneurysm repair (EVAR), aneurysm neck shape has not yet been neglected. As showed in **figure 1**, AAAs can be easily grouped into three distinctive categories (type I, II and III), and classified into five types, which comprise type I, IIA, IIB, IIC and III [32].

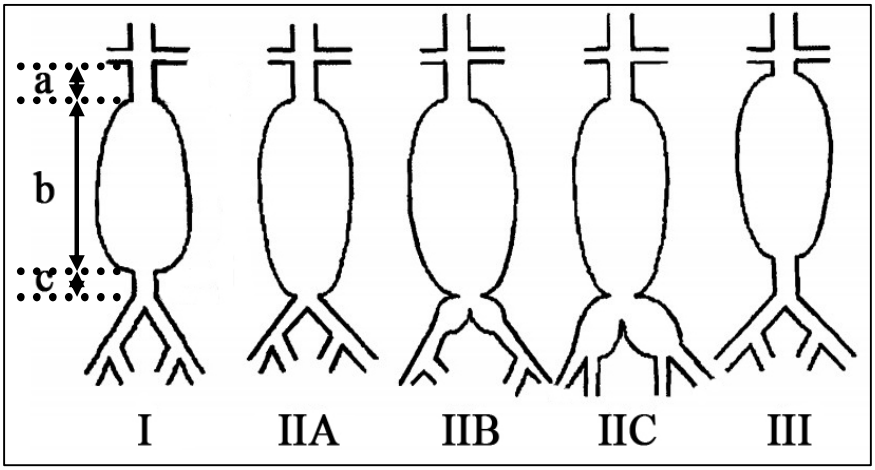

Figure1. Schematic model of AAA classification according to Schumacher et al. [32]. Type I: proximal neck (a) ≥ 15mm and distal cuff (c) ≥ 10mm; type IIA: proximal neck (a) ≥ 15mm and AAA down to aortic bifurcation; type IIB: proximal neck (a) ≥ 15mm and aneurysm with proximal common iliac artery involvement; type IIC: proximal neck (a) ≥ 15mm and AAA down to the iliac bifurcation; and type III: proximal neck (a) < 15 mm and distal AAA expansion.

1.4 Diagnostic

Symptomatic AAA patients are more likely to be associated with the clinical triad, which are abdominal or back pain, a pulsatile abdominal mass and hypotension. However, the clinical triad takes place just in about one third of AAA patients [33]. Thereunto, pain is the most continual complaint in AAA patients, and pain is always is occurred in the hypogastrium or the lower back. Pain gets AAA patients lasting for hours at any time, and is typically steady. In addition, AAA presenting in the young adult is more likely to be symptomatic and associated with more proximal aortic involvement than in elder patients [34].

1.4.1 Physical examination

Generally accepted, palpation of AAAs is safe and has not been reported to increase rupture risk. Abdominal palpation is moderate sensitivity for detecting an AAA that would be large enough to be referred for surgical repair [35], but abdominal palpation alone cannot be relied for smaller AAA. Abdominal palpation may be more adequate for screening thin AAA patients [36]. Most AAAs is asymptomatic and is discovered occasionally during medical examination for other purposes; therefore imaging diagnosis possesses undoubtedly an important clinical value for diagnosis of AAA. The following imaging techniques have its own advantages, limitations and their own indications.

1.4.2 X-ray plain films

The X-ray films can provide information about a curvilinear aortic wall calcification during an accidental clinical examination for other purposes [37]. Unfortunately, it

can be considered only as a hint that different stage of atherosclerosis are located in aneurysms walls. Sometimes, small calcified rings may demonstrate the presence of visceral artery aneurysms.

1.4.3 Ultrasonography

Ultrasound is an excellent screening test and the modality of choice for the detection of patients who suffered from an asymptomatic AAA [38]. This approach has the virtue of being widely available, noninvasive and having relatively low cost. Ultrasonography has a sensitivity of almost 100% for asymptomatic patients in the diagnosis of AAAs [39]. Screening for abdominal aortic aneurysms and monitoring the growth rate of aneurysms are most efficiently performed with ultrasonography. Undeniably, a limitation and disadvantage of ultrasonography is that aorta might not be visualized in patients with increased bowel gas and in obese individuals. Moreover, it cannot reliably ascertain the presence of periaortic disease and aneurismal of proximal or distal extent [40].

1.4.4 CT and CTA

For AAA, the computed tomography (CT) offers the physicians important information about not only the aneurysm but also the aneurismal surrounding anatomy. The use of CT is adequate to confirm inflammatory abdominal aortic aneurysm (iAAA), but CT is not sufficiently accurate to indentify abdominal arterial anatomy itself and adjacent collateral circulation [41]. The computed tomography angiography (CTA) is a powerful tool in screening AAA, and is able to detect the entire and detailed anatomical information including surrounding structures [42]. Moreover, three dimensional reconstructions make CTA a promising tool for displaying even the most complex aortic anatomy [43] (**Figure 2A**).

1.4.5 Intravascular ultrasound (IVUS)

Intravascular ultrasound is an invasive technique, and can provide accurate and reproducible measurements of abdominal aortic aneurysm. An advantage is to possibility of longitudinal images that are able to show the vascular structures and improve the spatial insight in abdominal aortic anatomy [44]. However, there are limitations of IVUS, which are the cause that this technique is not widely available and the technology has still to be improved.

1.4.6 Digital subtraction angiography (DSA)

Intra-arterial DSA is always “gold standard” for the preoperative assessment and diagnosis of AAAs. At the moment, DSA is used especially during and after the endovascular procedures. DSA is often reserved for special considerations, which is e.g. a suspicion of renovascular stenosis, renal hypertension, juxtarenal or suprarenal

AAAs [45]. Several advantages of DSA include renovascular disease confirmation and anomalous vessels identification (**Figure 2B**).

Figure 2. Reconstructed computed tomographic angiograms (CTA) and digital subtraction angiography (DSA) technique were applied to diagnose of AAAs. A: Reconstructed CTA in the frontal projection demonstrating the infrarenal aortic aneurysm (arrow heads). B: DSA Early arterial phase of a posteroanterior abdominal aortogram showing an abdominal aneurysm (arrows) originating below the renal arteries (outline arrow).

1.5 Therapy

1.5.1 Medical management

Several co-morbidities, for instance cardiovascular disease, pulmonary disease and neurological diseases, often coexist with AAA. Therefore, relative pre-operative medical strategies might promote post-operative outcomes e.g. relative complications and short-term mortality for the patients who underwent AAA. Consequently, the necessity to selected appropriate medical therapies which not only decrease the growth rate of AAA but also prevent short or long term effect is of highest priority. Smoking cessation, excise and effective medical drug for medical therapy of AAA patients are to reduce aneurysm evolve to rupture, decrease the short or long term after discharge and reduce accompanying complications.

1.5.2 Smoking cessation

A study based on the investigation of small aneurysms [20] suggested that persistent smoking predicted more rapid expansion of maximum AAA diameter. At the other side it is also well known and currently undoubted that smoking cessation is associated with improve of lung function. Although there is no evidence to support that smoking increases the risk of co-morbidities within AAA patients, patients who suffered from continuing nicotine intake have an increased risk of aneurysm rupture and poorer long-term survival [46].

1.5.3 Exercise

Nakahashi et al. suggested that aortic flow loading may decrease the expansion of AAA [47]. In addition, exercise might also reduce cardiovascular complications in the patients who suffer from AAA. Furthermore, a randomized trial demonstrated that exercise training is well tolerated and sustainable in small AAA patients who completed one year of follow-up [48].

1.5.4 Pharmacotherapy for AAA

1.5.4.1 Beta blockers

Many current guidelines recommend the use of medical treatment with beta blockers in the patients undergoing vascular surgery. Beta blockers may also play an important role in patients with AAAs who underwent endovascular or open surgical repair. There is no definite evidence or convincing studies proving potential efficacy of beta blockers in inhibiting expansion of AAAs. A randomized double blinded trial from Denmark suggested that propranolol might have a potential for minor inhibition of expansion of AAA [49]. Nevertheless, the superiority that beta blockers might significantly decrease the growth rate of AAA was not confirmed by another randomized control trials [50]. Furthermore, it was demonstrated that the patients with AAA did not tolerate propranolol well.

Beta blockers, especially metoprolol, did decrease the length of hospital stay in the patients undergoing infrarenal vascular surgery, though it did not reduce thirty-day cardiovascular events [51]. Yang et al also showed that metoprolol was not effective to decrease the thirty-day and six-month postoperative cardiac event [52]. The treatment with beta-blockers can be started one month before discharge and are to be used only in the AAA patients of highest cardiac risk [1]. The ESVS guidelines from 2011 advise such treatment as a Class A (level of evidence 1b) recommendation.

1.5.4.2 Statins

Perioperative use of 3-hydroxy-3-methylglutaryl coenzyme A reductase inhibitors, also known as statins, has been confirmed to reduce postoperative all-cause mortality in patients undergoing major vascular surgery [53]. For AAAs, use of statin in patients undergoing endovascular repair was still independently associated both with reduced overall and cardiovascular mortality [54]. Meanwhile, several clinical studies have provided evidence on the impact of statins on the AAA growth rate [55,56]. In contrast, Ferguson et al. showed no association between use of statin and AAA expansion [57]. Fortunately, because statins have been indicated for most of AAA patients with cardiovascular diseases, treatment should be started one month before a surgical treatment to decrease cardiovascular complication [1]. The ESVS guidelines from 2011 advise such treatment as a Class A (level of evidence 1a) recommendation.

1.5.4.3 Angiotensin converting enzyme inhibitor (ACE-I)

A Canadian study, a large population-based case-control study, demonstrated that ACE inhibitors are associated with a reduced risk of ruptured abdominal aortic aneurysm [58]. It was evidenced that AAA patients who were administered an ACE inhibitor before admission had significantly reduced occurrence of ruptured aneurysms. Nevertheless, the results were inconsistent, suggesting more likely that there was no significant association between ACE inhibitors and growth of AAA [59,60].

1.5.4.4 Tetracycline

Tetracycline (Doxycycline) is a broad-spectrum antibiotic, but suppressive effects on matrix metalloproteinases (MMPs) by tetracycline also were identified. Baxter et al. suggested that doxycycline is safe and well tolerated by patients with small asymptomatic AAAs and is also associated with a reduction of MMP-9 levels in blood [61]. However, doxycycline might have diverse effects on AAA. Another study confirmed that doxycycline treatment reduced expression of MMP-3 and MMP-25 at mRNA level in aortic wall, increased the level of Cystatin C and tissue inhibitor of metalloproteinase 1 (TIMP-1) [62].

Table 1. Potential evidence of pharmacotherapy for AAA growth according to ACC/AHA practice guidelines [63].

Drug	Effect on AAA growth	Level of evidence	Class of Recommendation
Beta-blocker	No inhibition	A	III
Statins	Inhibition	B	IIb
ACE inhibitors	No inhibition	B and C	IIb
Tetracycline	Inhibition	B	IIa

1.5.5 Open surgery for AAA

The aim of open surgical repair (**Figure 3A**) is to prevent rupture together with an acceptable rate of perioperative or postoperative morbidity and mortality. Conventional open surgery repair (OSR) is a traditional method for treatment of AAA and until now, it still remains to be an important surgical procedure for management of AAA with an advantage of definite and long lasting therapeutic results [64]. There are several prosthetic aortic grafts available to replace aorta ventralis: polytetrafluoroethylene (PTFE), knitted Dacron and collagen impregnated graft [65]. The graft replacement of the aneurysmatic aortic segment, represented by both tubular and bifurcated grafts, is still the standard of care for AAA. Access for OSR is either through a retroperitoneal approach or a trans-abdominal pathway. Incontestable, hemodynamic instability and reperfusion injury caused by aortic clamping and declamping subjected AAA patients to a deadly blow.

1.5.6 Endovascular repair for AAA

Since 1991, when alternative method for treatment of AAA was proposed, namely endovascular repair (EVAR), a continuous increasing number of patients who received EVAR as a predominant approach for therapy with promising initial results, was observed [66] (**Figure 3B**). Endovascular techniques and elective repair especially, has been widely applied in the treatment of abdominal aortic aneurysms. EVAR represents a less invasive procedure for AAA therapy [67]. For AAA patients treated with endovascular repair, there is a significant reduction in time for presentation to intervention, blood transfusion, intensive care and postoperative hospitalization stay [68]. Some successful procedures for the EVAR under local anesthesia have also been reported but only in a few large clinical centers [69,70].

The short-term results using EVAR for AAA treatment have been confirmed by several randomized controlled trial [71,72]. However, medium-term expanding to long-term outcomes of EVAR, such as all-cause mortality, aneurysm-related mortality and re-intervention rate remain still uncertain. Recently, the publication of the results of the DREAM trial [73] and EVAR-1 trial [74] with regard to EVAR versus OSR has shed light on long-term outcomes. The DREAM trial suggested that the rate of secondary interventions was significantly higher for endovascular repair in six years follow-up. The EVAR-1 trial, nevertheless, showed no differences in total mortality or aneurysm-related mortality in the long term follow-up.

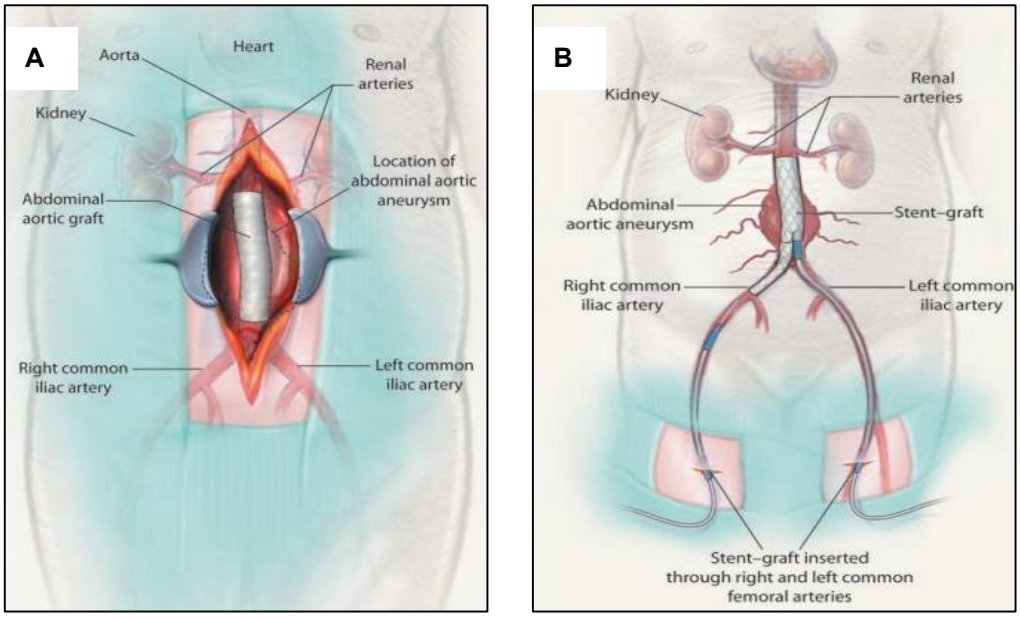

Figure 3. Schematic overview of open surgical repair (A) and endovascular repair (B) for an infrarenal abdominal aortic aneurysm according to Schermerhorn et al. [75]. In an endovascular repair (EVAR), a stent graft inserted through the right groin is placed just below the renal arteries, and the left limb of the bifurcated device is inserted through the left groin to overlap with the main body of the stent graft.

1.6 Etiology and Pathogenesis of AAA

Despite considerable advances in treatment of AAA, patients with a diameter exceeding 5.5 cm generally undergo surgical or endovascular repair [76,77]. Recently, developing of new therapies for treating small or asymptomatic AAA received greater efforts to investigate. However, for novel therapeutic strategies, better understanding of pathophysiologic processes and etiology leading to AAA wall destabilization until rupture is necessary and has become important issue to recognize patients at an increased risk.

The formation of AAA is associated with genetic variation [78], environmental factors [79], anatomical diversity [80], changes at biological level and other factors. Herein, it is considered that the interaction of multifactor is playing critical role rather than the effect of a single factor. For this purposes, it is becoming increasingly important to fully understand the formation and development of AAA and its etiology characteristics on molecular level.

At bio-molecular level, the pathogenesis of AAA is caused by multifunctional degenerative processes, including smooth muscle cells (SMCs) apoptosis/necrosis, extracellular matrix remodeling, and infiltration of inflammatory cells. Genetic disorder, estrogen deficiency and atherosclerosis are also causal underlying factors of destructive degeneration of the aortic wall. Among them, damage and degradation of elastin and collagen of the abdominal aortic wall are direct factors leading to AAA formation [81]. The exact etiology of AAA hasn't been absolutely understood yet, it is however certain that the progression of aneurismal degeneration involves destructive remodeling of the aneurysmal wall.

1.6.1 SMC apoptosis/necrosis

As the principal resident cells in the aortic wall, smooth muscle cells (SMCs), they synthesize proteins (elastin, collagen, gelatin, proteoglycan etc.), maintaining vessel wall elasticity, grant strength of the abdominal aortic wall and constitute the extracellular matrix (ECM) to the tunica media. Reduced SMCs may induce series of pathophysiological changes and boost the formation and development of AAA [82]. Previous study demonstrated that medial SMCs density is significantly decreased in human AAA tissues, which associated with evidence of SMC apoptosis [83]. Subsequently, another investigation has shown increased apoptosis of SMCs, which is most likely to be the factor of significant decrease of SMCs density in AAA [84]. It is believed that perforin and Fas/Fas Ligand in the immune cells might play a critical role in induction of apoptosis of SMCs in aneurysmal tissue [85]. Several mechanisms may contribute to induce SMCs apoptosis. Herein, infiltration of inflammatory cells in the media and adventitia is a key factor causing apoptosis of SMCs [86].

1.6.3 Infiltration of inflammatory cells

AAA is characterized by vascular inflammation and leucocyte infiltration throughout the media and adventitia of the vessel wall, which leads to the upregulation of expression and release of multiple cytokines [87]. Infiltration of inflammatory cells is associated with loss of smooth muscle cells (SMCs), breakdown of elastin and increase in degradation of extracellular matrix such as collagen and proteoglycans, which finally lead to aortic wall rupture.

1.6.3.1 Inflammatory cytokine

Several inflammatory cytokines, including IL-1β, IL-6, and TNF-α, have been abundantly detected in AAA tissue samples. Through measurement of tumor necrosis factor-alpha (TNF-α), interleukin 1 beta (IL-1β), interleukin 6 (IL-6) and interferon-gamma (IFN-γ) at circulating level, Juvonen et al suggested that the production of these cytokines is increased in these patients compared with healthy control individuals [88]. In addition, TNF-α and IL-1β concentration were significantly increased in the AAA specimens and further implicated an inflammatory process in the pathogenesis of AAA [89]. Furthermore, cytomegalovirus infection may also play a role in the pathogenesis of inflammatory aortic aneurysms [90].

1.6.3.2 Inflammatory cells and ECM

The inflammatory process results in protease-mediated degradation of the extracellular matrix. Furthermore, reactive oxygen species (ROS) play an important role in regulation of matrix metalloproteinases and induction of SMC apoptosis [91]. The recruitment of inflammatory cells into the adventitia, and elaboration of metalloproteinases (e.g. MMP-2 and MMP-9), may lead to the rapid growth and rupture of aneurysms. In addition, these inflammatory cells are likely to be the source of both the incremental amount of MMPs and a cascade of cytokines and markedly contribute to the aortic wall remodeling [92].

1.6.3.3 Autoimmunity

Both cellular and humoral immunity is involved in the pathogenesis of AAAs [93]. Indeed, AAAs shares many features of autoimmune diseases, including genetic predisposition, organ specificity, and chronic inflammation [94]. Several studies support the proposition that the chronic inflammation observed in AAA is a consequence of a dysregulated autoimmune response mediated by excessive autoreactive T cells against autologous components of the aortic wall [95, 96]. This loss of self-tolerance and further expansion of autoreactive lymphocytes lead to eventual destruction of aortic matrix and smooth muscle cells.

In conclusion, the AAA disease typically involves tissue inflammations, which have been widely seen by the presence of inflammatory leukocytes and various cytokines.

They are considered to participate in the immunopathogenesis of AAAs and results in the destruction of aortic wall.

1.6.4 Extracellular matrix remodeling

The matrix metalloproteinases (MMPs) are a family of regulated enzymes, and also thought to play a major role on the extracellular matrix remodeling, which in the aorta comprises especially collagen I and III and elastin. Each of MMPs has a different activity to disintegrate and remodel extracellular matrix. Several members of this family of enzymes have already been identified in aneurysmal aorta [97]. Herein, gelatinase B (MMP-9), gelatinase A (MMP-2), and macrophage elastase (MMP-12) have been suggested as the key mediators of the degradation of the structural proteins in the aneurysmal aortic wall [98,99].

MMP-9 (gelatinases B) has been proven to be the most abundant elastolytic proteinase, which is expressed by infiltrating macrophages not only in the human aneurysmal tissue [100] but also elevated in the plasma of AAA patients [101] (**Figure 4**). In addition, MMP-9 expression correlates also with increasing aneurysm diameter [102]. Therefore, therapeutic drug targeting MMP-9 may restrict the growth rate of AAA [103]. However, several studies suggested that additional enzymes, neutrophil elastase [104] or urokinase-type plasminogen activator (uPA) contribute to extracellular activation of proMMP-9 as well [105]. Meanwhile, other proteinases (MMP-2 and MMP-12) may amplify MMP-9 mediated degradation of elastic fibers.

MMP-2 is also considered to be in close association with the extracellular matrix in aneurysm tissues. Previously, Davis and colleague [106] demonstrated that MMP-2 was found to be primarily produced by mesenchymal cells. They also revealed that MMP-2 was prominent within AAA tissue when mesenchymal cells were surrounded by inflammatory cells, and suggested paracrine modulation of MMP-2 expression in AAAs. Subsequently, another study confirmed that macrophage-derived MMP-9 and mesenchymal cell MMP-2 are both required and cooperate with development of AAA [107].

MMP-12 is specifically expressed by macrophages within AAA tissue and considered to play a similarly important role in AAA development [108]. It is specifically localized to elastin fiber fragments, which represents a key component of aortic wall structure; therefore MMP-12 may have a direct and singular role in the pathogenesis of aortic aneurysms [109].

In conclusion, the MMPs families might become useful biological markers of AAA and have potential targets in terms of pharmacological treatment.

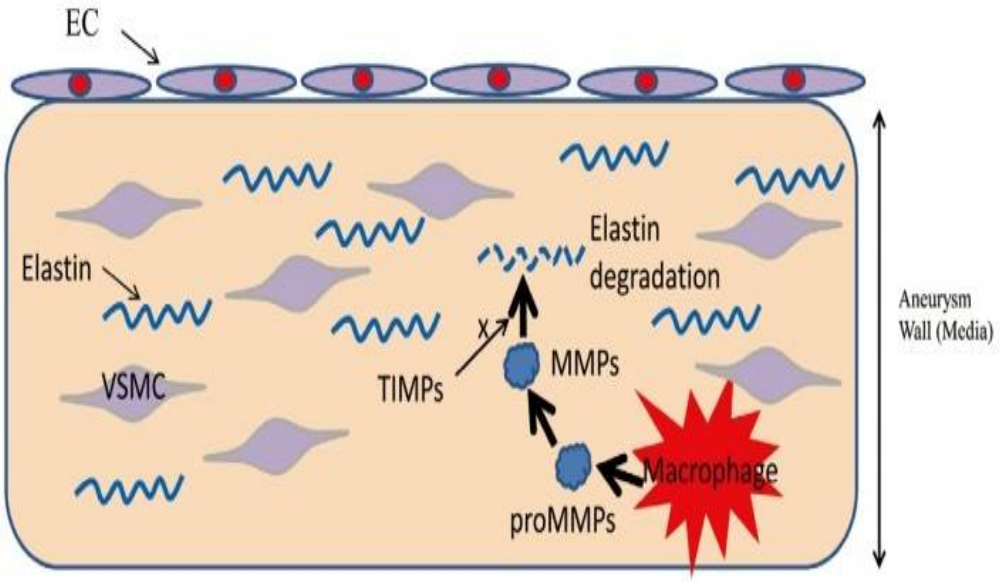

EC: endothelial cells
MMPs: matrix metalloproteinases
TIMPs: tissue inhibitor of metalloproteinase 1
VSMC: vascular smooth muscle cell

Figure 4. Elastin degradation in the aneurysmal wall according to Kurosawa et al. [110]. The schematic representation of the role of matrix metalloproteinases (MMPs) in the aneurysmal wall is shown.

1.6.5 Genetic variation

There is a familial tendency to abdominal aortic aneurysms [1]. Previous study demonstrated that genetic variation in the haptoglobin and cholesterol ester transfer protein genes appears to influence dilatation of the abdominal aorta [78]. In a nationwide survey in Sweden, the relative risk of developing AAA for first-degree relatives to persons suffered from AAA was approximately doubled (OR=1.9; 95%CI, 1.6-2.2, P<0.0001) compared to persons with no family history [111].

More recently genome-wide technique, Genome-Wide Association Studies (GWAS), was used to provide unbiased ways of identifying genetic risk factors for AAA. GWAS has confirmed a powerful technique to identify genetic risk factors associated with the presence of AAA. The following five chromosomal regions in the human genome especially contribute to the genetic risk for AAA and were listed in **table 2**.

Table 2: AAA genetic loci discovered using genome-wide association studies according to Kuivaniemi et al. [112].

Chromosomal location	Nearest gene (gene symbol; gene ID)	Polymorphism	RAF	OR [95%CI]	P value	Refer.
3p12.3	Contactin-3 (CNTN3;5067)	rs7635818	0.42	1.33 [1.10–1.21]	0.0028	[113]
9p21.3	CDKN2B antisense RNA 1 (CDKN2BAS1; 100048912)	rs10757278	0.45	1.31 [1.22–1.42]	1.2×10^{-12}	[114]
9q33.1	DAB2 interacting protein (DAB2IP;153090)	rs7025486	0.25	1.21 [1.14–1.28]	4.6×10^{-10}	[115]
12q13.3	Low density lipoprotein receptor-related protein 1 (LRP1;4035)	rs1466535	0.68	1.15 [1.10–1.21]	4.5×10^{-10}	[116]
19p13.2	Low density lipoprotein receptor (LDLR;3949)	rs6511720	0.88	0.76 [0.70–0.83]	2.1×10^{-10}	[117]

Note: RAF: risk allele frequency in population; OR: odds ratio; 95% CI: 95% confidence interval; rs number: unique identifier for each single nucleotide polymorphism (for more information, see http://www.ncbi.nlm.nih.gov/snp/). Gene symbols and IDs are available from http://www.ncbi.nlm.nih.gov/gene/

1.7 Epigenetics in general

Pathophysiological changes in gene expression are the basis of many human diseases. Among others, epigenetics have been already recognized to be a powerful tool to activate or silence gene transcription, which is a stably heritable phenotype resulting from changes in a chromosome without alterations in the DNA sequence [118]. Epigenetic changes comprise DNA methylation, various histone modifications (e.g. methylation, acetylation, phosphorylation, ubiquitinilation and sumoylation), and RNA-based mechanism, which capacitate the cells to respond rapidly to environmental changes [119].

1.7.1 Epigenetics - conception

Although epigenetic alterations in gene expression can not directly change DNA sequence, these alterations may affect expression of a gene or the availability of its product. Precisely, regulation of gene expression include following two components, which are traditional model and epigenetic regulation. The former is that gene expression is directly impacted by the DNA sequence though transcriptional

regulation approaches. The latter is that gene expression is indirectly influenced by changing chromatin structure though DNA methylation and histone modification [120].

Chromatin structure is affected by DNA methylation and histone modification. Short segment of DNA wrapped around eight histone protein cores (double of H2A, H2B, H3, and H4) constitute a nucleosome [121]. These nucleosomes are organized into chromatin, the building block of a chromosome (**Figure 5**). Histone protein play structural and functional role in all nuclear progressions.

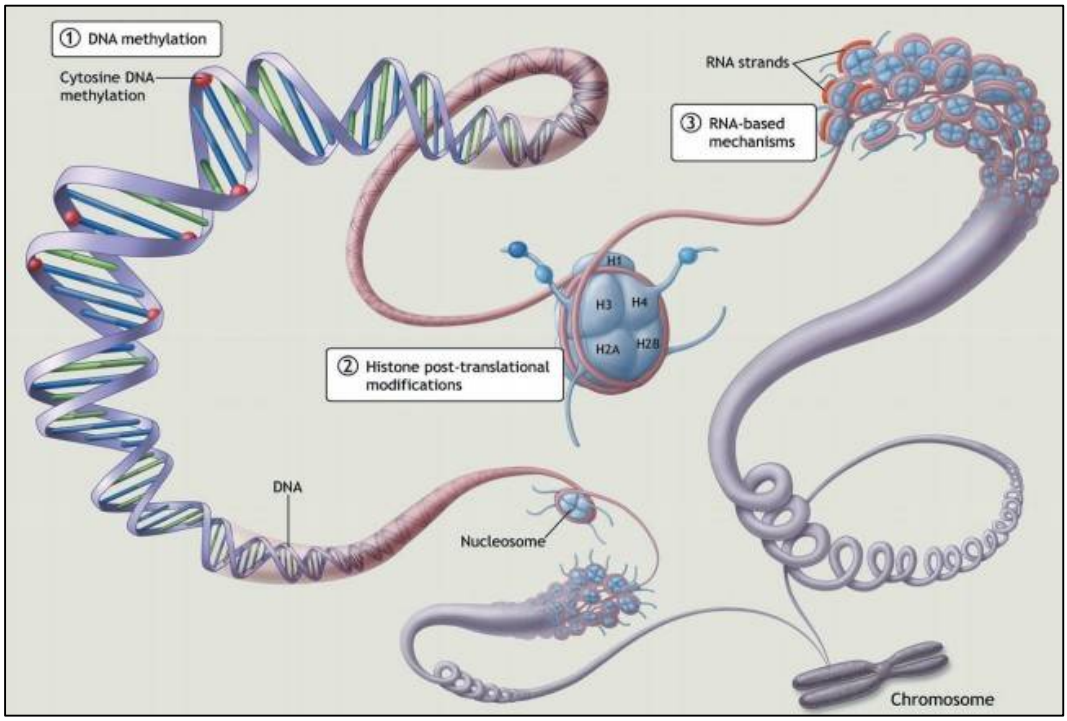

Figure 5. Epigenetic mechanisms of gene regulation according to Matouk et al [122]. The mechanisms of epigenetic mainly in the control of gene expression including the following three pathways: (1) DNA methylation, (2) histone posttranslational modifications, and (3) RNA-based pathways.

1.7.2 Epigenetics - adaptation to the environment

Positive natural selection has played an important role in our development, which is the force that propels the increase in prevalence of advantageous traits [123]. Advantageous traits differ widely and may resist to infections (e.g. malaria) or affects food preferences [124]. This positive natural selection has been ascribed to genetic variants. Recently, there has been a dramatic increase in the use of genome-wide detection to identify adaptively evolving loci in the human genome [125]. Epigenetics, specifically DNA methylation, are highlighted as mechanisms of adaptation and response to environmental factors [126].

1.7.3 Epigenetics - current situation

Although variation of epigenetic regulation may facilitate to explain genetic diversity, significant alterations of epigenetic regulation can result in diseases. Most studies relating epigenetics to human pathogenesis have targeted on cancer or other serious diseases. Recently the role of epigenetics as a potential mechanism to control genes has also been proposed in cardiovascular disease. Only very few studies to date have investigated these epigenetic alterations in human atherosclerosis. Although present topic and hotspot is epigenetic mechanisms of disease yet, epigenetic procedures are requisite to investigate normal growth, homeostasis and development.

1.8 DNA methylation

DNA methylation plays a key role in maintaining the normal structure of the DNA, chromatin stability, and X-chromatin inactivation [127]. In human and other mammals, DNA methylation is almost exclusively restricted to CpG di-nucleotides. DNA methylation can silence genes and repetitive elements which lead to the alteration of chromatin structure [128]. DNA methylation is catalyzed by three different DNA methyltransferases (DNMTs) encoded by different genes on distinct chromosomes: DNMT1, DNMT3a, and DNMT3b. The DNA methylation status is constantly changing, and is involved in the regulation of pathological changes in arterial atherosclerosis, diabetes, and hypertension [129,130,131].

1.9 Histone modification

Histones are modified at plenty of sites. There are more than sixty different residues on histones where modifications have been confirmed by both specific antibodies and mass spectrometry [132]. Different modifications locate to the N-terminal tails of histones molecules within the nucleosome, and change the chromatin structure or hence regulate the accessibility of transcription factors to DNA. Modification of histone tails include following several types, which are methylation, acetylation, ubiquitination, phosphorylation, ADP ribosylation, biotinylation and sumoylation. In fact, histone methylation and acetylation are the most important modifications and the most studies so far have been focused on these changes.

1.9.1 Histone methylation

The numerous histone modification types acknowledged represents a huge the number of modifications that can take place on histones. For instance, additional complexity of modification procedures comes partly from the fact that methylation at lysines or arginines could have different forms: mono-, di-, or trimethyl for lysines and mono- or di- (asymmetric or symmetric) for arginines [132]. Histone that is methylated at specific residue can either silent or activate gene expression. The balance between

these transforms is achieved through the action of enzymes, which are named methyltransferases (HMTs) [133]. HMTs are enzymes that are facilitating the transfer of the methyl group to a certain site of histone.

1.9.2 Histone acetylation

The acquaintance of the molecular level of histone acetylation is promptly emerging. Histone acetylation was first observed in 1964 by Allfrey and co-workers [134]. They proposed that histone acetylation plays an important role in the regulation of gene transcription, which is found in actively transcribed regions of chromatin. Histones are hyperacetylated if the gene is active and conversely in silenced regions histones exert to be hypoacetylated (**Figure 6**). Subsequently, several studies have solidified and extended this theory and found that histone acetylation is performed by the action of histone acetyl transferases (HATs), which add an acetyl group to a lysine residue of the histone protein, attributing that way to chromatin activation. Oppositely, corresponding acetyl group can be removed by histone deacetylases (HDACs), resulting in chromatin inactivation [135,136].

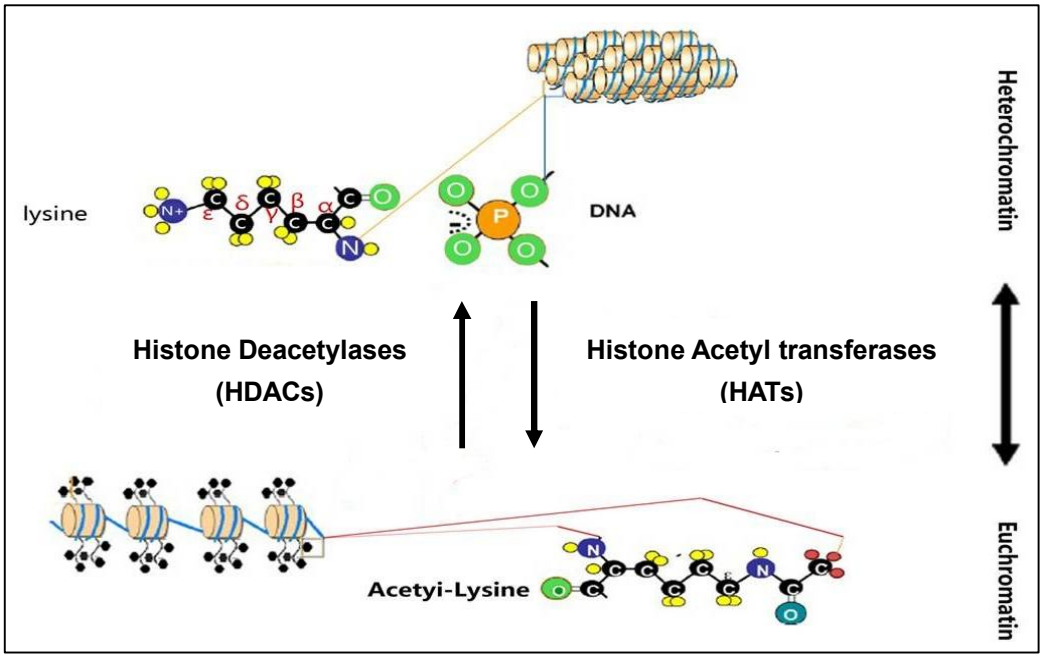

Figure 6. Histone acetylation and transition of heterochromatin to euchromatin. The figure depicts the molecular structure of acetylated and deacetylated lysine and the resultant charges/neutralization responsible for the interaction of histones with chromatin. Adapted from Khan et al [137].

1.10 Histone acetyltransferases in details

Transferring of acetyl groups to lysines by histone acetyltransferases (HATs), as well as the effect of steric hindrance, facilitate binding of transcription factors to DNA and consequently lead to increased gene expression. Histone acetyltransferases (HATs) are often capable of acetylating multiple lysine (K) residues in vitro. Most HATs

require protein partners and function within HATs complexes to perform their specific actions. The interoperable interactions between HATs and their complexes afford functional regulation and substrate specificity [138,139].

1.10.1 New nomenclature

Despite the names of these enzymes called HAT, histones are not their only substrates. Non-histone substrates include other components such as transcription factors, chromatin remodeling factors, and diverse cytoplasmic/mitochondrial proteins. Meanwhile, hundreds of these proteins have already been found to be susceptible to acetylation [140]. For this reason, it has been suggested that the term HAT is far too general and should be replaced by KAT, wherein the K stands for lysine. Therefore, these new terminology was also used in the following sections of this study [141].

1.10.2 HAT family in general

So far, four families of HATs were discovered, which include all together more than eleven enzymes. Every HAT possesses an acetyl transferases domain, however, sequence comparison distribute them into subfamilies according to additional shared domains (**Table 3**).

Table 3. Summary of histone acetyltranserases (HATs) selected in the study according to Santos-Rosa [142] and Furdas [143].

Family	HAT	KAT*	Histone substrate	Function
GNAT	GCN5	KAT2A	H3K9,14,18,36	transcriptional activation, DNA repair
	P/CAF	KAT2B	H3K9,14,18,36	
p300/CBP	CBP	KAT3A	H2AK5 H2BK12,15 H3K14,18 H4K5,8	transcriptional activation
	p300	KAT3B	H2AK5 H2BK12,15 H3K14,18 H4K5,8	
MYST	Tip60	KAT5	H4K5,8,12,16	transcriptional activation, DNA repair, replication
	MOZ/MYST3	KAT6A	H3K14	
	MORF/MYST4	KAT6B	H3K14	
	HBO1/MYST2	KAT7	H4K5,8,12	
	HMOF/MYST1	KAT8	H4K16	
TF-related HATs	TAF1	KAT4	–	transcriptional activation, Pol III transcription
	TFIIIC90	KAT12	H3K9,14,18	

*Note: The abbreviations used in the study are: KAT, lysine [K] acetyltransferase

1.10.3 GNAT (Gcn5-related N-Acetyltransferases) family

GCN5 (KAT2A)
The yeast protein Gcn5 (general control nonderepressible 5) provides clear molecular evidence to directly link histone acetylation and gene activation, which was the first discovered transcription-related HAT [144]. The recent evolution and cognition of Gcn5 suggested that it can be divided into two histone acetyl transferases (HATs) from metazoan organisms: GCN5 (KAT2A) and P/CAF (KAT2B). They two are highly homologous GCN5-like paralogous. GCN5 exerts a widely range of functions with regard to cell proliferation, cell cycle regulation, differentiation, and DNA damage repair [145]. Furthermore, GCN5 has been found to function as a transcription co-activator for estrogen receptor α (ER-α) [146].

P/CAF (KAT2B)
Although most of the metazoan genomes code for one GCN5 type factor, vertebrates have another gene encoding P/CAF (p300/CBP-associated factor), which is approximate in 73% identical to GCN5. It has been suggested that P/CAF could locally achieve an open chromatin configuration and accelerate transcriptional activity, when it is bound to specific promoters through interaction with p300/CBP [147]. There is also increasing evidence that P/CAF modulates non-histone proteins [148]. For cardiovascular disease, a study base on three large prospective studies suggested that a variation in the promoter region of P/CAF is associated with coronary heart disease-related mortality [149].

Relevance
The GCN5 and P/CAF have been demonstrated to acetylate numerous transcription factors directly. The GCN5 knockout mice result in early embryonic lethality, while P/CAF knockout mice show no obvious phenotype. Deletion of GCN5 and P/CAF may result in severe developmental defects, which exert a partial functional redundancy between GCN5 and P/CAF [150].

1.10.4 CBP/p300 family

Among the mammalian CBP and p300 is another pair of ubiquitously expressed paralogous proteins that belong to next family of HATs. CBP/p300 family is more efficient and has less substrate specificity than the other HATs enzymes [151].

CBP (KAT3A)
CBP (CREB-binding protein) is ubiquitously expressed and is involved in the transcriptional co-activation with several different transcription factors. CBP was named after its original description as an interacting partner of the transcription factor CREB (cAMP responsive element binding) [152]. CBP is involved in the acetylation

of H3 and interacts with cell cycle regulators (c-Myc and c-jun) [153]. Furthermore, the activated CBP also may acetylate other transcription factors (p53 and TFIIB transcription factor complex) to facilitate their binding to DNA [154]. Additional mechanism by which CBP is thought to stimulate transcription is by recruiting the P/CAF to the promoter.

P300 (KAT3B)
P300 was initially described as the 300-kDa protein (p300) interacting with the adenovirus E1A protein, which shares high conserved regions with CBP [155]. It possesses multiple domains that bind to diverse proteins containing many transcription factors [156]. It has been confirmed that p300 facilitates gene transcription by histone acetylation and is capable to interact with transcription factors such as p53, NF-κB, and P/CAF [157,158]. These co-activator molecules control gene transcription and most of them have intrinsic HAT activity.

Relevance
CBP and p300 are highly homologous proteins (with >70% of overall identity) and share most of their known functional domains. Such findings explain why these both proteins have widely overlapping functions via their interactions with similar partners and substrates [159]. Many studies have suggested that CBP/p300 is critically involved in control of development, proliferation, differentiation, and apoptosis [160].

1.10.5 MYST family

MYST (Moz, Ybf2/Sas3, Sas2, and Tip60) proteins constitute the largest family of HATs and are present in all eukaryotes. Recently, several studies have found out that member of MYST family are required for a diverse cellular processes, not only in health but also in disease. Translocations affecting MYST member may e.g. result in leukemia and solid tumors [161].

Tip60 (KAT5)
Tip60 (HIV Tat-interacting protein of 60 kDa) was firstly identified as an HIV-1 Tat associating protein in yeast [162]. The Tip60 has a well-characterized involvement in transcriptional regulation, functioning as a co-activator for such crucial proteins as nuclear hormone receptors [163], NF-κB [164], and c-Myc oncoprotein [165]. Through the RNA interference (RNAi) technique, a study has revealed that Tip60 is required for induction of p53 apoptosis [166]. Precisely, an important function is emerging between Tip60 and transcription mediated by the p53 tumor suppressor.

MOZ/MYST3 (KAT6A)
The MOZ (Monocytic Leukemia Zinc Finger Protein) is a human proto-oncogene, which has a homology with yeast Sas3. Besides, the MOZ has intrinsic HAT activity,

and aberrant acetylation by abnormal MOZ proteins leads to leukemogenesis. MOZ displays significant sequence similarity to MORF (overall identity is nearly 60%; similarity is approximate 66%) [167]. All MOZ fusion partner genes are involved in histone modification and transcriptional regulation. Precisely, MOZ specifically interacts with transcription factors such as AML1, p53 and NF-κB functioning as their transcriptional co-activator [168,169,170].

MORF/MYST4 (KAT6B)

MORF (monocytic leukemia zinc finger protein-related factor) is ubiquitously expressed in adult human tissues, and its gene is located at human chromosome band 10q22. MORF has intrinsic HAT activity [171]. Unlike known HATs, MORF possesses a transcriptional repression domain at its N terminus and an activation domain at its C terminus [172]. The MORF generates fusion of genes associated with CBP in various disorders, including acute myelocytic leukemia (AML) and uterine leiomyomata [173,174].

HBO1/MYST2 (KAT7)

HBO1 (HAT bound to ORC1) was originally identified in a screen for proteins interacting with origin recognition complex protein 1 (ORC1) [175]. ORC initiates recruitment of components of several pre-replication complexes (pre-RC) such as Cdc6/Cdc18 and the minichromosome maintenance complex [176]. Earlier studies suggested that HBO1 might play an active role in DNA replication. Recently, Iizuka and co-workers confirmed that HBO1 positively regulates pre-RC assembly and initiation of DNA replication [177].

HMOF/MYST1 (KAT8)

The human MOF (males-absent on the first) is a member of the MYST family, and is believed to be responsible for histone H4K16 acetylation in human cells. MOF is ubiquitously expressed and is clearly targeted to all chromosomes [178]. Besides, MOF plays critical roles by acetylating non-histone substrates such as p53 [179]. Base on mammalian study, Hilfiker et al. revealed that hMOF forms at least two individual multi-protein complexes, MSL and NSL [180]. Depletion of hMOF in cells results in genomic instability including following aspects, which are early embryonic lethality, defective DNA damage repair, and reduced transcription of certain genes [181,182]. Over-expression of the hMOF and its corresponding substrate modification of H4K16 have been confirmed in breast cancer and medulloblastoma [183].

Relevance

The function of members of MYST family is rather diverse, including roles in transcription, epigenetic control, DNA replication, and repair.

1.10.6 TF-related HATs family

TAF1 (KAT4)
Transcription initiation is mediated by RNA polymerase II and pre-initiation complex (TFIIA, -B, -D, -E, -F and -H) that are highly conserved in human [184]. Herein, TFIID plays a role in pre-initiation complex assembly on protein-coding genes, which comprised of the TATA box binding protein (TBP) and fourteen TBP-associated factors (TAFs). TAF1 is the largest component of the transcription complex TFIID and acetylates histones H3 and H4 in vitro [185]. The TAF1 protein possesses intrinsic protein kinase activity and histone acetyltransferase activity [186]. The point that TAF1 modulates transcriptional activity of proteins such as c-Jun has been investigated [187]. Recently, another study demonstrated that TAF1 is also a co-activator of androgen receptor (AR) that binds and enhances AR transcriptional activity [188].

TFIIIC90 (KAT12)
TFIIIC is necessary for transcription of tRNA and 5S RNA genes by RNA polymerase III, and is composed of six subunits, five of which are conserved in humans [189]. TFIIIC is a multifunctional protein complex required for promoter recognition, recruitment of TFIIIB, RNA polymerase III and chromatin-mediated transcription. There is an evidence that the three TFIIIC subunits (220, 110, and 90 kDa) possesses HAT activity and intrinsic HAT activities have been verified as well [190]. Herein, 90-kDa subunit (TFIIIC90) directly binds to tRNA and 5S RNA gene promoters [191]. Current evidence suggests that hTFIIIC90 cooperates with hTFIIIC63 in facilitating the recruitment of TFIIIB and RNA polymerase III [192].

1.11 HDACs in detail

Histone deacetylation is mediated by histone deacetylases (HDACs) and, in contrast to HAT, has been associated with gene repression and their discovery came almost in parallel to the discovery of HATs enzymes. Precisely, histone deacetylases (HDACs) can remove acetyl groups and thus influence transcription vice versa.

1.11.1 Non-updated nomenclature

As already mentioned above with regard to the nomenclature of HATs, HDACs could have been renamed as KDACs as well. However, the scientists suggested that renaming them would serve to confusion rather than clarity; because of HDAC families already had a coherent nomenclature. Therefore, they proposed to adopt old nomenclature and regulation [141].

1.11.2 HDAC family

Base on yeast studies, Class I HDACs (HDACs 1, 2, 3, 8) are homologues of yeast PRD3 and are found exclusively in the nucleus. Class II HDACs (HDACs 4-7, 9 and 10), homologues of yeast Hda1, are found in both the nucleus and the cytoplasm [193]. Furthermore, to these classical HDACs, Mammalian HDACs are classified into three major classes, with at least 11 isozymes having been indentified [194] (**Table 4**).

Table 4. Summary of histone acetyltranserases (HATs) selected in the study according to Gray et al. [193].

Family	Name	Substrate	Role
Class I:	HDAC1,2,3,8	Histones, TP53, E2F1	transcription corepressor
Class II:	HDAC4,5,6,7,10	Histones	transcription corepressor
Class III:	SIRT1,2 (5,6,7)	Histones, p53	cell proliferation, cell cycle

1.11.3 The role of HDACs

HDACs have been widely considered to have transcriptionally repressive effect. Herein, HDACs fabricate chromatin less available for transcription factors though condensation of chromosomes. HDACs act as components of co-repressor complexes. This is confirmed by the facts that HDACs are found to cooperate with transcription repressors, and HDAC inhibitors induce expression of certain genes [195].

1.12 Potential role of epigenetics in AAA

There is very limited evidence of epigenetic mechanism in AAAs, with most of the recent investigations being concluded from studies on atherosclerosis. With regard to atherosclerosis lesions, it was recently observed that genomic DNA isolated from human atherosclerotic lesions is hypomethylated [196]. Inversely, data from peripheral blood lymphocytes in patients with coronary heart disease were inconsistent [197] regarding the methylation status. Likewise, no consistent data are available about histone modification in human atherosclerosis, and nothing is known about such processes and possible mechanisms in abdominal aortic aneurysms. Krishna et al. have hypothesized that epigenetic mechanisms might play a role in the pathogenesis of AAA; however so far, there is no direct evidence to support this assertion to date [198].

Fortunately, DNA methylation and histone acetylation have already been investigated in other context with regard to inflammation, cellular proliferation and remodeling, processes that take place also during AAA development and progression. Therefore, these epigenetic alterations may also be relevant to the pathology of AAAs. Important risk factors for AAA, including cigarette smoking, older age, male gender and hypertension have already been linked with epigenetic effects and thus could act to

promote AAA. Consequently, epigenetic changes could play an important role to the in AAA pathophysiology.

1.13 Aim of study

The aim of the present study is therefore to attain a better insight into the epigenetics and its role in human AAA. The global object of this study was to find possible contribution of histone acetylation, of the expression of the corresponding enzymes histone acetyl transferases (HAT) and the possible molecular mechanisms to the development and progression of AAA.

The specific aims of these studies were:
1. To perform a semi-quantitative histological and immunohistochemical analysis in the diseased and healthy aortic tissue samples and to find possible relationships between epigenetic changes and individual cell types within AAA wall (e.g. inflammatory cell infiltrates, endothelial cells of the neovessels and smooth muscle cells with their different phenotypes).

2. To compare the expression of HATs at mRNA level between the AAA tissue samples and age-and gender- matched healthy controls. Furthermore, to correlate the expression of the individual HATs with the cells located within AAA, the expression of specific markers representing these individual cells at mRNA level was analyzed as well.

3. To investigate, whether histone acetylation is altered in the biopsy samples of patients with AAA compared with healthy control tissue at protein level.

4. To determine, whether histone acetylation and the expression of HATs are changed in AAAs compared with age- and gender matched controls. Furthermore, whether the expression of HATs can be related to the individual cells within AAA and whether it is altered in aneurysmal tissue samples compared with controls.

2. MATERIALS AND METHODS

Collection of human tissue samples (abdominal aortic aneurysm and normal healthy abdominal aorta) for experimental research was conducted according to the ethical guidelines of Technische Universität München, Klinikum rechts der Isar. This study was approved by the local ethics committee and corresponding informed consent form was written by the patients and donors. The investigation conformed to the principles outlined by the Declaration of Helsinki [199] for use of human tissue.

2.1 Tissue sampling and processing

2.1.1Tissue collection

Samples of 37 patients (30 males, 7 female) with asymptomatic AAA were obtained during conventional surgical repair from the Department of Vascular and Endovascular Surgery (Klinikum rechts der Isar). Average age was 66.8±11.4 (range 40–87 years) and average maximum AAA diameter size determined by CT scan was 62.8 ± 16.7 mm (range 40–90 mm). All AAAs were accompanied by atherosclerotic changes within the vessel wall. Patients with Ehlers-Danlos syndrome, Marfan syndrome, other known vascular or connective tissue disorders were excluded from the study. Furthermore, the included patients had no evidence or medical history of any cancer disease.

Healthy aortic tissue samples from 12 organ donors were used as a control (7 males, 5 female). These donors, whose average age was 59.2 ± 19.4 (range 21 to 86 years) were obtained from the Department of Trauma Surgery (Klinikum rechts der Isar). None of the control samples showed any signs of atherosclerosis and no evidence or medical history of aneurysm and the other vascular disorders was known. Exclusion criteria also included cancer, infection, or any other immune-mediated disease, as far as these data were available.

2.1.2 Tissue processing

During open surgical repair of an abdominal aortic aneurysm the incision in the abdomen was performed and the diseased aorta was exposed. Following excision of a superfluous part of the AAA, the tissue samples were immediately transferred into a physiological solution (130 mmol/l sodium chloride, 5 mmol/l potassium chloride, 2 mmol/l calcium chloride, and 3 mmol/l sodium lactate) and delivered contemporary to the lab for further processing. There the AAA-wall was divided in two parts. One part (AAA: n=37, Ctrl: n=12) was segmented in blocks of 1-4 cm, and immediately fixed in 4% formalin for up to 24h, followed by dehydration and embedding in paraffin. The other part (AAA: n=37, Ctrl: n=12) of the specimen was immediately frozen in

liquid nitrogen (**Figure 7**). Fresh frozen samples were used for protein extraction and quantitative western blot analyses; quantitative real-time reverse transcriptase-PCR (RT–PCR) and histological and IHC analyses were performed using the formalin-fixed samples.

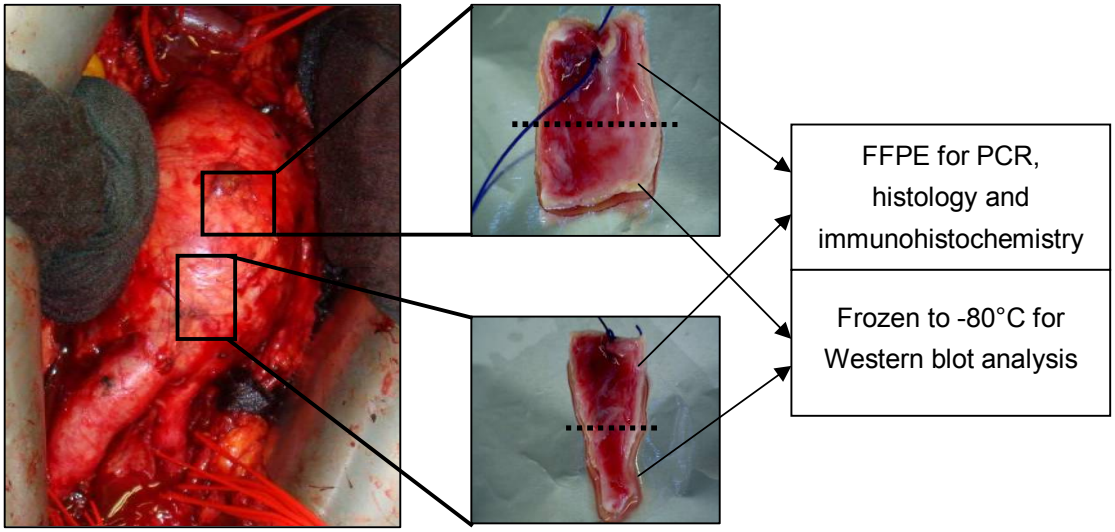

Figure 7. An Example of biopsy tissue recovered from AAA patients. FFPE: formalin fixed paraffin-embedded.

2.2 Histochemistry

For a proper histological characterization, 2-3 µm thin sections were prepared (Leica RM2255 rotary microtome, Leica Biosystem, Germany) from each sample block followed by haematoxylin-eosin (HE) and elastica van Gieson (EvG) staining. The HE and EvG staining were performed in order to evaluate the general aortic wall morphology, degree of degradation of extracellular matrix, cellularity, extent of inflammation, and neovascularization of each sample.

2.2.1 Haematoxylin-Eosin (HE) staining

The hematoxylin-eosin staining (HE) is the primary staining in histochemistry. Generally, the staining of nuclei by hemalaun is blue, cytoplasm and extracellular tissue is stained in various shades of red, pink and orange. The HE staining of this study was carried out according to a standard histochemical protocol of the Department of Pathology (Klinikum rechts der Isar). Specific content as follows, the sectioned tissue slides were deparaffinized by xylene three times for 5 minutes at room temperature, followed by treatment in alcohol series (100% isopropanol - 96% ethanol - 70% ethanol) twice each incubated for 3 minutes and then transferred to distilled water.

Following integrated deparaffination, cellular nucleus was dyed by incubating the section in Mayer's hematoxylin for 10 minutes at RT. Thereafter, the slides were

washed by tap water and transferred in distilled water. According to the protocol, the slides were incubated with acidified eosin. After renewed rinsing in distilled water, dehydration procedure was performed by alcohol series (ethanol 70% - 96% ethanol - 100%isopropanol) followed by xylene. Finally, the slides were mounted in Dako mounting medium (DAKO, Humburg, Germany) and covered with cover slips (Thermo Scientific™ Cover Slips, Thickness 1, Germany).

2.2.2 Elastica van Gieson (EvG) staining

The Elastica van Gieson staining (EvG) is a combination of elastica staining and van Gieson's staining, the former included Weigert's iron haematoxylin and the later is a mixture of picric acid and acid fuchsin. Collagen and elastin fractions are distinguished; generally, elastica van Gieson staining will result in the visualization of black-brown nuclei, black-stained elastic fibers, bright red-stained collagen and yellow-stained cytoplasm, muscle, fibrin and red blood cells.

Preparation for slides: The slides were incubated and dried at 56°C overnight.

Preparation for Weigert's iron haematoxylin: Equal parts of Weigert's solution A and Weigert's solutions B (Weigert's Hematoxylin Kit, Pharmacy, Klinikum rechts der Isar, München) were combined before use.

Preparation for van Gieson solution: Van Gieson was used to differentiate between collagen and smooth muscle and to evaluate the increase rate of collagen within AAA.

Procedure: The sectioned slides were initially deparaffinized by xylene twice for 10 minutes at RT, followed by alcohol series (100% isopropanol - 96% ethanol - 70% ethanol) twice, each incubated for five minutes and then transferred to distilled water. Subsequently, the nuclear staining was made in a Weigert's Hematoxylin solution for ten minutes and the slides were then rinsed with distilled water for ten minutes again. Furthermore, the cytoplasm staining was performed by incubating the samples in van Gieson solution for three minutes at RT. After a short moistened with distilled water, the procedure of dehydration was performed (70% ethanol- 96% ethanol -100% isopropanol), followed by a brief treatment with xylene. Finally, the slides were mounted using Dako mounting medium (DAKO) and covered with appropriate cover slips (Thermo Scientific™ Cover Slips, Thickness 1, Germany).

2.3 General Immuhistochemistry

In order to identify the individual cell types within each tissue sample, corresponding general immunohistochemistry using CD45 for leukocytes, CD3 for T-cells, CD68 for macrophages, CD34 for neovessels and Smooth muscle cells Myosin heavy chain 1+2

for SMCs was performed. For all immunohistochemical procedures carried out in this experimental study LSAB (LASB kit; DAKO, Humburg, Germany) was used and the recommended manufacturer's protocol was followed.

2.3.1 Pretreatment

All staining was performed on a 2 µm thin sections from AAA tissue and healthy aorta, which were fixed in formalin and embedded in paraffin (FFPE). The sectioned tissue was mounted on appropriate glass slides (SuperFrost Plus, VWR International, Darmstadt, Germany), incubated 56°C overnight, and deparaffinized by twice incubation for 10 minutes in xylene, followed again twice by alcohol series (100% isopropanol - 96% ethanol - 70% ethanol) each 5 minutes. Subsequently, the slides were transferred to distilled water.

The heat induced epitope retrieval was performed within this study. The slides were heated at 100°C under pressure for 7 minutes in sodium citrate solution (pH = 6; 2.1 g citrate monohydrate in 1000 ml distilled water).

2.3.2 Target antibodies for AAA

Depending on the target antigen, corresponding antibodies were selected and the recommended heat induced epitope retrieval methods were performed (**Table 5**).

Table 5. Antibodies performed for characterization of AAA.

Name	Dilution	Clone	Clone/ typing	Isotype	Corresponding cells	Method	Brand /Code
CD45	1:200	2B11+ PD7/26	Monoclonal Mouse	IgG1	T- and B- lymphocytes	LSAB	DAKO M0701
CD3	1:400	–	Polyclonal Rabbit	IgG	T- lymphocytes	LSAB	Abcam Ab5690
CD34	1:400	EP373Y	Monoclonal Rabbit	IgG	Endothelial cell/ neovascularization	LSAB	Abcam Ab81289
CD68	1:2000	Kb1	Monoclonal Mouse	IgG1	Macrophages/ monocytes	LSAB	DAKO M0184
MHCII	1:1000	–	Polyclonal Rabbit	IgG	Smooth muscle cells	LSAB	Abcam Ab53219

Note: MHCII, Myosin heavy chain 11

2.3.2 LSAB method

Labelled streptavidin-biotin immunohistochemistry assay (LSAB) method is one of the most common methods for immunohistochemical detection. The LSAB method is based on the high affinity of streptavidin to biotin. In this study, a universal DAKO LSAB kit and peroxidase (LSAB+ Kit, HRP; biotinylated goat anti-mouse/anti-rabbit; Dako, Germany) were used.

Procedures: Following antigen retrieval, all slides were retreated with 3% H_2O_2 solution and incubated for 15 minutes at RT. The slides were placed into a chamber and rinsed with one fold TRIS buffer for 3 minutes three times at RT. The 1x TRIS buffer were prepared from 10x TRIS buffer (pH = 7.6; 60.5 g Trizma base and 90 g NaCl in 1 liter distilled water, pH adjusted with HCl) and diluted in distilled water. Followed by one hour incubation with corresponding primary antibodies, appropriate/optimized dilutions were used as described in **table 5**; the slides were covered with 100 µL antibody solution and incubated at RT. During this procedure, all slides were kept in a humid environment to avoid-light chamber, followed by rinsing with 1x TRIS buffer 3 minutes for three times. Thereafter, all the slides were incubated with biotinylated secondary antibody (solution A, pink solution) for 25 minutes and streptavidin-peroxidase (solution B, yellow solution) for another 25 minutes at RT, followed by washing in one fold TRIS buffer 3 minutes for 3 times, respectively. Finally, the chromogenic visualization was performed by diaminobenzidine (DAB, solution C) and HRP substrate (solution D). Precisely, 15µL solution C dissolved in 750µL solution D, which was dropped onto the slides 100µL (C+D).

After the sufficient color development, the slides were rinsed with TRIS buffer 3 times and counterstained with hematoxylin for 20 seconds. Subsequently, a dehydration in alcohol series was performed (70% ethanol- 96% ethanol -100% isopropanol), followed by a brief treatment with xylene. Finally, the slides were mounted by Dako mounting medium (DAKO) and covered with appropriate cover slips (Thermo Scientific™ Cover Slips, Thickness 1, Germany).

2.4 Microcopy and histological assessment

All stained tissue samples (slides) were captured with a digital image capture device-Aperio ScanScope CS2 system (Aperio, Leica Biosystems GmbH, Germany) and magnified by Aperio Image Library software (Leica Biosystems GmbH, Germany) from department of Pathology (Klinikum rechts der Isar). Precisely, with five slides load capacity and 20x and 40x magnification the ScanScope CS2 was used in this study as digitalization image capture device.

For the conventional and standard staining, the histological classification was performed by characterizing vessel wall cellularity and degree of calcification. Subsequently, grade was assessed though baseline cell count and intensity of corresponding cells e.g. SMCs, elastin, collagen, infiltrates, macrophages, and neovascularization.

Histological evaluation: The quality of each slide was assessed two times independently as the follows: no staining (-), weak positive staining (+/-), scattered

positive staining (+), majority of positive staining (++), and strong overall positive staining (+++). These score analyses were performed for all cells within the vessel wall and for all specimens. In addition, for inter-related quality-evaluation between the above mentioned quality evaluation following scoring was used: +/++ and ++/+++.

Translate order of magnitudes: Light microscopic results were graded semi-quantitatively from 0 (to the corresponding no staining change) to +3 (to the corresponding strong staining change: +++). This histopathological grading was performed for endothelial cell, inflammatory infiltrate, collagenous and elastic fiber in the AAA tissue samples as well as in healthy aorta.

2.5 Immunohistochemistry of histone acetylation

Regarding to histone acetylation, IHC procedures were divided in two parts. One part concerned KATs and their expression at cellular level, whereas the other part concerned their corresponding substrates such as H3K9, H3K14 and H3K18, which are the most common substrates for KATs analyzed in this study.

2.5.1 Cellular localization of KATs in AAA and control determined by IHC

All staining procedures were performed on 2 µm thin sections from FFPE tissue samples of AAA and healthy aorta. To associate the expression of KATs with the individual cells within the aortic wall, consecutive sections were prepared accordingly to Reeps and co-workers [200]. Precisely, the consecutive slides from each specimen were prepared and incubated with the individual antibodies.

Depending on the target antigen, the corresponding antibodies as summarized in **table 6** were selected. Again, a heat epitope retrieval method was used. In all cases, one slide was stained with an antibody to detect the specific cell type (CD45, CD3, CD34, CD68, or MHCII) and a consecutive slide was stained with antibody against the KATs of interest (KAT2B, KAT3B, and KAT6B).

Table 6. Antibodies performed for KATs.

Antibodies	Dilution	Clone/ typing	Isotype	Method	Brand	Code
KAT2B	1:200	Polyclonal Rabbit	IgG	LSAB	Abcam	Ab96510
KAT3B	1:100	Polyclonal Rabbit	IgG	LSAB	Abcam	Ab61217
KAT6B	1:400	Polyclonal Rabbit	IgG	LSAB	Abcam	Ab58823

2.5.2 Acetylation of histone H3 substrates by IHC

All sliced tissue samples were pre-treated as those listed in the Chapter 2.5.1. Depending on the target antigen, corresponding antibodies were selected (**Table 7**). In

accordance with consecutive staining, one slide was stained with an antibody to detect the specific cell type (CD45, CD3, CD34, CD68, or MHCII) and a consecutive slide was stained with antibody against the KATs of interest (H3K9, H3K14, and H3K18).

Table 7. Antibodies performed for histone 3 substrate.

Antibodies	Dilution	Clone/ typing	Isotype	Method	Brand	Code
H3K9	1:1500	Polyclonal Rabbit	IgG	LSAB	Abcam	Ab4441
H3K14	1:1000	Monoclonal Rabbit	IgG	LSAB	Abcam	Ab52946
H3K18	1:1500	Polyclonal Rabbit	IgG	LSAB	Abcam	Ab1191

2.6 Gene expression analysis at mRNA level using RT-PCR

2.6.1 RNA extraction from FFPE tissue samples

RNA was isolated from FFPE tissue sections adjacent to slides used for histological characterization by the High Pure RNA Paraffin Kit (Roche, Mannheim, Germany) according to the manufacturer's instructions. In addition, the corresponding glass and microtome surface decontaminant (RNaseZap® Solution, USA) has been used in order to avoid RNA digestion/degradation.

Procedure: Two AAAs or healthy aorta tissues slices were obtained from FFPE blocks, each of 10 µm thickness, and transferred into a 1.5 ml clean and RNase-free Eppi tube (PCR tube, Eppendorf, Germany). The deparaffinization procedure was performed as follows: to each Eppi tube 800 µl Xylene was added, incubated 5 minutes at room temperature and mixed overhead during incubation several times. Then, the Xylene was replaced by 400 µl absolute ethanol, mixed and centrifuge for 4 minutes at 12000 rpm. The supernatant was discarded and add 1 ml absolute ethanol by overhead shaking followed by centrifuge for 4 minutes at 12000 rpm. The supernatant was then discarded and dried for 10-15 minutes at 55°C.

Extraction procedure was continued according to the instruction of the manufacturer's protocol (Roche) as follows: A mix with 10% SDS, Proteinase K (Vial 2, Roche Kit) and Lysis buffer (Bottle 1, Roche Kit) was prepared and added to the dried samples. The so pretreated samples were incubated overnight and additional Proteinase K (Vial 2, Roche Kit) was added again next day to completely dissolve the tissue. Proportional Binding buffer (Bottle 3, Roche Kit) and absolute ethanol were prepared and added to the High-Puffer-Filter-tube (Roche Kit), which were telescoped in the Collection-tube (Roche Kit). It was followed by several series of washing steps (washing buffer: Bottle 4 and Bottle 5, Roche Kit) and centrifugation, respectively. Subsequently, the Collection-tube was removed and the High-Puffer-Filter-tube was placed into a sterile Eppi tube. The samples were then incubated with Elution buffer (Vial 8, Roche Kit) and centrifuged again.

RNA was finally eluted in 60 µl of RNase-free water. The concentration and quality of RNA was measured with a Nanodrop 2000c spectrophotometer (peqlab, Erlangen, Germany). The A260/A280 ratio of more than 1.8 was considered high-quality RNA samples. Followed the measurement of RNA concentration, eluted RNA was directly used to synthesize cDNA or stored at -80°C until analysis.

2.6.2 cDNA synthesis

Total RNA was reverse-transcribed with M-MuLV reverse transcriptase and oligo-dT primer (cDNA Synthesis Kit RevertAid) according to the manufacture's instructions (Fermentas, St. Leon-Rot, Germany).

Procedure: Each time 11 µl of RNA was transferred into a RNase-free Eppi tube (PCR tube, Eppendorf, Germany). To each RNA sample 1µl Oligo (dT)18 primer was added, mixed gently, centrifuged briefly and incubated at 65°C for 5 minutes in order to resolve GC-rich RNA template. The following components were then added to each reaction tube: 4 µl of 5×Reaction Buffer, 1µl of RiboLock RNase Inhibitor, 2µl of 10 mM dNTP Mix, and 1µl ReverAid M-MuLV Reverse transcriptase,, mixed gently, briefly centrifuged and incubated for 60 minutes at 42°C. Subsequently, the reaction was terminated by heating at 70°C for 5 minutes. Finally, the reaction tubes contained 20 µl of cDNA in total, which were then further diluted to a final concentration of 10 ng/µl for each sample.

The cDNA, prepared as described above, was then directly used in RT-PCR applications or stored short-termed at -20°C.

2.6.3 Real-Time PCR

Quantification was performed by SYBR Green-based-PCR (peqlab) using StepOnePlus Real Time PCR-System (ABI) and the corresponding software.

Such real time polymerase chain reaction (Real-time PCR) is also called quantitative polymerase chain reaction (qPCR). In contrast to a conventional PCR, which is characterized by an end point analysis, the real-time PCR is a quantifiable method and amplified DNA or cDNA is detected as the reaction progresses in "real time". Real-time PCR technique that avoids disadvantage of conventional PCR to monitor final signals can either use specific fluorochromes (e.g. SYBR Green I) or hybridization probes (e.g. TaqMan probe). This technology has been widely used to monitor difference in mRNA expression level in cells or mRNA expression differences with different tissues or organs.

SYBR Green I dye binds all double stranded DNA (dsDNA). The detection of SYBR Green I dye was monitored though measuring the increase in fluorescent reaction

throughout the individual PCR cycles. In this study following SYBR Green I dye was used: KAPA^{TM}, SYBR$^{®}$ FAST qPCR MasterMix Universal (peqLab).

Most of primers used in this study were purchased from Qiagen (QuantiTect Primer Assay; Hilden, Germany) as primers already optimized for the corresponding mRNA expression product (**Table 8**). Because these primers are property of Qiagen, corresponding primer sequences cannot be provided.

Table 8. Primer used for real time PCR detection.

Gene	Name	Cat. No./ID	Amplicon (bp)	Gene bank Locus	Brand
KAT2A	Hs_KAT2A_1_SG	QT00067704	88	NM_021078	Qiagen
KAT2B	Hs_KAT2B_1_SG	QT00092267	149	NM_003884	Qiagen
KAT3A	CREBBP	qHsaCIP0033238	114	NG_009873	Biorad
KAT3B	Hs_EP300_1_SG	QT00094500	72	NM_001429	Qiagen
KAT4	TAF1	qHsaCED0034994	101	NG_012771	Biorad
KAT5	Hs_KAT5_1_SG	QT00096600	127	NM_182709	Qiagen
KAT6A	Hs_KAT6A_1_SG	QT00081984	145	NM_001099412	Qiagen
KAT6B	Hs_KAT6B_1_SG	QT00008638	102	NM_001256468	Qiagen
KAT7	Hs_KAT7_1_SG	QT00006132	78	NM_001199155	Qiagen
KAT8	Hs_KAT8_1_SG	QT00090636	94	NM_032188	Qiagen
KAT4	Hs_TAF1_1_SG	QT00027482	99	NM_138923	Qiagen
KAT12	GTF3C4	qHsaCID0015897	135	NT_035014.4	Biorad
CD45	Hs_LTK_2_SG	QT01665307	134	NM_001135685	Qiagen
CD3	Hs_CD3D_1_SG	QT00998214	72	NM_000732	Qiagen
MSR-1	Hs_MSR1_1_SG	QT00064141	91	NM_002445	Qiagen
SMTN	Hs_SMTN_1_SG	QT00026677	132	NM_001207017	Qiagen
MYH10	Hs_MYH10_1_SG	QT00005117	72	NM_001256012	Qiagen
MYH11	Hs_MYH11_1_SG	QT00069391	130	NM_001040113	Qiagen
VCAM-1	Hs_VCAM1_1_SG	QT00018347	106	NM_080682	Qiagen
Col. I	Hs_COL1A1_1_SG	QT00037793	118	NM_000088	Qiagen
GAPDH	Hs_GAPDH_1_SG	QT00079247	95	NM_002046	Qiagen

The rest of primers for gene KAT3A (CREBBP), KAT4 (TAF1), and KAT12 (FGIII90) were purchased from Biorad (PrimerPCR SYBRGreen Assay) as ready-to-use primer mix as demonstrated in **Table 8**. The corresponding primer sequences were also not available.

All PCR reactions were performed using the StepOnePlus device (Applied Biosystems/Life Technologies, Darmstadt, Germany). The PCR reaction designed as shown in **Table 9**. The PCR reactions were performed in 96-well plates (MicroAmp$^{®}$ Fast Optical 96-Well Reaction Plate, Applied Biosystems, Germany) and sealed with a specially adhesive sealing foil (Adhesive Sealing Tape for PCR, Sarstedt, Germany). The PCR plate was prepared as shown in **Figure 8**. In total, reaction volume of 25 µl for each real-time PCR per well was used.

Table 9. Protocol of loading RT-PCR reaction system.

Ingredient	Per reaction (µl)
SYBR® FAST qPCR MasterMix Universal	12.5µl
Water (sterile, DNase and RNase free)	8.5µl
Primer	2µl
cDNA	2µl

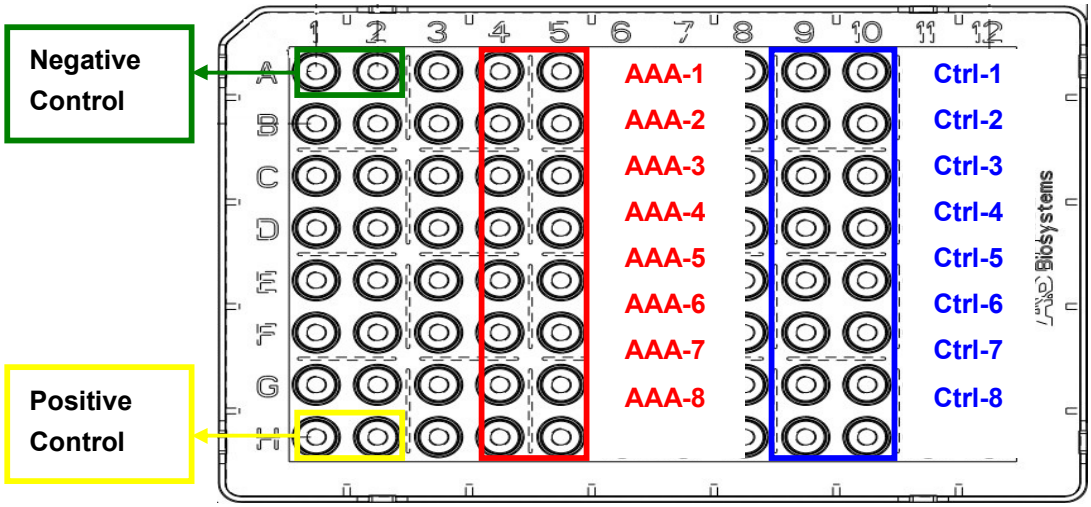

Figure 8. Sampling design for the SYBRGreen-based PCR reaction used in the present study. All PCR reactions were performed in 96-well plates in duplicates for each sample. Note: negative control is DNA- and RNA- free water replacing the cDNA. Positive control is known concentration of RNA from a selected AAA tissue sample, where the PCR reaction was working all the time. This positive control was also used to adjust all PCR plates at the same cycle threshold.

Each PCR reaction was performed in duplicates. After activation of the thermo-stable DNA polymerase at 95 °C for 5 minutes, the PCR reaction followed by further 45 cycles as shown in **Table 10**.

Table 10. Program and procedure of RT-PCR reaction system.

Temperature	Time	Purpose
95°C	30 seconds	denaturation
60°C	30 seconds	annealing
72°C	30 seconds	Primer Extension
77°C	15 seconds	Elimination of primer dimer

Data analysis of real-time PCR:

A non-template well reserved as negative control, which was replaced as sterile and RNase-DNase free water was used to prove the specificity of PCR reaction and to avoid or detect possible contamination. Normalization was performed for the house-keeping gene glyceraldehyde-3-phosphate dehydrogenase (GAPDH), which is an enzyme of glycolysis and is expressed in every cell of the human body constitutively widely at the same level. Furthermore, a selected control aortic RNA

(positive control, see also **Figure 8**) was used to compare the results of all samples and between the individual PCR plates.

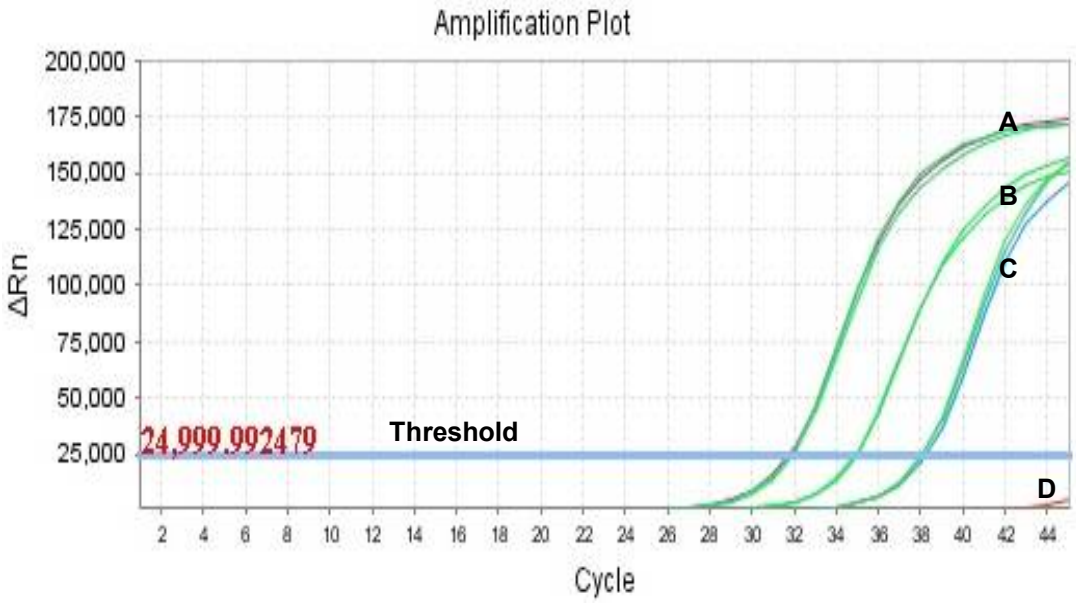

Figure 9. An example of the amplification plot of real-time PCR using KAT2A target mRNA and different study groups. In this view, the X-axis shows the number of cycles; the Y-axis shows Rn (The n PCR cycle of fluorescence signal intensity) minus the baseline-ΔRn. (A) is amplification curve of positive samples for KAT2A gene (Ct value is 32 approximately). (B) is amplification curve of AAAs group for KAT2A gene (Ct value is 35 approximately). (C) is amplification curve of healthy aorta group for KAT2A gene (Ct value is 38 approximately). (D) is amplification curve of negative substrate (equivalent water not cDNA) for KAT2A gene (Ct value is undetermined).

A widely used method to analyse relative gene expression is the comparative C_T value and describes as the $2^{-\Delta CT}$ method. The C_T value, also called threshold cycle, is the intersection between an amplification curve and a threshold (**Figure 9**). To compare the expression of target gene with GAPDH as control for normalization and the following formula was performed:

$$\text{Relative expression}=2^{-\Delta CT}=2^{CT(\text{housekeeping gene})-CT(\text{Target gene})}$$

Furthermore, to prove the quality and specificity of each PCR reaction, melting curve analysis was performed all time (**Figure 10**). Melting curve analysis is an assessment of the dissociation characteristics of double-stranded DNA during heating and is specific for the primer binding to cDNA product. Potential primer dimer or other unspecific DNA binding leads to the shift of the melting peak.

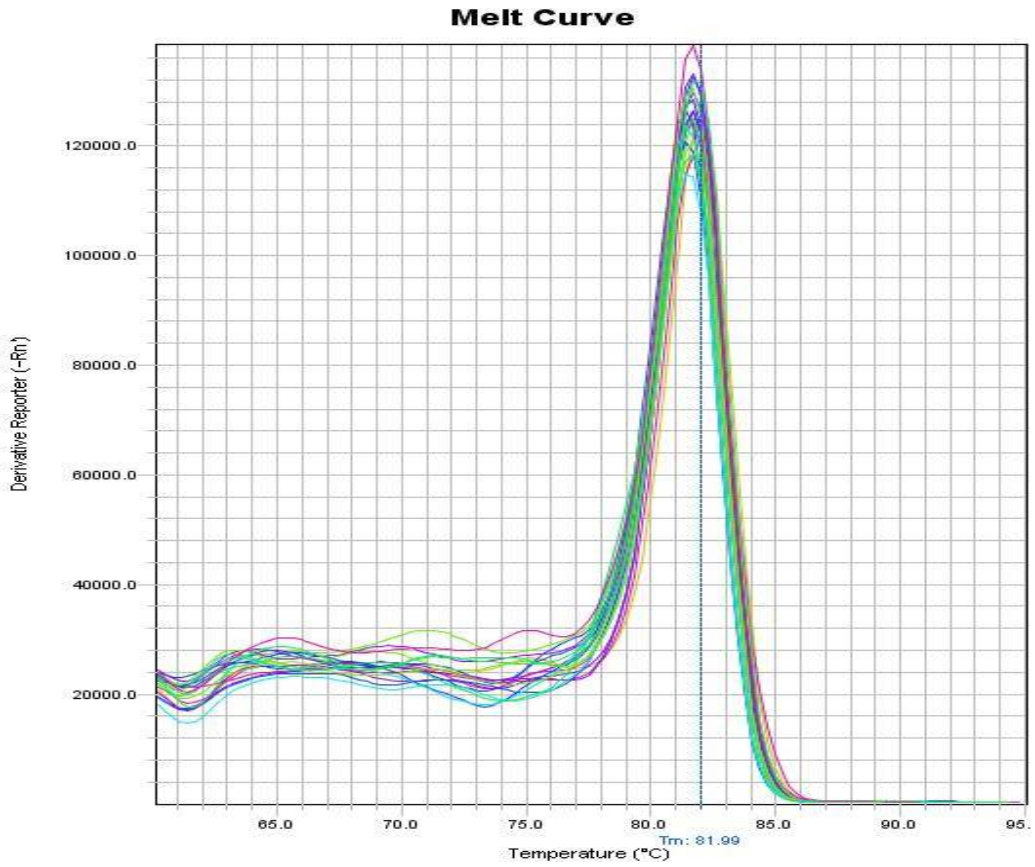

Figure 10. Melt curve example as a result for KAT2B generated within AAA group. In this view, the X-axis shows the temperature; the Y-axis shows derivative reporter. This graph showed the correlation between fluorescence and temperature during melting-curve analysis.

Due to the non-parametric distribution of the PCR results, a modified ΔC_T method was applied: $\Delta C_{Ti} = C_T(KATi) - C_T(GAPDHi)$ (i = corresponds to the individual samples 1 to n) and $2^{-\Delta CTn}$ was determined. These values from each study group were then tested for normal distribution. Because none of the samples was normal distributed, whiskers box plot was created for the ΔC_T values determining median with the 1th and 3th quartile as a variance (stable versus unstable carotid lesions), and $\Delta\Delta C_T$ (ΔC_T(unstable) - ΔC_T(stable)) was calculated comparing medians (non-parametric statistical tests) of the study groups for all factors analyzed in the study.

2.7 Western Blot

The western blot, also called immunobloting, is a widely used molecular biological technique to analyzed proteins of interest in an extracted tissue samples or cells. The critical points of this technique are including the following four aspects: (i) Following protein denaturation and treatment with sodium dodecyl sulfate (SDS), proteins are separated by gel electrophoresis according to their individual weight. (ii) Subsequently, the denatured proteins are transferred onto a special membrane (e.g. polyvinylidene fluoride (PVDF) or nitrocellulose). (iii) After transfer, the membrane

is treated with appropriate antibodies against the target protein by antigen-antibody reaction. (iv) Finally, using specific chemiluminescent indicator, the target protein is visualized as a band in an appropriate imaging system.

2.7.1 Protein preparation from tissue

2.7.1.1 Total protein extraction

The AAA and healthy aortic tissue were transferred to a mortar with liquid nitrogen and homogenized with a pestle (Sigma-Aldrich, Germany). The frozen tissue powder was quickly transferred into a 1.5 ml tube (Eppi tube, Eppendorf, Germany) and pretreated with a RIPA lysis buffer (**Table 11**). The miscible suspensions were incubated for 30 minutes on ice, followed by homogenate vortex for 20-30 second and centrifugation for 12,000 rpm at 4°C. The supernatant was transferred to a new 1.5 ml Eppi tube in order to determine protein concentration and frozen at -20°C until further analysis.

Table 11. The protocol of PIPA buffer for Western blot.

Tris-HCl	50mM	pH=7.5 with HCl
NaCl	150mM	-
NP-40	1% (v/v)	or 1% Triton X-100
SDS	0.1% (w/v)	-
Natriumdeoxdesoxychoat	0.5% (w/v)	-
Sodium azide	0.02% (w/v)	-

2.7.1.2 Histone extraction

Histone extraction was carried out using an EpiSeeker Histone Extraction kit (Abcam, ab113476, Cambridge, UK), according to the manufacturer's instructions. Pretreatment: Tissues were homogenized with a 1x Pre-Lysis buffer and centrifuged by 3000 rpm for 5 min at 4°C. Procedure: The supernatant was discarded, the tissue pellets were resuspended in Lysis Buffer (Histone Extraction Kit) and incubated on ice for 30 min. After centrifuging at 12,000 rpm for 5 min at 4°C, the supernatant was moved to a new 1.5 ml Eppi tube. Balance-Dithiothreitol (DTT) buffer was added at a ratio of 1:500 (1µl DTT solution + 500 µl of Balance Buffer) and 0.3 volumes of this balance-DTT buffer were added to the supernatant. The supernatant was transferred to a new 1.5 ml Eppi tube in order to determine the protein concentration and frozen at -20°C until analysis.

2.7.1.3 Protein quantification

Protein concentrations were determined using the enhanced BCA Protein Assay Kit (23225-Pierce® BCA Protein Assay Kit, Thermo Scientific, Germany). The reactions were performed in 96-well plates (96-Well Polystyrene Plates, Corner Notch, Thermo Scientific, Germany) in duplicates for each sample. Fifty parts of solution A and one

part solution B, totally 200 µl working solution, were added to each sample and the standard sample and incubated at 37°C for 30 minutes. The whole protein was quantified by device for OD value, with 280 nm Absorbance as the reference value. A very rough protein concentration can be obtained by making the assumption that the protein sample has an extinction coefficient of 1 (1 OD = 1 mg/ml protein).

2.7.2 Preparation polyacrylamide gel electrophoresis (PAGE)

Depending on the size of the target proteins, three different separation gels and same stacking gel were used. The following reagents (**Table 12**) were pipetted sequentially, and the polymerization was triggered with N,N,N',N'-Tetra-methylethylenediamene (TEMED) for separation gel. Subsequently, the separation gels were covered with absolute ethanol. After 20 minutes thepolymerization was terminated.

Table 12. Separation gel recipes.

Formulations	15%	10%	7.5%
Distilled water	2.400 ml	4.100 ml	4.900 ml
1.5M Tris-HCl, pH=8.8	2.500 ml	2.500 ml	2.500 ml
Acylamide, 30%	5.000 ml	3.300 ml	2.500 ml
SDS, 10%	0.100 ml	0.100 ml	0.100 ml
APS, 10%	0.050 ml	0.050 ml	0.050 ml
TEMED	0.005 ml	0.005 ml	0.005 ml

Furthermore, the following reagents were pipetted sequentially and the polymerization was triggered with TEMED still for stacking gel. The unmodified stacking gel was covered by a separation gel, the comb was inserted and kept for 20 minutes at RT to allow the complete polymerization. For the stacking gel, the composition was described in **Table 13**.

Aliquots of 30 µg were used from each protein sample, mixed with 2x Laemmli Buffer (0.0625M Tris-Cl (pH 6.8), 30% glycerol, 2% sodium dodecyl sulfate, 0.01% bromphenol blue) and denatured at 95°C for 5 minutes. Following short cooling on ice, the protein samples were then loaded into stacking gels.

Table 13. Stacking gel recipe.

Formulations	5% Stacking gel
Distilled water	2.750 ml
0.5M Tris-HCl, pH=6.8	1.250 ml
Acylamide, 30%	0.850 ml
SDS, 10%	0.050 ml
APS, 10%	0.025 ml
TEMED	0.005 ml

2.7.3 Procedure of electrophoresis

Electrophoresis chamber (Mini-PROTEAN Tetra Cell for Mini Precast Gels, Bio-Rad Laboratories GmbH, Germany) was prepared adding appropriate Electrophoresis buffer (3.03 g Trizma base, 14.4 g glycine and 1.0 g SDS in 1000 ml distilled water). The prestained marker (IV, peqlab, Germany) and the denaturated protein samples were then loaded into the wells of the polymerized gel (**Figure 11**). The electrophoretic run through the stacking gel was carried out firstly at 100 V (approx. 60 mA) for about 20 minutes. As soon as the proteins achieved the separating gel, the run was continued at 200 V for at least 40 minutes.

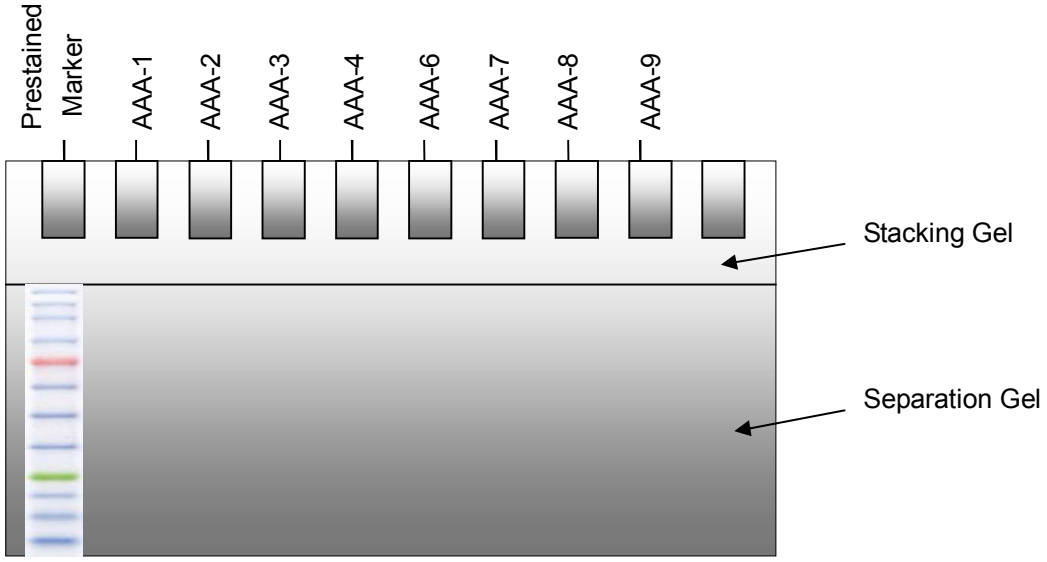

Figure 11. Sampling design program of Stacking gel and Separation gel system.

2.7.4 Blotting

After the electrophoresis was finished, the separated proteins were transferred onto a PVDF membrane. The protein transfer was performed either in 10% methanol containing Transfer Buffer (3.03 g Trizma base, 14.4 g Glycine and 100 ml methanol in 900 ml distilled water) for large molecular weight proteins, or in 15% methanol containing Transfer Buffer (3.03 g Trizma base, 14.4 g Glycine and 150 ml methanol in 850 ml distilled water) for small molecular weight proteins. The PVDF membrane was shortly activated in a pure methanol before transfer and the gel together with several filter papers were equilibrated in the corresponding Transfer Buffer described above (**Figure 12**). The semi-dry transfer device (Trans-Blot® SD Semi-Dry Electrophoretic Transfer Cell, Bio-Rad Laboratories GmbH, Germany) was used to transfer protein onto the PVDF membrane. For small molecular weight protein 10V for 60 min were applied. The wet transfer device (Mini Trans-Blot® Cell, Bio-Rad Laboratories GmbH, Germany) was used for large molecular weight protein overnight.

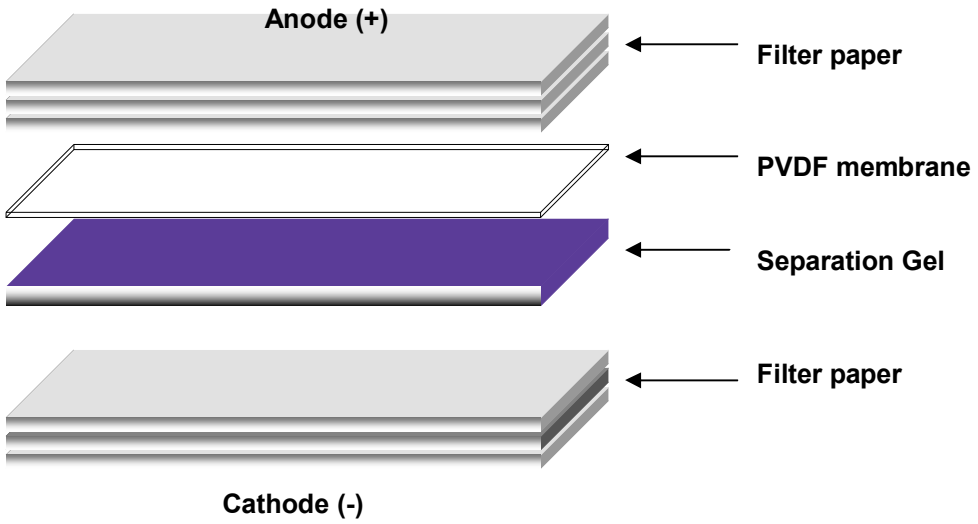

Figure 12. Assembling of transfer sandwich.

To control the protein separation, the gel was treated with Coomassie Brilliant Blue solution (0.5mg Coomassie Brilliant Blue, 50 ml methanol, 10 ml acetic acid in 40 ml distilled water) following the protein transfer. Furthermore, the PVDF membrane was prestained with Ponceau-S solution.

2.7.5 Immunoblot

Membranes containing target proteins were blocked in 1x Blocking Buffer (5% fat-free and skimmed milk powder in TBS Buffer) for one hour at room temperature at slow shacking. The TBS Buffer included 2.42 g Trizma base, 8.0 g NaCl in 800 ml distilled water, and adjust pH value to 7.6 with HCl (2N) filled to 1000 ml by distilled water.

The PVDF membrane containing the desired proteins was incubated with the primary antibody detecting KATs, H3 substrate and GAPDH at 4°C overnight. Each antibody was diluted in 1x Blocking Buffer and followed by one hour incubation for GAPDH and overnight incubation for KATs and H3, respectively. Regarding corresponding primary antibodies, appropriate dilutions were used as described in **Table 14** and **Table 15**.

Table 14. Antibodies used for KATs.

Antibodies	Dilution	Clone/ typing	Isotyoe	Size (kDa)	Brand	Code
KAT2B	1:1000	Polyclonal Rabbit	IgG	93	Abcam	Ab96510
KAT3B	1:1000	Polyclonal Rabbit	IgG	290	Abcam	Ab61217
KAT6B	1:1000	Polyclonal Rabbit	IgG	231	Abcam	Ab58823
GAPDH	1:1000	Monoclonal Rabbit	IgG1	36	Abcam	Ab8245

Table 15. Antibodies used for H3 substrate.

Antibodies	Dilution	Clone/ typing	Isotyoe	Size (kDa)	Brand	Code
H3K9	1:1000	Polyclonal Rabbit	IgG	17	Abcam	Ab4441
H3K14	1:500	Monoclonal Rabbit	IgG	17	Abcam	Ab52946
H3K18	1:1000	Polyclonal Rabbit	IgG	17	Abcam	Ab1191

2.7.7 Protein detection

Membranes were rinsed with TBS Buffer three times and incubated with HRP-conjugated secondary antibody Buffer (antibody diluted by Blocking Buffer) for one hour at room temperature. Proteins were visualized with an ECL working solution (Solution A: Solution B is 1:1) of SuperSignal ® West Pico Chemiluminescent Substrate (Thermo Scientific, Bonn, Germany).

The PVDF membrane was exposed to FUJI Medical X-Ray Film (FUJI film Europe GmbH, Germany), and Films were processed with a Medical Film Processor (SRX-10A, Konica Minolta Medical and Graphic Imaging Europe GmbH, Germany).

Protein quantification:
Protein quantification was performed by analyzing the band intensities of each sample for the same amount of protein using free software ImageJ 1.44p (National Institutes of Health, USA) [201] and normalized for the band intensity of the expression of GAPDH.

Briefly: The western blot radiogram was scanned and saved as a TIFF file. In the ImageJ program the image was cropped so that it included just the gel and then using Gel Analyzer Options. A rectangle was drawn around the individual protein lanes, the background threshold was adjusted and plot lanes analysis was performed. The resulted values are a measure of the relative density of each peak, compared to the standard, which will obviously have a relative density of 1, corrected for background. In order to test for significant differences between the study groups, first the relative density of each target protein was corrected/normalized for the relative density of GAPDH and then the fold-change value (between a control samples and AAA tissue specimens) was determined.

2.8 Statistical analysis

The data obtained in the present work were first tested for a normal distribution assessed by the One-Sample Kolmogorov-Smirnov test. Normal distributed samples were analyzed using independent t-test for n=2 and ANOVA test for n>2. Non-parametric data were analyzed by Mann-Whitney-U-test for n=2 and Kruskal-Wallis for n>2. For categorical variables, such as gender, smoking history,

hypertension, diabetes and coronary disease, comparison between groups was done using a Chi-quadrate (χ^2) test. Continuous data in RT-PCR results are presented as mean±SD. The two groups were tested by homogeneity of variances, after which the differences between groups were tested by repeated measurements using One-way ANOVA. In all cases, a value of $P<0.05$ was set as the threshold for significance. Correlations between continuous or categorical variables were quantified by using Spearman's rank correlation coefficient. The analyses were performed using SPSS version 16.0 (SPSS Inc., Chicago, IL, USA).

3. RESULTS

3.1 Characterization of study subjects

3.1.1 Characteristics (demographic data) of the AAA patients

The experimental study group included 37 patients (30 male, 7 female) who underwent elective open surgical repair of infrarenal abdominal aortic aneurysm. The youngest AAA subject was 40 years and the oldest 87 years old. The average age was 66.8 ± 11.4 years. The mean maximum diameter of abdominal aortic aneurysm was 62.8 ± 16.7 mm. Eighty-one percent of AAA patients had hypertension, 29.7% were smokers. In addition, forty-one percent suffered from hyperlipidemia and only one AAA patient (2.7%) was diagnosed with diabetes mellitus and one individual had chronic kidney disease (2.7%). The baseline characteristics of the AAA patients are summarized in **Table 16**.

3.1.2 Characteristics of the control group

As control subjects, twelve healthy abdominal aorta tissues (kidney transplant donor of abdominal aorta from the Department of Trauma Surgery) were included. The youngest control subject was 21 years old and the oldest 86 years old. The average age was 59.2 ± 19.4 years. None of the control subjects had any obvious atherosclerotic changes within the aortic wall assessed by light microscopy. The only visible changes in the aortic wall morphology were the slightly enlarged intima (**Table 16**).

Regarding comparison of the study groups (AAA patients versus healthy control subjects) as shown in **Table 16**, no significant differences were observed in gender (P=0.111). Furthermore, the study groups were also matched with regard to the age (P=0.057). In this context, it is to mention that it is very difficult to obtain control healthy aortic samples.

Table 16. Characteristics of study subjects.

Variable	AAA group		Control group		*P* value
No. of subjects	37		12		
	n*	N	n*	N	
Male	30 (81.1)	37	7 (58.3)	12	0.111[#]
Rupture	7 (18.9)	37	-	-	-
Age (Yr)	66.8±11.4	37	59.2±19.4	12	0.057[†]
Max AAA diameter (mm)	62.8±16.7	37	-	-	-
Morbidities					
Hypertension	30 (81.1)	37	-	-	-
Diabetes mellitus	1 (2.7)	37	-	-	-
Hypercholesterolemia	1 (2.7)	37	-	-	-
Hyperlipidemia	15 (40.5)	37	-	-	-
Smoking	11 (29.7)	37	-	-	-
Chronic kidney disease	1 (2.7)	37	-	-	-
Medication					
ASA+Clopid	30 (83.3)	36	-	-	-
Beta blocker	22 (61.1)	36	-	-	-
ACE-I	15 (41.7)	36	-	-	-
Statins	22 (61.1)	36	-	-	-
Antihypertensives	7 (20.0)	35	-	-	-
Diuretics	14 (38.9)	36	-	-	-
Laboratory indexes					
hsCRP (mg/dl)	4.7±6.7	14	-	-	-
Fibrinogen (mg/dl)	620.5±245.7	6	-	-	-
Urea (mg/dl)	22.3±9.6	33	-	-	-
Creatinine (mg/dl)	1.4±1.0	37	-	-	-
Creatinkinase (U/l)	418.2±1531.4	25	-	-	-
Leukocytes (1000/µl)	9.3±4.1	37	-	-	-
Erythrocytes (Mio./µl)	4.5±0.7	37	-	-	-
Thrombocytes (1000/µl)	247.1±99.7	37	-	-	-
Hemoglobin (g/dl)	13.8±5.2	37	-	-	-
Hematocrit (%)	38.7±6.1	37	-	-	-
MCH (pg)	29.4±2.6	36	-	-	-
MCV (fl)	87.7±5.8	36	-	-	-
MCHC (g/dl)	33.5±1.4	36	-	-	-
Sodium (mmol/l)	139.3±3.6	36	-	-	-
Potassium (mmol/l)	4.6±0.5	37	-	-	-

Note: [#]Chi-square test and values in parentheses are *percentages. †: The result of age data for two groups (Shapiro-Wilk test: *P*=0.951 for AAA group and *P*=0.587 for control group) was normally distributed, therefore, T-test was performed. ASA: acetyl salicilic acid. hsCRP: high sensitivity C reactive protein. MCH: mean corpuscular hemoglobin. MCV: mean corpuscular volume. MCHC: mean corpuscular hemoglobin concentration.

3.2 Histological and immunohistochemical characterization of tissue specimens

3.2.1 General morphology assessment using H&E staining

Healthy aortic tissue:
First, hematoxylin and eosin (HE) staining was performed to assess the morphology and cellular composition of the aortic wall (**Figure 13**). Healthy infrarenal abdominal aorta of the control subjects included three intact parts of the vessel wall, tunica-intima, tunica-media and tunica-adventitia. The tunica-intima of the aorta was smooth with an intact layer of endothelial cells and almost no inflammatory cells and no atherosclerotic plaque formation were observed. The only visible changes between the individual tissue samples of these control study subjects were found to be the variability in the thickness of the intima layer.

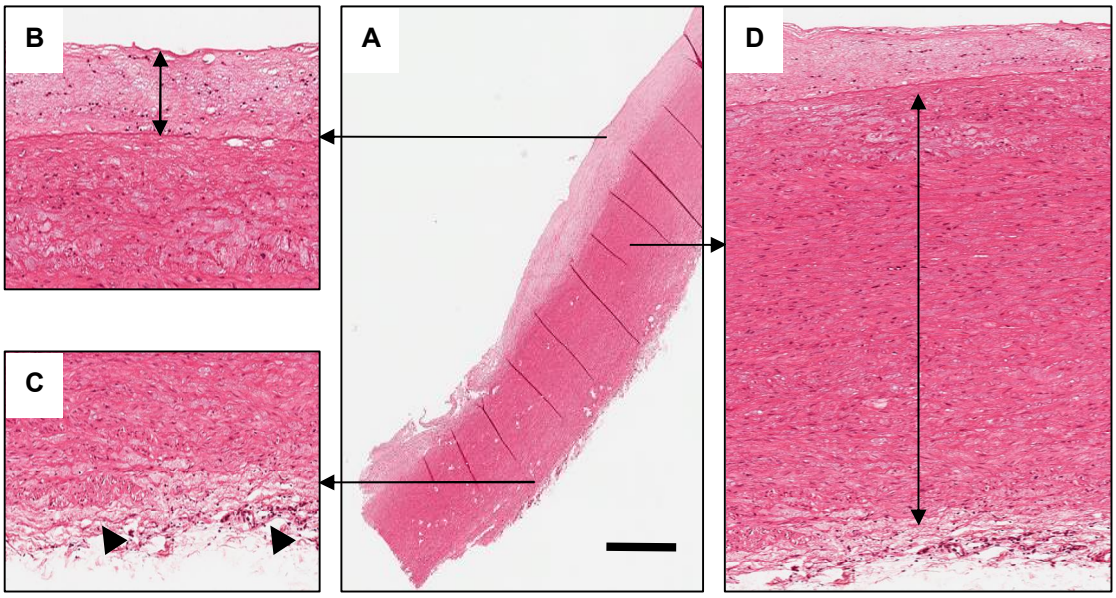

Figure 13. An example of morphology of healthy aortic wall used in this study (HE staining). (A) Overview image of the segmental infrarenal abdominal aorta (scale bar represents 1 mm). (B) The tunica-intima (double-headed arrow) consists of a monolayer of endothelial cells in close apposition to a thick continuous internal elastic lamina (original magnification x 10). (C) A network of vasa vasorum (arrowheads) was detected throughout the tunica-adventitia (original magnification x 10). (D) The tunica-media (double-headed arrow) consists of vascular smooth muscle, collagen and elastic fibers (original magnification x 4).

AAA tissue:
Histological characterization of AAA tissue showed that pathophysiological processes in the infrarenal abdominal aortic aneurysm involved all three layers of the aortic wall, comparing with those demonstrated in healthy abdominal aortic tissue (**Figure 14**). The histological HE staining of abdominal aortic aneurysm was associated with a considerable thickening of tunica-intima, which was frequently colocalized with

infiltrated inflammatory cells. In addition, enlarged tunica-intima coexists with massive aggregates of extracellular lipids even atherosclerotic plaque. Furthermore, enhanced neovascularization (**Figure 14D**) was observed mainly in the tunica-media and partially also in the intimal layer. Neovessels were predominantly associated with inflammatory infiltrates (**Figure 14C**).

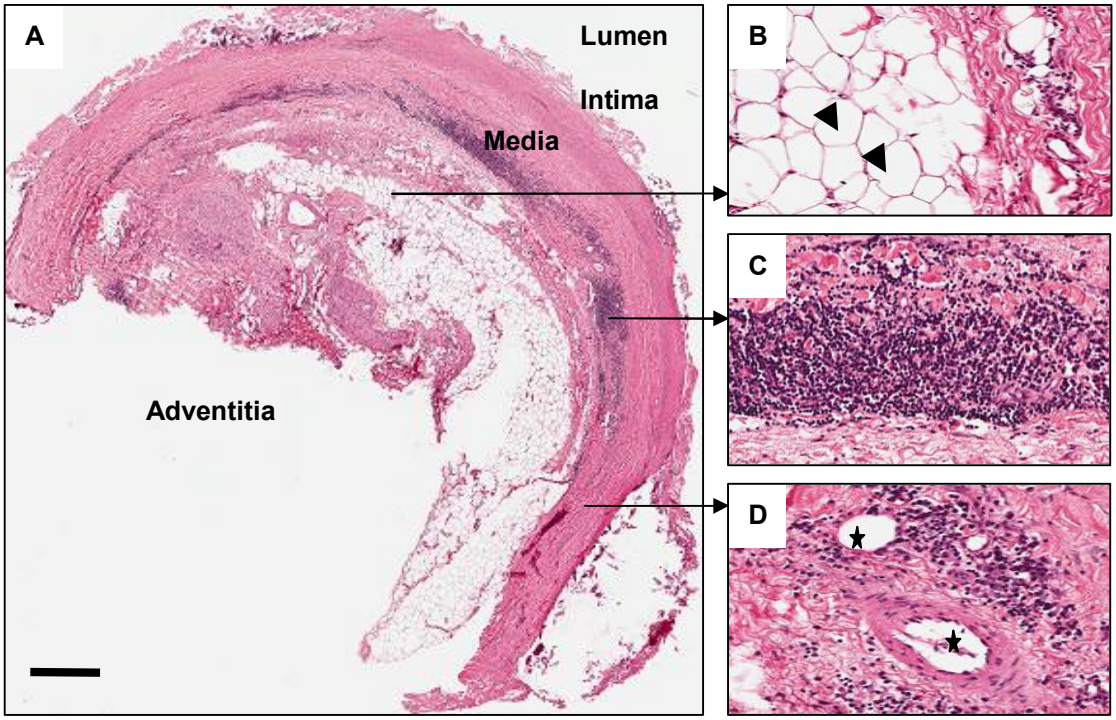

Figure 14. An example image of a typical histopathology of diseased AAA wall used in this study (HE staining). (A) Overview image of the segmental infrarenal abdominal aorta aneurysm (scale bar represents 1 mm). (B) Cholesterol crystals and inflammatory foam cells (arrows) within the adventitia, (C) Infiltration/Accumulation of Inflammatory cells in the deeper part of tunica-media (often conterminous with adventitia), (D) Neovascularization (asterisks), frequently associated with inflammation. B-D original magnification x 20.

3.2.2 Elastic and collagen fibers assessment using EvG staining

Healthy aorta tissue:
Elastic van Gieson (EvG) staining was performed to identify the extracellular composition and pathomorphology of aortic wall with regard to collagen and elastin (**Figure 15A and 15B**). Light microscopic findings demonstrated that collagen fibers in healthy aorta were arranged regularly and well defined elastic lamina of tunica-media was observed, associated with the collagen.

AAA tissue:
In contrast to healthy aorta, the EvG staining in AAA wall demonstrated by widely degenerated tunica-media containing disorganized and fractured collagen fibers. Light microscopic findings showed furthermore significant degradation of extracellular elastic fibers. In addition, an increased collagen volume fraction of AAA was detected

in the histological sections (**Figure 15C and 15D**).

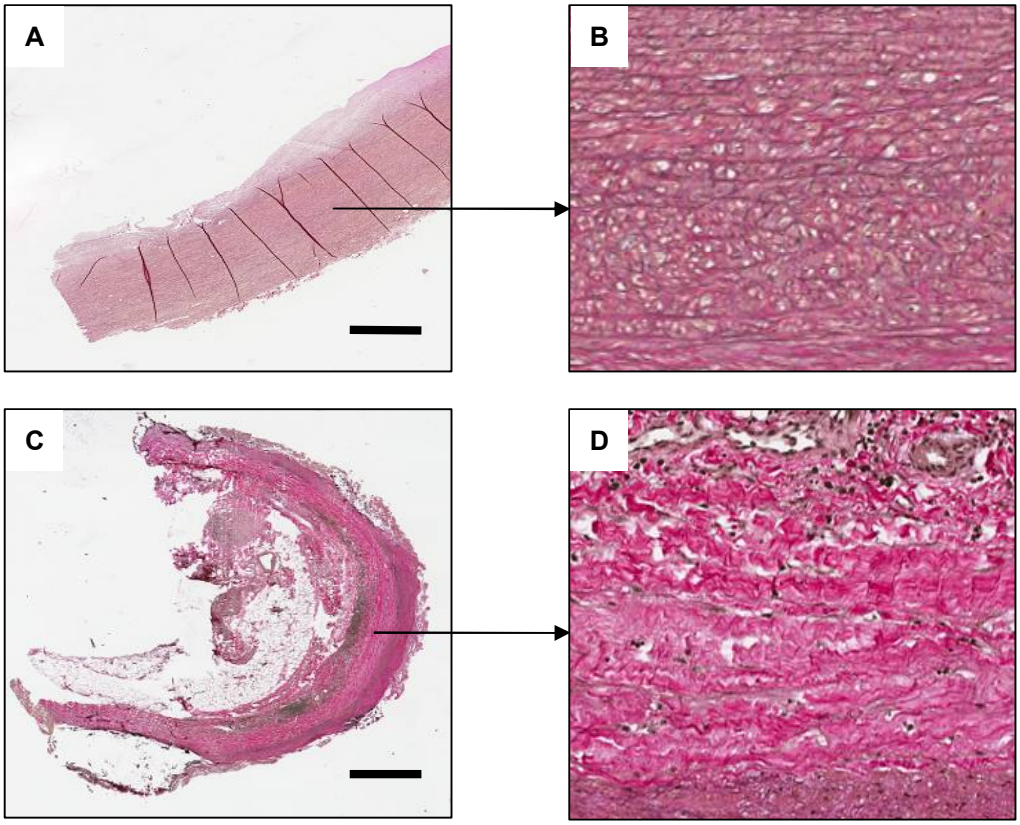

Figure 15. Representative images of healthy abdominal aorta (A, B) and AAA wall (C, D) using elastic van Gieson (EvG) staining. (A and B) The healthy aortic tissue showed compact media with well organized collagen and elastic fibers, free of neovessels and inflammatory cells. (C and D) AAA wall demonstrated disorganized and heterogeneous distribution of collagen and only few fragmented elastic fibers. A and C: scale bar represents 1 mm, B and D: original magnification x 20.

3.2.3 Inflammatory cells in aortic wall - Leukocytes

For the detection of inflammatory leukocytes, the CD45 antibody was used that reacts with the CD45 leukocyte common antigen (LCA), a common marker of human white blood cells [202]. It is expressed particularly in T and B lymphocytes.

AAA tissue:
Former studies of human AAA tissues indicated that inflammation is a critical element in aneurismal pathology [203]. In the present study, extensive inflammatory infiltrates were also detected in AAA wall in contrast to healthy aorta, where only few scattered leukocytes were detected in adventitia (data not shown). The immunohistochemical results showed that especially the tunica-media and tunica-adventitia were infiltrated by these mononuclear lymphocytes (**Figure 16A and 16B**). Furthermore, leukocytes were frequently associated with neovessels and were found at the border between adventitia and media.

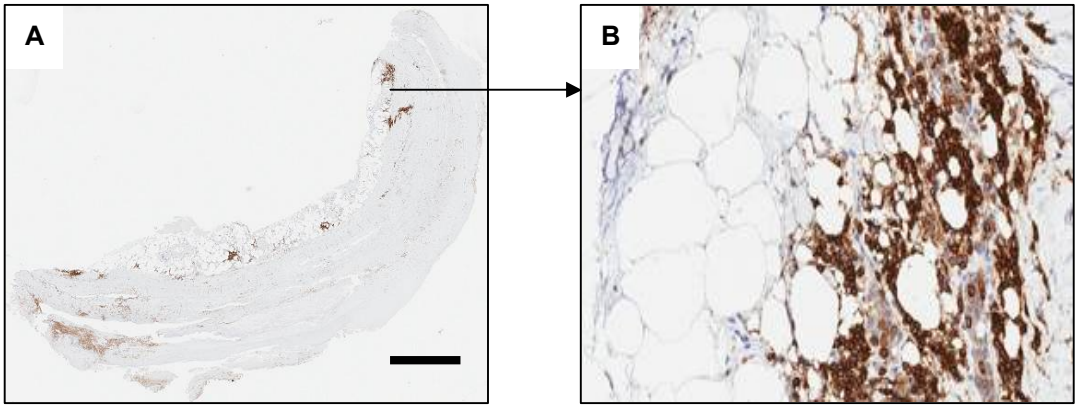

Figure 16. An example of immunohistochemical staining of leukocytes in AAA wall using CD45 antibody. Predominantly tunica-media and tunica-adventitia were infiltrated by these mononuclear lymphocytes. (A) Scale bar demonstrates 1 mm, (B) original magnification x 20.

3.2.4 Inflammatory cells in aortic wall - Leukocytes - Macrophages

Macrophages as well as leukocytes are the most common inflammatory cells in AAA wall. Therefore, in this study macrophages were identified using the CD68 antibody. CD68 is a well known marker of macrophages, monocytes, and macrophages-derived foam cells. Besides, it is especially useful as a marker for the various cells of the macrophage lineage [204].

AAA tissue:
The CD68 positive cells were located in the atherosclerotic areas mainly in the extended intima of the AAA wall and at the border between intima and media (**Figure 17A and 17B**). In contrast to leukocytes, the occurrence of macrophages was not so apparent and abundant. Furthermore, macrophages were not found in deeper parts of the aortic wall but mainly in the intima or within the upper parts of media. They were mainly associated with atherosclerotic plaques within AAA.

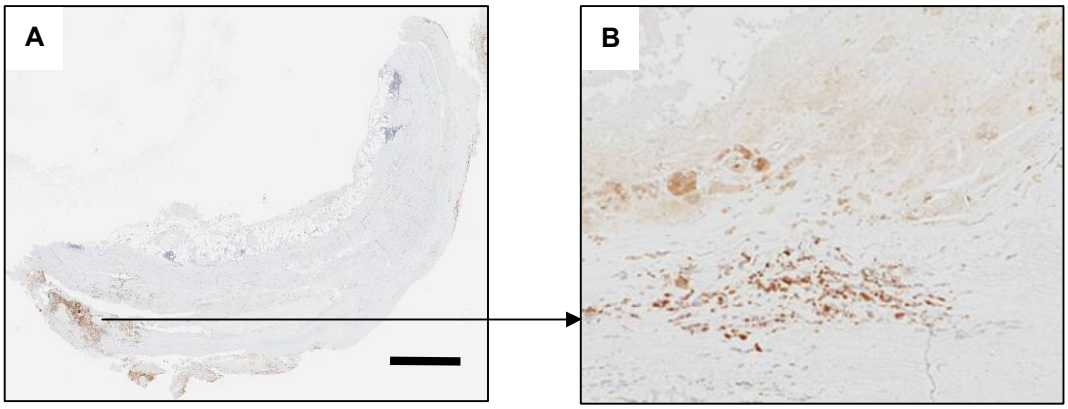

Figure 17. An example of immunohistochemical staining of macrophages in AAA wall using CD68 antibody. Predominantly tunica-intima and tunica-media were infiltrated by these macrophages and were associated with atherosclerotic plaques. (A) Scale bar shows 1 mm, (B) original magnification x 20.

3.2.5 Smooth muscle cells (SMCs) assessment

For detection of SMCs an antibody against Myosin heavy chain 1 and 2 was used (MHCII = Myosin heavy chain 11). Myosin heavy chain is highly conserved among vertebrates and is ubiquitously expressed in human smooth muscle rather than in striated muscle within vasculature. The SMCs (MHCII) antibody used in this study does not cross react with myosin of non muscle tissue. Furthermore, this antibody was selected because it is able to detect contractile and synthetic phenotype of SMCs.

Healthy aorta tissue:
The results demonstrated an expected histology of healthy aortic wall. The smooth muscle cells were located mainly in the tunica-media of the healthy aorta and were arranged in parallel with collagen and elastin fibers (**Figure 18A and 18B**).

AAA tissue:
Light microscopic findings of AAA tissue specimens showed significant reduction in the number of vascular smooth muscle cells in comparison to healthy aorta. The arrangement of SMCs was quite heterogeneous and not circularly in parallel layers as in control tissue. Furthermore, the dissociation from collagen was frequently observed. Moreover, some of the neovessels located in media or at the border between media and adventitia were also surrounded by smooth muscle cells (**Figure 18C and 18D**).

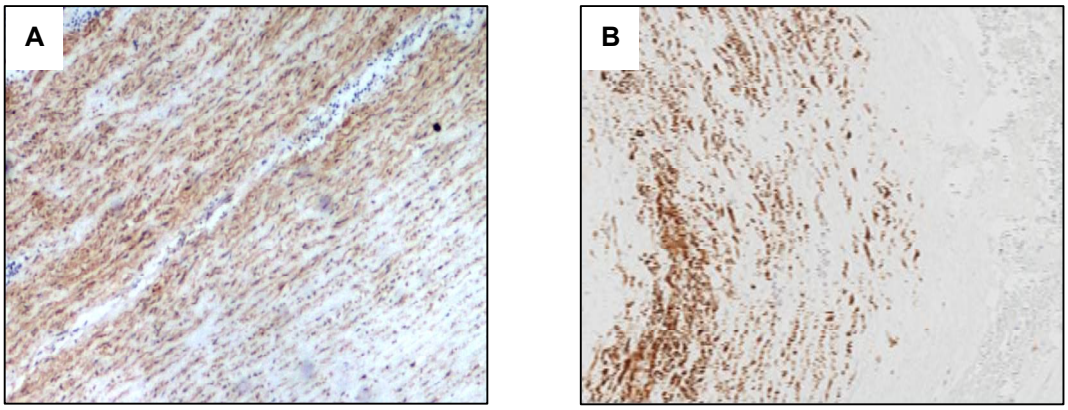

Figure 18. An example of SMCs staining using smooth muscle Myosin heavy chain 11 in the healthy aorta (A) and AAA (B). In healthy aorta SMCs were located and well organized mainly in media (original magnification x 20). In contrast, SMCs in AAA were discontinuous and scattered heterogeneously throughout the AAA wall (original magnification x 20).

3.2.6 Neovascularization-CD34

The standard staining procedure with CD34 antibody does not detect all ECs. It has been described previously that the human hemopoietic stem cell maker CD34 is a good endothelial marker of ECs, especially for angiogenesis, therefore CD34 was used to evaluate the extend of neovascularization within AAA [205].

AAA tissue:
An increase in medial neovascularization was detected in biopsies of abdominal aortic aneurysmal tissue (**Figure 19A**). Neovessels were found in the deeper parts of the media and at the border between media and adventitia. These neovessels were widely associated with inflammatory cells and contained only the endothelial layer independent of their size (**Figure 19B**) assuming their instability or fragility. Furthermore, scattered neovessels were found also in adventitia. These neovessels contained often and additional stabilizing layers of SMCs and were seldom accompanied by inflammation. There was almost no positive staining for neovessels in the atherosclerotic areas, which means that few neovessels are detectable in the atherosclerotic intima.

In contrast to AAA tissues samples, almost no CD34 positive staining was observed in healthy aorta tissue. For this reason, the staining of CD34 of the control study group is not shown in this study.

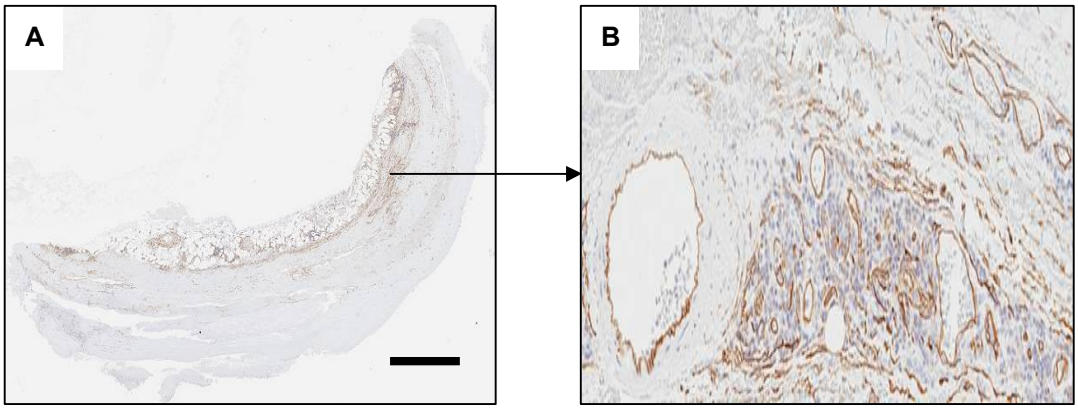

Figure 19. An example of neovascularization in human AAA wall using CD34 staining. (A) Conspicuous neovascularization, especially within media and at the border to adventitia was accompanied by accumulation of inflammatory cells (scale bar corresponds to 1 mm). (B) Higher magnification (original magnification x 20) showing plethora of neovessels at the border between media and adventitia accompanied with inflammatory cells (blue).

3.2.7 Semi-quantitative grading of the histopathology of AAA

To assess the extension of the individual histopathological features in AAA wall, a semi-quantitative histological characterization of all AAA tissue samples was performed (**Table 17**). Furthermore, to compare the histopathological features of AAA with a healthy aorta, the semi-quantitative scoring was done also in the control group. Because controls tissue samples showed the same results regarding the scoring, **Table 17** contain only one example of the histological characterization of the control group (ctrl), as shown in the last row of the **Table 17**.

Table 17. Overview of the classification of the AAA group.

Patient	Cellularity (HE)	Collagen (EvG)	Elastin (EvG)	Infiltrates (CD45)	Macrophages (CD68)	SMCs (MHCII)	Neovessel (CD34)
1	++	++	+	++/+++	+	+	++/+++
2	+	+/++	+/-	++/+++	+	+/-	++
3	+	+/++	+/-	++/+++	+/-	+	+/++
4	+	++	+/-	+	+/-	++	++
5	++	+++	+	+++	-/+	+	++
6	++	++	+/-	++/+++	-/+	++/+++	++/+++
7	+/++	++/+++	+/++	+	+ (+/-)	+++	+/-
8	+++	++/+++	+/++	++	+	+++	++/+++
9	+++	+/++	+/++	+/-	-	+++	+/++
10	+++	+++	+/-	+++	+	++/+++	+++
11	+/++	++/+++	+/-	++++	+ (+/-)	+/++	+++
12	+/-	++	+/-	+	-/+	+ (+/++)	++/+++
13	++	+/++	-/+	++	+/-	++	++
14	+	++/+++	+/-	+	-/+	++/+++	+/-
15	++	+/++	+	+++	+	+/++	+++
16	+/++	++/+++	-/+	++/+++	+/++	+ (+/-)	++/+++
17	+	++/+++	++	++	+	++	++
18	+	+	+/-	+/++	+ (+/++)	++	+ (+/++)
19	+	+/++	+/++	+++	+ (+/-)	+ (+/++)	++/+++
20	+/++	++	-	+/-	-/+	++/+++	-/+
21	++	++	+/-	++	-/+	+	+
22	+	++/+++	-/+	+/++	-/+	+/-	+/++
23	++	+++	+/++	+/-	-	+++!	+/-
24	+	+++	+	+/++	-/+	-/+	+
25	+/++	++	+/-	+++	+	+	++/+++
26	+/++	++	+/-	+/++	++	+ (+/-)	+/++
27	+	++	-/+	++	++	+	++
28	++	+++	+	++	+/++	+/++ (+)	+++
29	+/-	+/++	-/+	+/-	+	+/-	-/+
30	+/-	+/++	+/-	+/++	+ (+/++)	+/++	-/+
31	+	+/++	-	++/+++	+ (+/-)	++	+/++
32	+/++	++	+/-	++++	++	++ (+/++)	+/++
33	+	++	+	+/++	+	+/++	+
34	+/++	+/++	+/-	+/++	+	++	+
35	+	++/+++	+	+	+ (+/++)	+/++	+/-
36	+	+	+/-	++	++ (++/+++)	+/-	+/-
37	++	+++	+/-	+/++	+ (+/-)	++/+++	+
Ctrl	++	+++	+++	-	-	+++	-

Note: Ctrl is healthy aorta tissue group.

3.3 Analysis of histone acetylation at mRNA level

Following a detailed characterization of the study objects, the histone acetylation within AAA was approached. The transfer of acetyl functional group on the histone lysine residues is accomplished by histone acetyltransferases (HATs). Therefore, as first steps to evaluate the changes in histone acetylation in AAA in comparison to healthy aorta, the expression of these HATs was analyzed at mRNA level. A total of 37 AAAs and 12 healthy aorta tissues were studied for the individual genes by the RT-PCR method using SYBR Green fluorescence dye and optimized PCR conditions were used to avoid primer dimer. In addition, the quality of all PCR reactions was proved by melting curve analysis. Gene expression was normalized to the expression of GAPDH.

3.3.1 Expression of HATs at mRNA level

To investigate the expression profiles of HATs in AAA (n=37) and normal controls (n=12) aorta tissues, mRNA levels of HATs (**Table 3**) were evaluated by quantitative real-time PCR. For better understanding and in accordance to the nomenclature of human histone acetyltransferases (HATs), the HATs analyzed in our study were named KATs (lysine[K]-histone acetyltranserases) (**Table 3**).

3.3.1.1 GNAT family

Following the quantitative Real-Time-PCR and data collection, first the Kolmogorov-Smirnov test (K-S test) for normal distribution was applied. For KAT2A, the expression could not be detected in the healthy aortic tissue (**Figure 20A**). In contrast, in AAA KAT2A was measured in all AAA specimens. The P value from the K-S test was 0.174, revealing that the data were normal distributed. For KAT2B, expression at mRNA level was detected in both, control aorta and AAA tissue. Test for normality showed P values of 0.200 and 0.193, again the data were normal distributed. Therefore, data was analyzed using *t*-test. For both histone acetyl transferases, KAT2A (**Figure 20A**) and KAT2B (**Figure 20B**), the mRNA levels were significantly higher in AAA than in control group ($P<0.001$ and $P<0.001$, respectively).

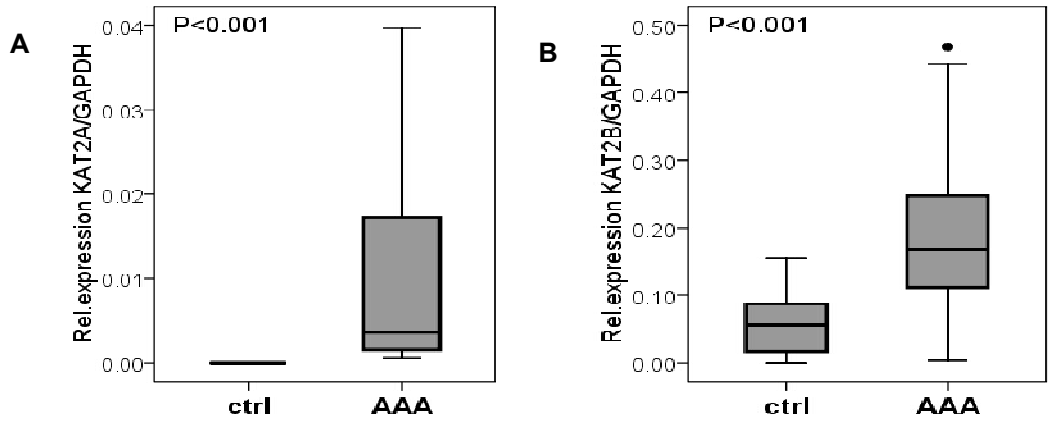

Figure 20. Expression of KAT2A (A) and KAT2B (B) at mRNA level in the AAA tissue samples compared with the control healthy aorta, analyzed by quantitative real time PCR and SYBR green fluorescence dye. AAA, abdominal aortic aneurysm; ctrl, healthy aorta tissue. Data are normalized to the expression of GAPDH and show x-fold decrease in comparison to that of the house-keeping gene.

3.3.1.2 CBP/P300 family

Normal distribution of these data was not found using the normality test and distribution curve (K-S test). For KAT3A (**Figure 21A**), its expression was not detected in healthy control samples, only in AAA wall. Kolmogorov-Smirnov test for AAA group achieved P value of 0.017. For KAT3B, the same test showed P values of 0.002 for control group and less than 0.001 for AAA group, respectively. Thus, the samples were not normal distributed and Mann-Whitney-U-test was used for comparison. The expression of the second group of HATs, the CBP/P300 family in biopsy tissues from abdominal aortic aneurysm (AAA, n=37) patients was significantly increased compared to that from normal controls (Ctrl, n=12) (P<0.001 for KAT3A in **Figure 21A** and P=0.007 for KAT3B in **Figure 21B**).

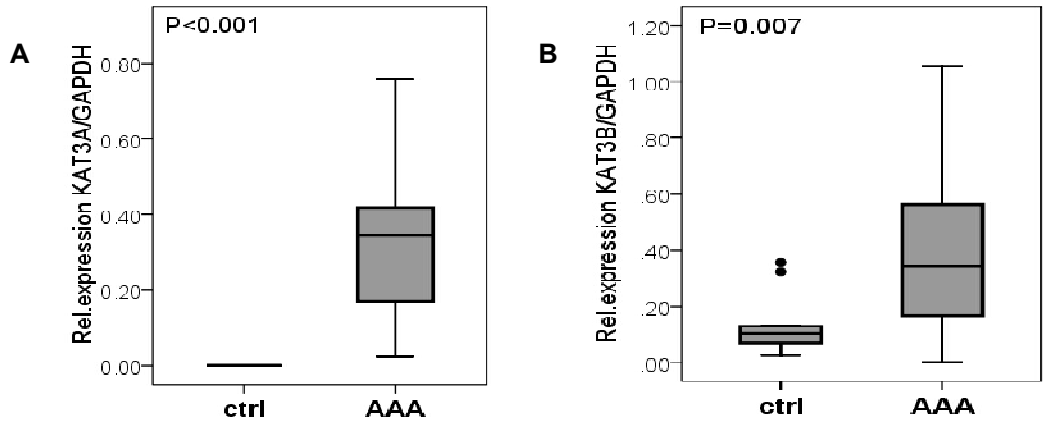

Figure 21. Expression of KAT3A (A) and KAT3B (B) at mRNA level in the AAA tissue samples compared with the control healthy aorta samples, as analyzed by quantitative real time PCR and SYBR green fluorescence dye. AAA, abdominal aortic aneurysm; Ctrl, healthy aorta tissue. Data are normalized for the expression of GAPDH.

3.3.1.3 MYST family

The normality tests of RT-PCR data for MYST family are shown in **Table 18**. In accordance with the distribution, corresponding Mann-Whitney or *t*-test was performed. The expression of KAT6B was significantly increased in AAA group compared to healthy aorta group and was the strongest expression observed among the MYST family of KATs within the AAA group. The mRNA level of KAT5, KAT6A, KAT7 and KAT8 were 67-fold, 6.9-fold, 113-fold and 6.3 fold less expressed than that of mRNA level of KAT6B among the AAA group (**Figure 22**).

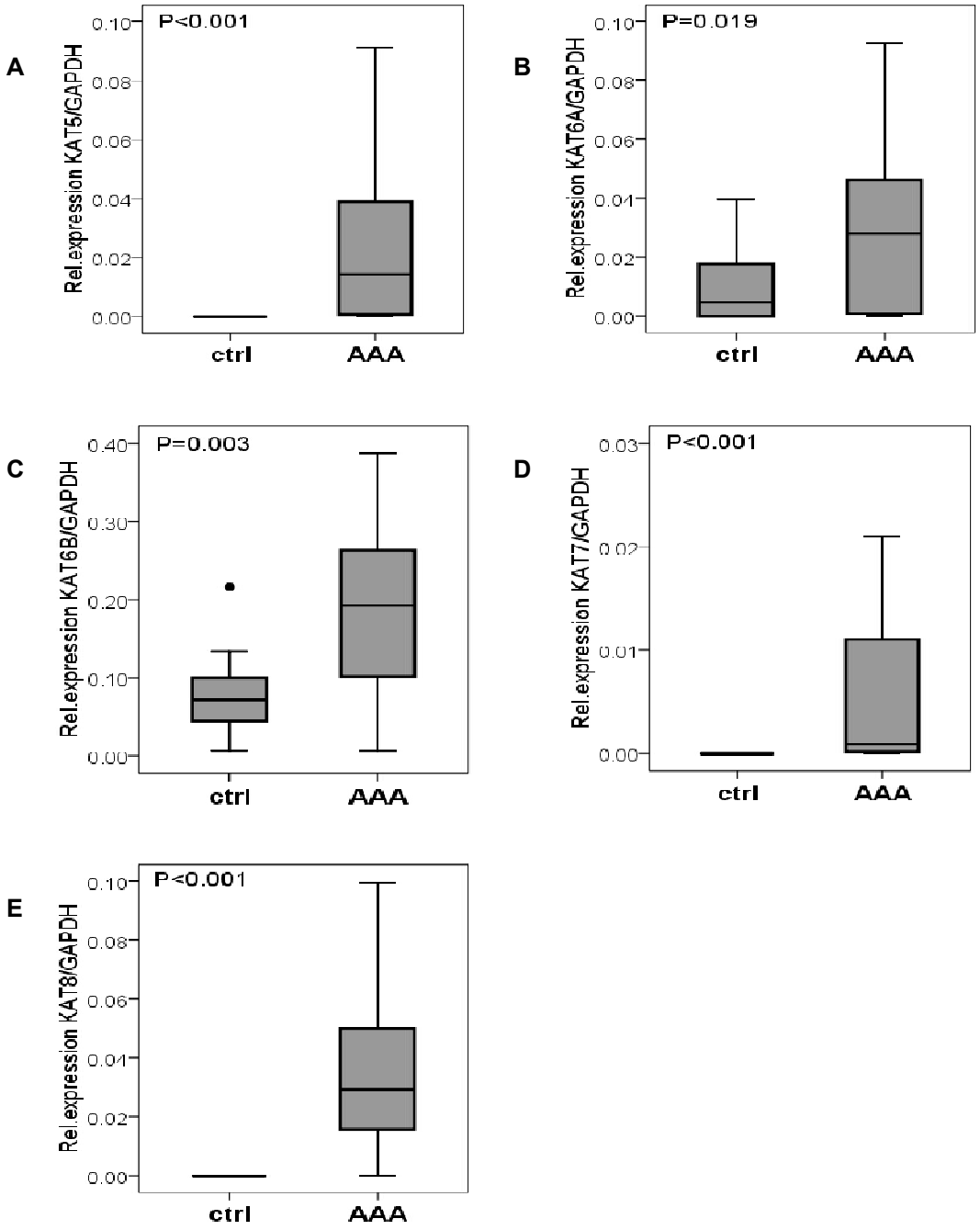

Figure 22. Expression of KAT5 (A), KAT6A (B), KAT6B (C), KAT7 (D) and KAT8 (E) at m RNA level in the AAA tissue samples compared with the control healthy aorta, analyzed by quantitative real time PCR. AAA, abdominal aortic aneurysm; Ctrl, healthy aorta tissue.

Table 18. Normality test results of RT-PCR data for MYST family.

Normality test	Control group		AAA group		test
	expression	P	expression	P	
KAT5	undet	NC	0.0177	<0.001	Mann-Whitney
KAT6A	0.0177	0.139	0.0280	0.059	*t*-test
KAT6B	0.0694	0.200	0.1930	0.200	*t*-test
KAT7	undet	NC	0.0017	<0.001	Mann-Whitney
KAT8	undet	NC	0.0307	<0.001	Mann-Whitney

Note: undet=undetermined, NC=not calculated.

3.3.1.4 TF-related Family

For the TF-related family of KATs normal distribution of the individual values for each acetyltransferases was detected. For KAT4, the P value was 0.002 for control group and 0.007 for AAA group, respectively. So Mann-Whitney was used for comparison. Interestingly, in contrast to the other families of HATs, the mRNA level of KAT4 was 2.21-fold stronger expressed in the controls than in the AAA group (P=0.002) (**Figure 23A**). No expression at mRNA level, whether in AAA or in control group was found for KAT12 (**Figure 23B**).

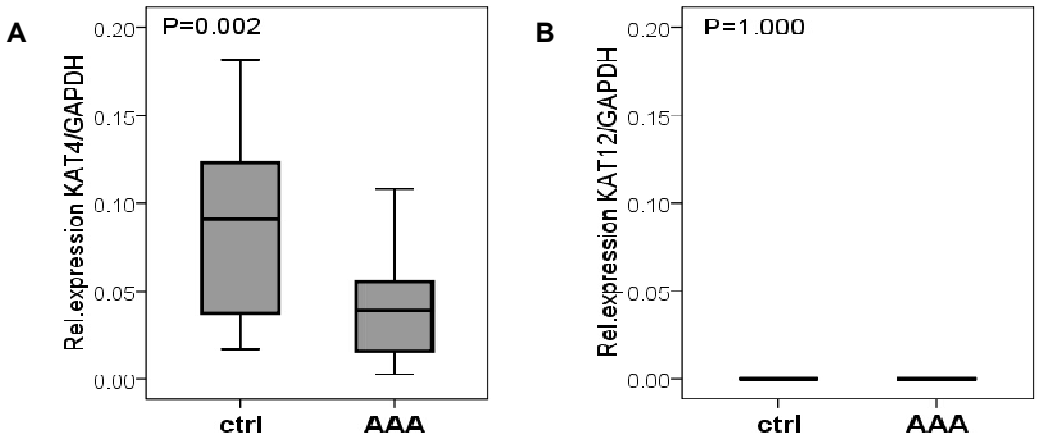

Figure 23. Expression of KAT4 (A) and KAT12 (B) at mRNA level in the AAA tissue samples compared with the control healthy aorta samples, as analyzed by quantitative real time PCR. AAA, abdominal aortic aneurysm; Ctrl, healthy aorta tissue.

3.3.1.5 Summary of expression analysis of KATs

The overview of the expression profiles of KATs in AAAs and healthy aorta tissue samples at mRNA level analyzed in this study is summarized in **Table 19**. As already mentioned above, the individual values demonstrate a relative expression at mRNA level related to the expression of the house keeping gene for GAPDH and thus displays the x-fold expression of GAPDH.

Table 19. Expression of KATs at mRNA level.

Family	KATs	AAA group	Healthy aorta group	*P value
GNAT	KAT2A	0.0042	undet	<0.001[t]
	KAT2B	0.1673	0.0663	<0.001[t]
CBP/P300	KAT3A	0.3451	undet	<0.001[u]
	KAT3B	0.343	0.0894	0.007[u]
MYST	KAT5	0.0177	undet	<0.001[u]
	KAT6A	0.028	0.0177	0.019[t]
	KAT6B	0.193	0.0694	0.003[t]
	KAT7	0.0017	undet	<0.001[u]
	KAT8	0.0307	undet	<0.001[u]
TF-related	KAT4	0.0389	0.0677	0.002[u]
	KAT12	undet	undet	1.000

Note: *P-values show statistical differences in expression between AAA tissue samples and healthy control aorta using either *t*-test (t) for normal distributed samples or non-parametric Mann-Whitney-U-test (u). Undet: expression was not detected.

3.3.2 Expression of markers representing individual cells within AAA at mRNA level

The next goal of the study was to associate the expression of KATs with the cells localized in AAA. Because we were not able to extract individual cells existing within the aortic wall, the expression of the KATs analyzed in this study was correlated with the cells within AAA indirectly by evaluation of the expression of specific markers of these cells. The most common cells in AAA are: SMCs, inflammatory cells such as T-and B-cells and macrophages and endothelial cells [200].

Therefore, representative markers of these cells were selected and their expression at mRNA level analyzed accordingly to correlate their expression with the expression of KATs. Following markers were used for inflammatory cells: CD45 for both T- and B-cells, CD3 for T-cells, and MSR1 as a surface scavenger receptor of macrophages. For SMCs, because in AAA two different forms of smooth muscle cells may exist, namely synthetic and contractile phenotype, markers specific for these individual cell types were used: smoothelin (SMTN) and SM myosin heavy chain (SM-MHC, MYH11) representing the contractile phenotype, SMemb/non-muscle MHCB (MYH10) and collagen I representing the synthetic phenotype [206]. Furthermore, the expression of vascular cell adhesion molecule-1 (VCAM-1) as a representative marker of endothelial cells and neovascularization was analyzed as well.

To obtain an overview of the expression levels of the above described markers representing the individual cells, the expression data at mRNA level are summarized in **Figure 24**. The MYH11 demonstrated the highest expression in AAAs. In contrast, the lowest expression was observed for SMTN, which was about 200-fold lower than

the expression of MYH11. Because the aim was to correlate the expression of KATs in the individual cells within AAA, the analysis of these markers was omitted in the healthy aortic tissue samples. Furthermore, in controls, inflammatory cells are not present or uncommon, the comparison between AAA and control would not show any interesting data.

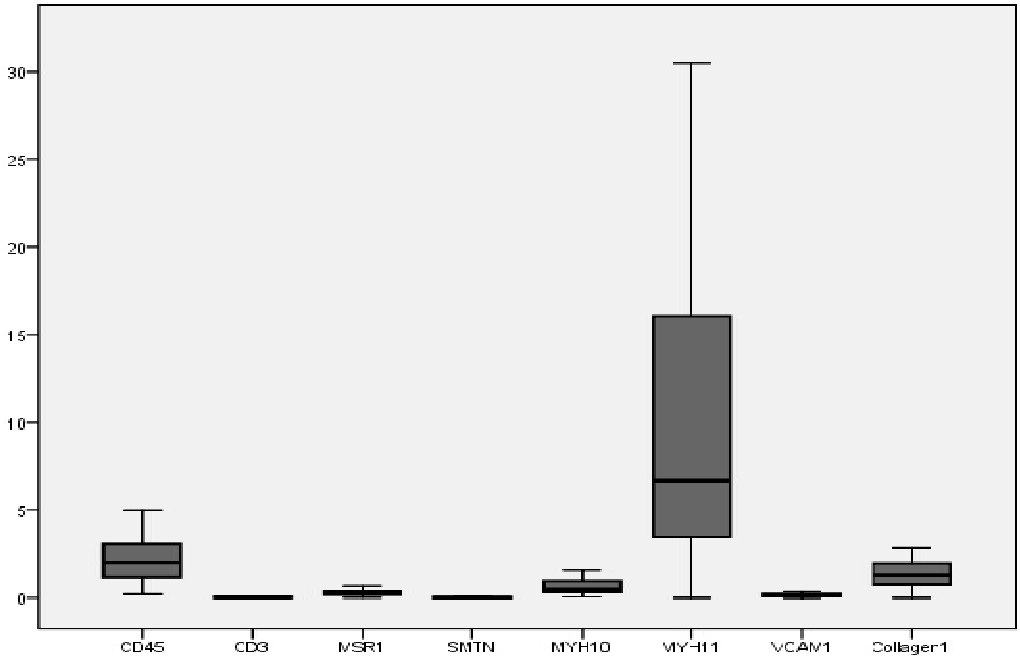

Figure 24. An overview of expression of markers of cells located within AAA: CD45, CD3, MSR1, SMTN, MYH10, MYH11, VCAM-1 and Collagen I. Analysis was performed by quantitative real-time PCR and SYBR Green fluorescence dye, normalized against the expression of GAPDH.

3.3.3 Correlation analysis

In the evaluation of the expression of KATs in different cells located within AAA, various correlations analyses were performed from the data collected as described above using markers representing individual cells and also with regard to the histological classifications of the AAA tissue samples.

3.3.3.1 Correlation between expressions of interclass KATs in AAA

First, all individual KATs were examined for correlations with each other using the Spearman's rang correlation coefficient due to the heterogeneous distribution of the experimental data (**Table 20**). The results demonstrated that KAT2B was significantly correlated with KAT3A, KAT3B and KAT6B (r=0.705; P<0.001, r=0.564; P=0.001 and r=0.528; P=0.007, respectively), and KAT5 with KAT8 (r=0.443, P=0.001). In addition, KAT6B correlated significantly with KAT3A, KAT3B and KAT6A (r=0.407, r=0.500 and r=0.531; P<0.05 in all cases) (**Figure 25)**.

Table 20. Correlations between individual KATs analyzed in the study using Spearman rank correlation coefficient.

r	KAT2A	KAT2B	KAT3A	KAT3B	KAT5	KAT6A	KAT6B	KAT7	KAT8	KAT4
KAT2A	-	n.c.	n.c.	n.c.	n.c.	n.c.	n.c.	n.c.	n.c.	n.c.
KAT2B		-	0.705***	0.564**	n.c.	n.c.	0.528**	n.c.	n.c.	n.c.
KAT3A			-	n.c.	n.c.	n.c.	0.407*	n.c.	n.c.	n.c.
KAT3B				-	n.c.	n.c.	0.500**	n.c.	0.342*	n.c.
KAT5					-	n.c.	n.c.	0.357*	0.443**	n.c.
KAT6A						-	0.531**	n.c.	n.c.	n.c.
KAT6B							-	n.c.	n.c.	n.c.
KAT7								-	n.c.	n.c.
KAT8									-	0.648**
KAT4										-

Note: * Significant (p <0.05), ** highly significant (p <0.01), *** highly significant (p <0.001)

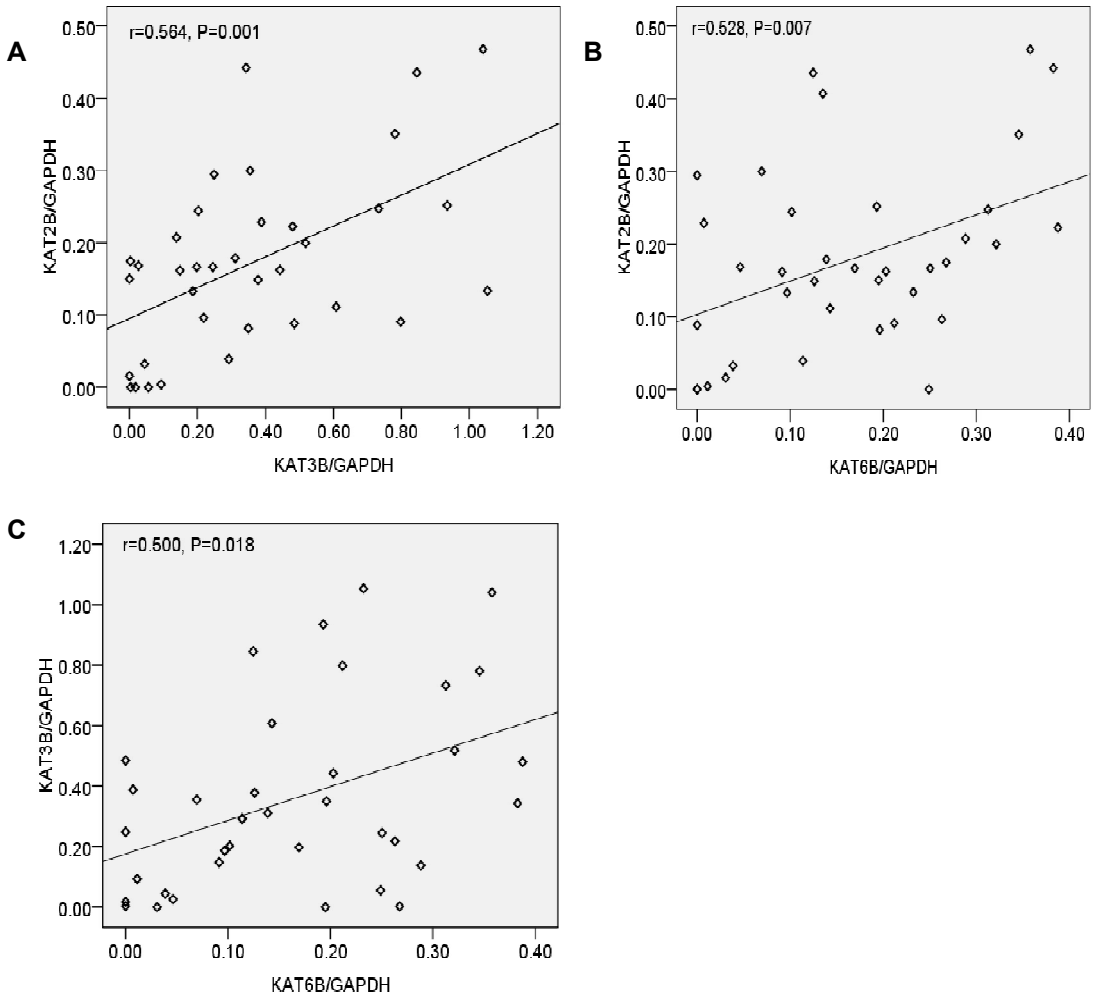

Figure 25. Selected positive correlations between the expressions of individual histone acetyltransferase at mRNA level in the AAA group. Correlations shown in Figure are between KAT2B and KAT3B (A); KAT2B and KAT6B (B); KAT3B and KAT6B (C).

3.3.3.2 Correlation between expression of KATs and AAA histology

The semi-quantitative histological characterization and the results of RT-PCR were analyzed again by calculating of the Spearman's rank correlation coefficient in order to explore any relationships between mRNA level and the morphology within AAA.

Several significantly positive correlations between the histological and immunohistochemical classification and mRNA level expression of KATs were observed. First, neovascularization level was positively associated with mRNA level of KAT5 and KAT7 (r=0.487, P=0.003 and r=0.531, P=0.002, respectively). Furthermore, a significant positive correlation was found between the amount of smooth muscle cells and expression of KAT2A (r=0.425, P=0.014). Beyond that, no significant correlation was detected between the other histological assessments and the expression of KATs (**Table 21**).

Table 21. Correlations between expressions of KATs and histology of AAAs using Spearman rank correlation coefficient.

r	Infiltrates	Neovessel	Collagen	Elastin	Macrophages	SMCs
KAT2A	.105	.186	-.144	-.067	-.246	.425*
KAT2B	-.160	-.154	-.056	.104	-.251	-.223
KAT3A	-.156	-.061	-.163	.054	-.314	-.342
KAT3B	-.057	-.063	.147	.025	-.020	.042
KAT5	.147	.487**	.095	-.037	.089	-.098
KAT6A	.066	.009	-.066	.146	-.014	.306
KAT6B	.112	.324	-.038	.117	-.034	-.249
KAT7	.295	.531**	-.007	-.065	.294	.145
KAT8	-.148	.166	.069	-.201	-.072	.255
KAT4	.002	.255	-.067	-.324	-.202	-.089

Note: * P <0.05, ** P<0.01, *** P<0.001.

3.3.3.3 Correlation between expression of KATs and markers representing the individual cells within AAA

In order to address the relationship between mRNA level of KATs and markers representing the individual cells within AAA, correlation analysis was performed between the expression of KATs and the expression of specific markers for the individual cells: CD45, CD3, MSR1, SMTN, MYH11, MYH10, collagen I and VCAM-1 (**Table 22**).

The correlation analyses of expression of the representative markers for inflammatory cells, which are CD45 for T- and B-cells, CD3 for T-cells and MSR1 for macrophages, and the individual KATs demonstrated that KAT3B seemed to be associated with all inflammatory cells, correlating with CD45, CD3, as well as MSR1 (r=0.339, P=0.039;

r=0.361, P=0.028 and *r*=0.351, P=0.032, respectively). The results are illustrated in **Figure 26A, 26B and 26C**. Furthermore, strong correlation was seen between KAT6B and CD45 or CD3 (*r*=0.609, P<0.001 for CD45 and *r*=0.553, P<0.001 for CD3, respectively) (**Figure 26D and 26E)**.

In addition, a strong negative correlation was detected between expression of KAT2A and expression of collagen I at mRNA level (*r*= -0.528, P<0.001). Furthermore, correlation coefficient of *r*=0.541 (P<0.001) provided a good measure of the strength of the relationship between KAT6A and expression of vascular cell adhesion molecule-1 (VCAM-1).

Table 22. Correlation analyses of the expression between individual KATs evaluated in this study and specific markers for cells localized within AAAs using Spearman rank correlation coefficient.

r	CD45	CD3	MSR1	SMTN	MYH10	MYH11	VCAM1	Coll I
KAT2A	-.196	.088	.002	.083	.228	-.081	-.083	-.528***
KAT2B	.323	.217	.388*	.267	.286	.271	.486**	.293
KAT3A	.396*	.106	.223	.152	.031	.211	.290	.250
KAT3B	.339*	.361*	.351*	.063	.171	.082	.264	.267
KAT5	.378*	.190	.136	.064	-.077	-.131	-.125	-.005
KAT6A	.171	.389*	-.085	.163	.425**	.180	.541***	.240
KAT6B	.609***	.553***	.288	.150	.081	.013	.254	.308
KAT7	.219	.277	.201	-.029	-.146	-.377*	-.258	.074
KAT8	.175	.084	.036	.166	.242	.248	.211	-.015
TAF1	.052	-.009	.115	.256	.042	.059	.012	-.218

Note: * Significant (p <0.05), ** highly significant (p <0.01), *** highly significant (p <0.001)

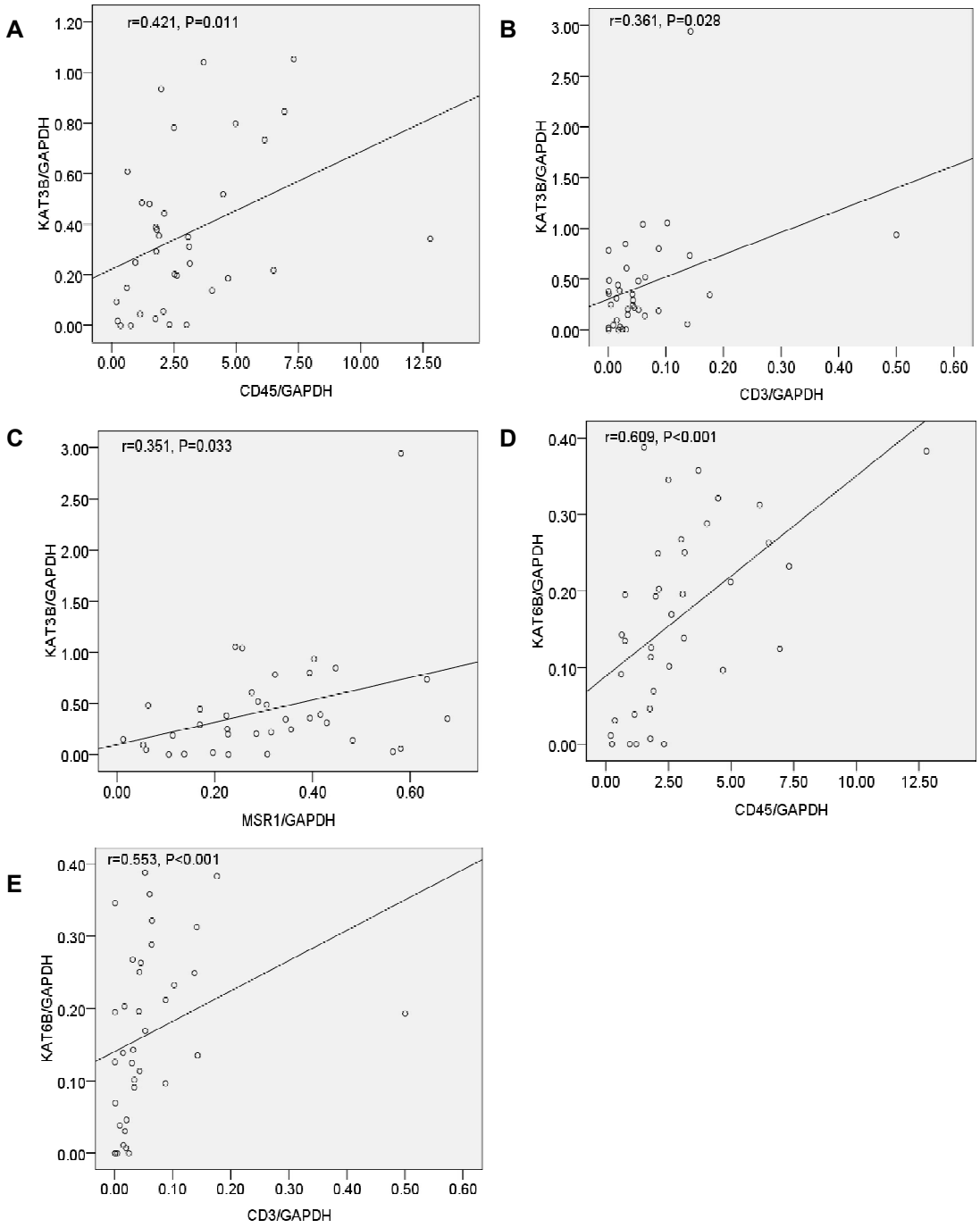

Figure 26. Correlation analysis between the expression levels of selected individual histone acetyltransferases in AAA and the expression of specific markers of cells localized in AAA wall. Correlations between KAT3B and CD45 (A), KAT3B and CD3 (B), KAT3B and MSR1 (C), KAT6B and CD45 (D), KAT6B and CD3 (E).

3.4 Immunohistochemical analysis of histone acetylation

The previous results from PCR at mRNA level showed significant differences in the expression of all KATs analyzed in this study between AAA and healthy aorta with the exception of KAT12, which was not detected in any tissue sample. Furthermore, association between the expression of these KATs and individual cells localized in AAA was observed as described in the previous section.

As a next, expression of KATs was analyzed by means of IHC to confirm the affiliation of these KATs with the cells within AAA (**Table 3**).

The expression level of many of these KATs was however very low, compared to that of GAPDH to which the expression was normalized. Therefore, according to the result of the PCR analysis at mRNA level, especially KAT2B, KAT3A, KAT3B and KAT6B were strong in their expression among the KAT family. Therefore, dependent upon these results, IHC of these corresponding acetyltransferases (KAT2B, KAT3B and KAT6B) was performed. It is to note that the antibody against KAT3A was not commercial available for FFPE tissue samples and IHC for KAT3A was therefore omitted.

Furthermore, in accordance with the known substrate specificity for the above mentioned KATs and according to the aim of this study to evaluate acetylation especially on histone H3, the acetylation at the lysine residues at lysine 9 (H3K9ac), lysine 14 (H3K14ac), and lysine 18 (H3K18ac) was analyzed, because these are the targets for KAT2B, KAT3A, KAT3B, and KAT6B.

Consequently, consecutive staining for histone acetylation of H3 at lysine 9, 14 and 18 was performed and associated with the individual type of cells in AAA and control group.

3.4.1 IHC analysis for histone acetyltransferases in AAA

3.4.1.1 KAT2B in AAA

KAT2B seemed to be expressed mainly in inflammatory cells (both T-cells and B-cells) and macrophages, because the staining intensity was the highest (**Figure 27**). Furthermore, the staining of the luminal ECs and neovessels were positive for KAT2B as well. In contrast, smooth muscle cells were only weak positive for KAT2B and not all cells seemed to express this acetyltransferase.

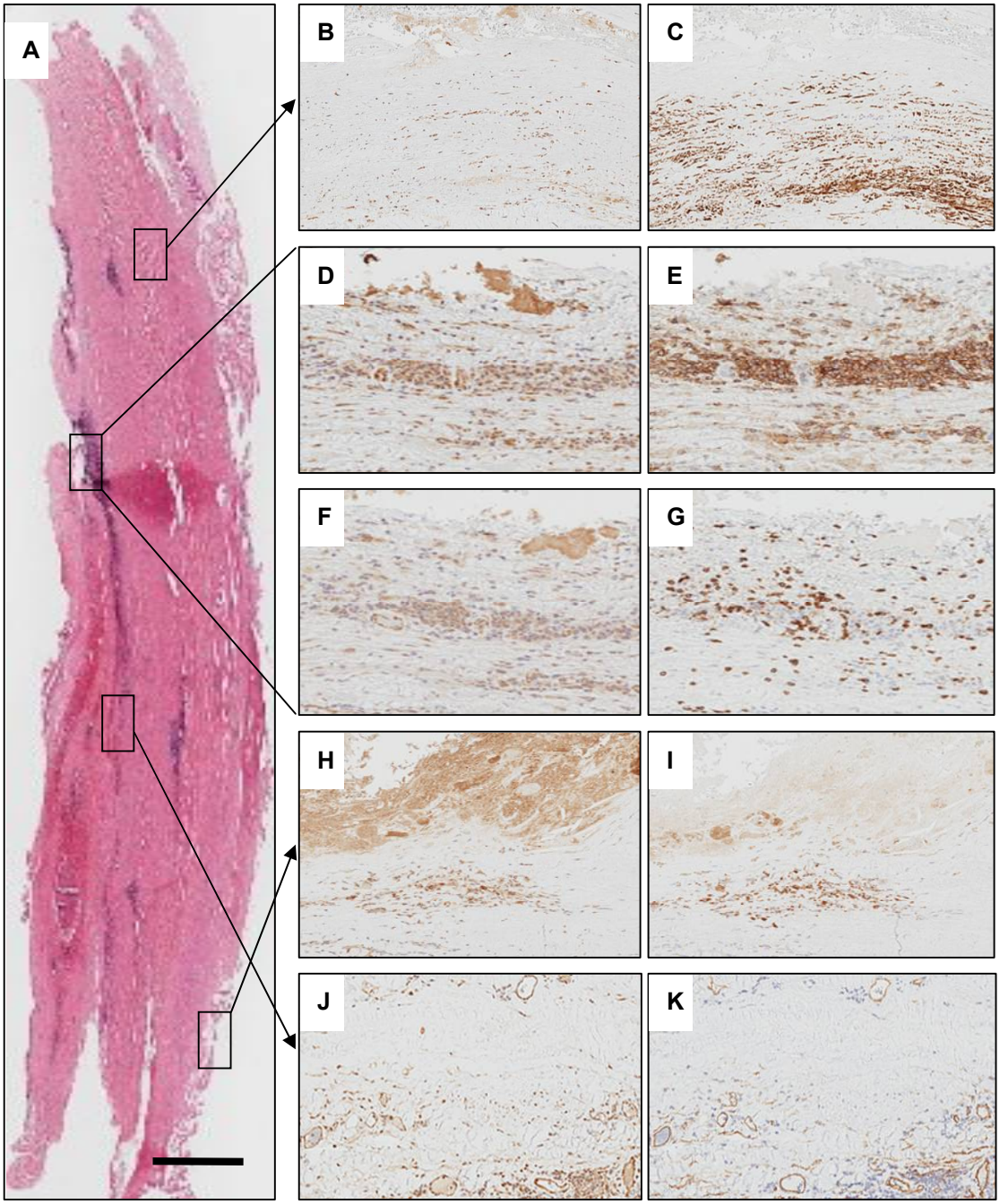

Figure 27: Selected AAA example of IHC for cellular localization and expression of KAT2B by consecutive staining. (A) Overview of selected AAA tissue by HE staining (scale bar represents 1 mm). (B, C) KAT2B and SMC staining; (D, E) KAT2B and CD45 staining; (F, G) KAT2B and CD3 staining; (H, I) KAT2B and CD68 staining; (J, K) KAT2B and CD34 staining. B-K: original magnification x 20.

3.4.1.2 KAT3B in AAA

Regarding KAT3B, inflammatory cells were strongly positive for this acetyltransferase similar to KAT2B. KAT3B was however detected particularly in T-cells. In contrast, medial SMCs, macrophages and neovessels were negative for KAT3B (**Figure 28**).

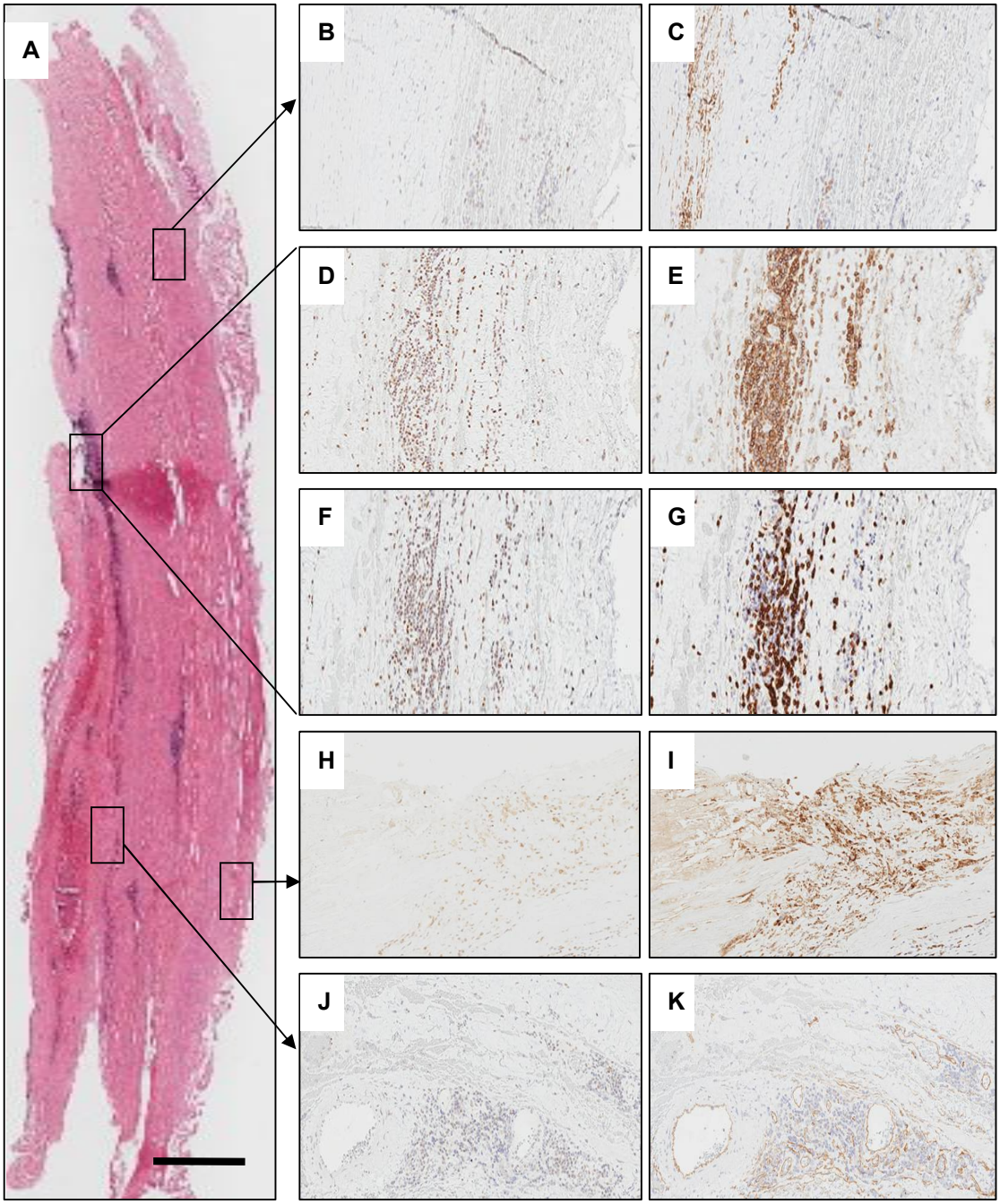

Figure 28: Selected AAA example of IHC for cellular localization and expression of KAT3B by consecutive staining. (A) Overview of selected AAA tissue by HE staining (scale bar represents 1 mm). (B, C) KAT3B and SMC staining; (D, E) KAT3B and CD45 staining; (F, G) KAT3B and CD3 staining; (H, I) KAT3B and CD68 staining; (J, K) KAT3B and CD34 staining. B-K: original magnification x 20.

3.4.1.3 KAT6B in AAA

Regarding KAT6B, inflammatory cells were in this case only weak positive for this acetyltransferase (**Figure 29**). Furthermore, the staining of the luminal ECs and neovessels was negative for KAT6B and not all cells seemed to express this acetyltransferase. In addition, SMCs were also negative for this staining.

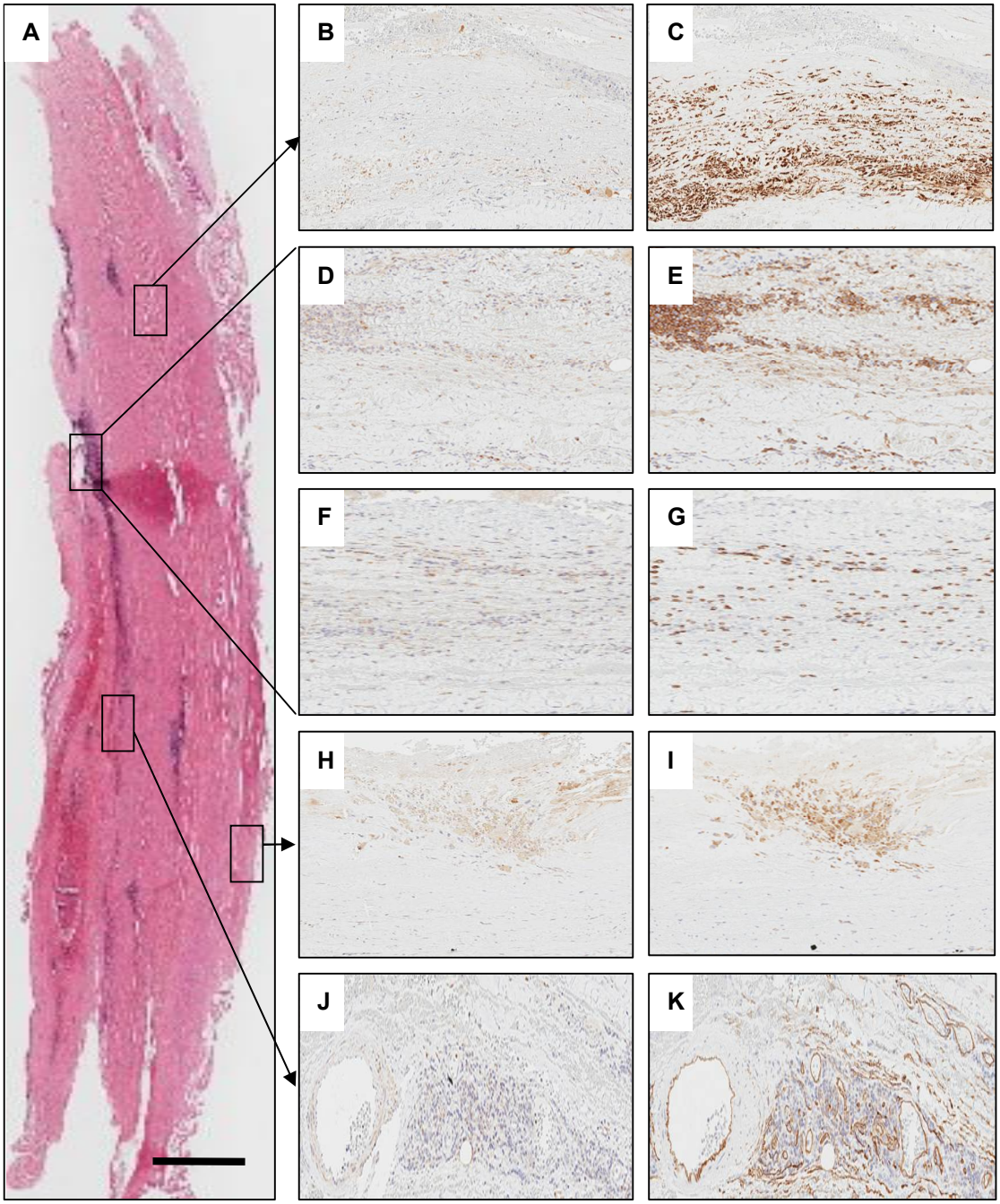

Figure 29: Selected AAA example of IHC for cellular localization and expression of KAT6B by consecutive staining. (A) Overview of selected AAA tissue by HE staining (scale bar represents 1 mm). (B, C) KAT6B and SMC staining; (D, E) KAT6B and CD45 staining; (F, G) KAT6B and CD3 staining; (H, I) KAT6B and CD68 staining; (J, K) KAT6B and CD34 staining. B-K: original magnification x 20.

3.4.2 IHC analysis of acetylation on histone H3 in AAA

In the above described IHC analysis, cellular expression of selected acetyltransferases was investigated. In the next approach their substrates, the specific acetylation sites of histone H3, namely K9, K14 and K18 were investigated. For this purpose, AAA samples were further stained with antibodies against the acetylated H3K9, H3K14 and

H3K18. It is to note that H3K36 is also a common target of the above analyzed KATs and in the study and there was intention to analyze also the acetylation of this lysine residue by means of immunohistochemisty. However, the corresponding antibody against H3K36 for IHC was unfortunately not available and therefore the staining against this location could not be performed.

3.4.2.1 Acetylation of H3K9 in AAA

H3K9 seemed to be acetylated mainly in inflammatory cells and macrophages (**Figure 30**). Furthermore, the staining of the luminal ECs and neovessels was positive for the acetylated H3K9 as well. In contrast, smooth muscle cells showed only weak acetylation of H3K9 and not all cells seemed to be acetylated at this lysine residue at all.

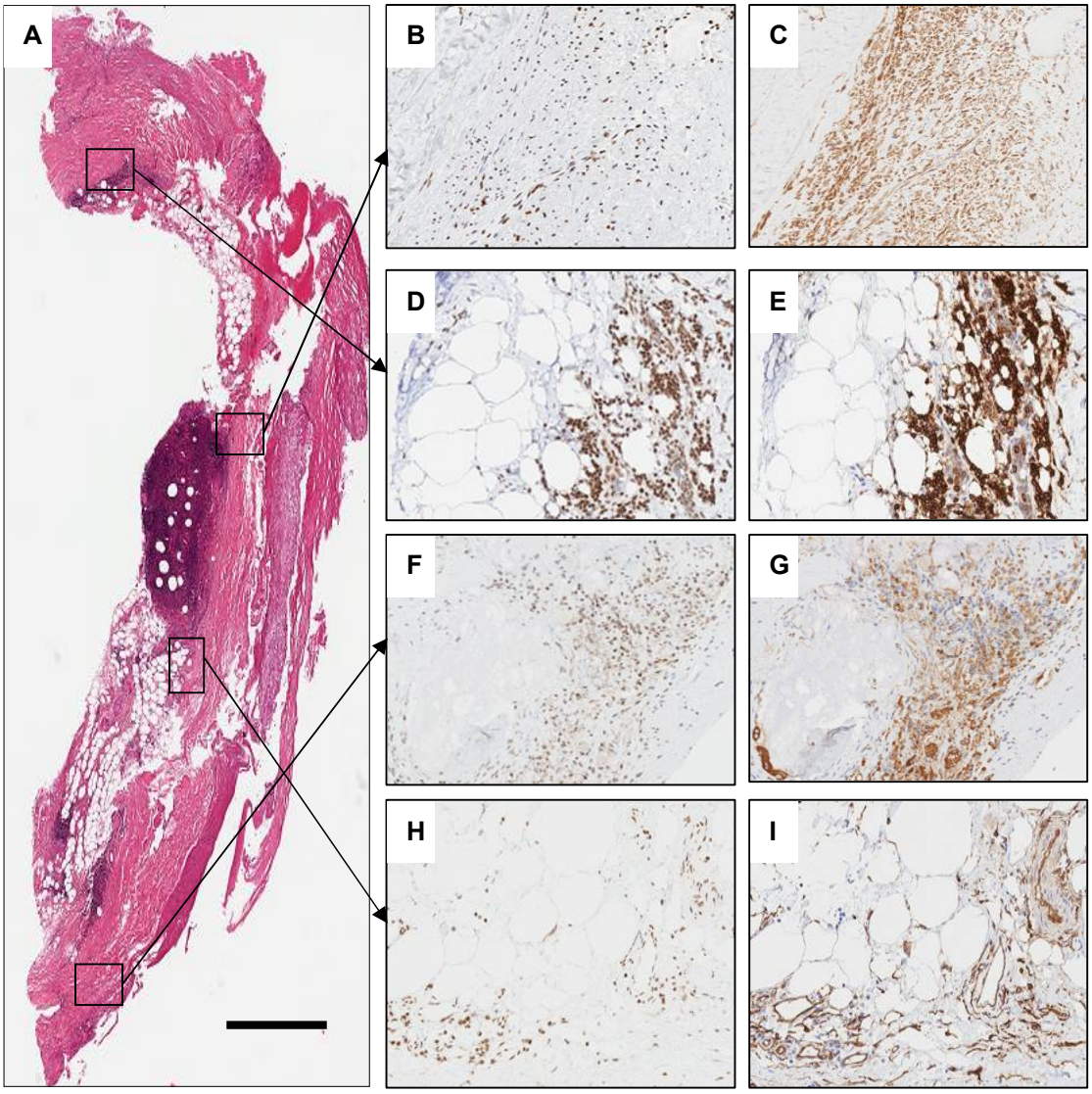

Figure 30. Selected AAA example of IHC for cellular localization and acetylation of H3K9 by consecutive staining. (A) Overview of selected AAA tissue by HE staining (scale bar represents 1 mm). (B, C) acetylated H3K9 and SMC staining; (D, E) acetylated H3K9 and CD45 staining; (F, G) acetylated H3K9 and CD68 staining; (H, I) acetylated H3K9 and CD34 staining. B-I: original magnification x 20.

3.4.2.2 Acetylation H3K14 in AAA

H3K14 also seemed to be acetylated mainly in inflammatory cells and macrophages (**Figure 31**). Furthermore, the staining of the luminal ECs or neovessels was positive for H3K14 as well, similar to the acetylation of H3K9. The same staining results were observed also for SMCs. Inferential, acetylation of H3K9 and H3K14 seems to follow the same pattern.

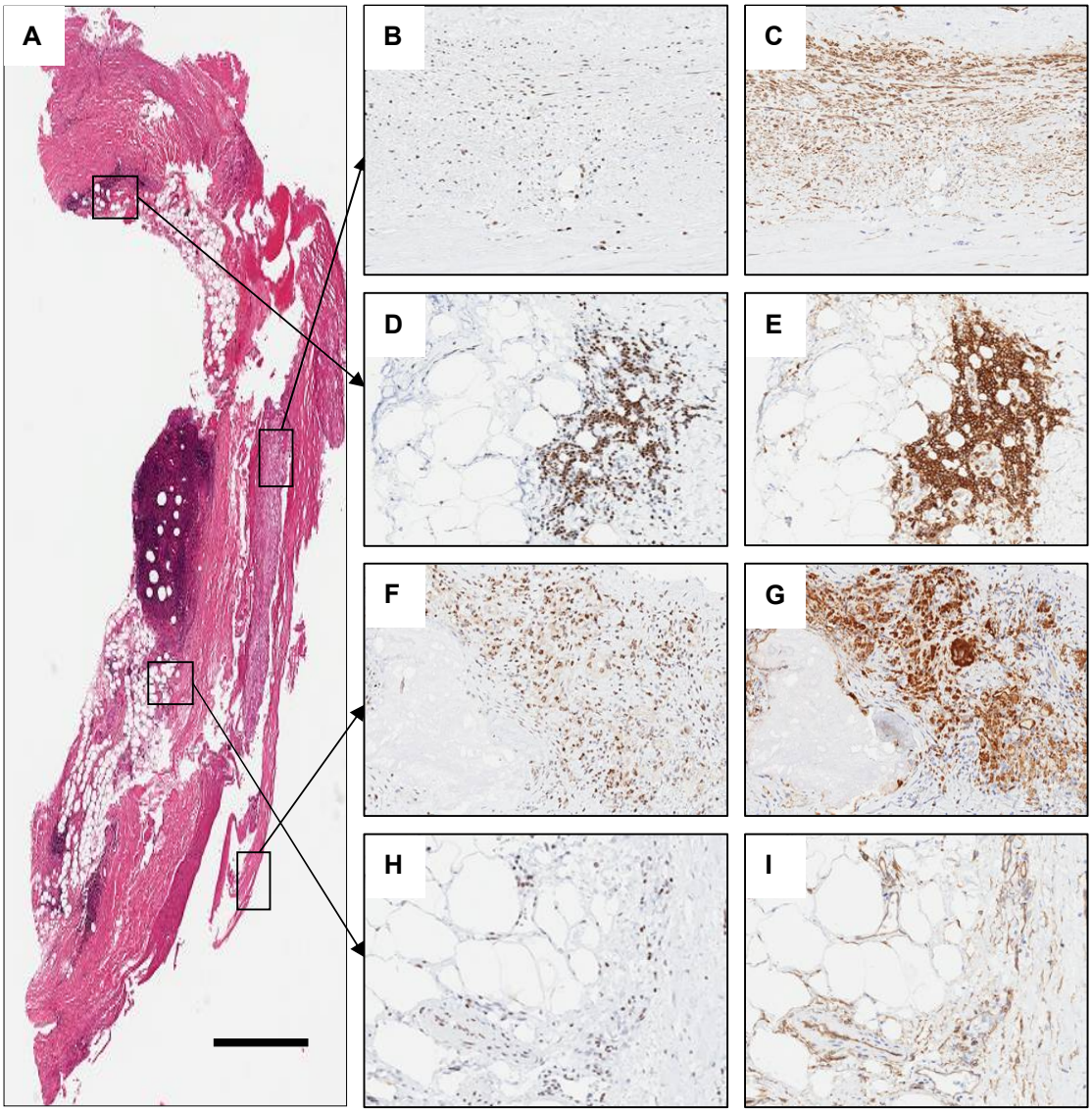

Figure 31. Selected AAA example of IHC for cellular localization and acetylation of H3K14 by consecutive staining. (A) Overview of selected AAA tissue by HE staining (scale bar represents 1 mm). (B, C) acetylated H3K14 and SMC staining; (D, E) acetylated H3K14 and CD45 staining; (F, G) acetylated H3K14 and CD68 staining; (H, I) acetylated H3K14 and CD34 staining. B-I: original magnification x 20.

3.4.2.3 Acetylation H3K18 in AAA

Acetylation of H3K18 was most intensive in inflammatory cells and macrophages (**Figure 32**). In contrast, ECs of the lumen and neovessels, as well as SMCs were only weak positive for acetylated H3K18 and not all cells seemed positive at all. Again, it was the same pattern as for the above described acetylation of H3K9 and H3K14.

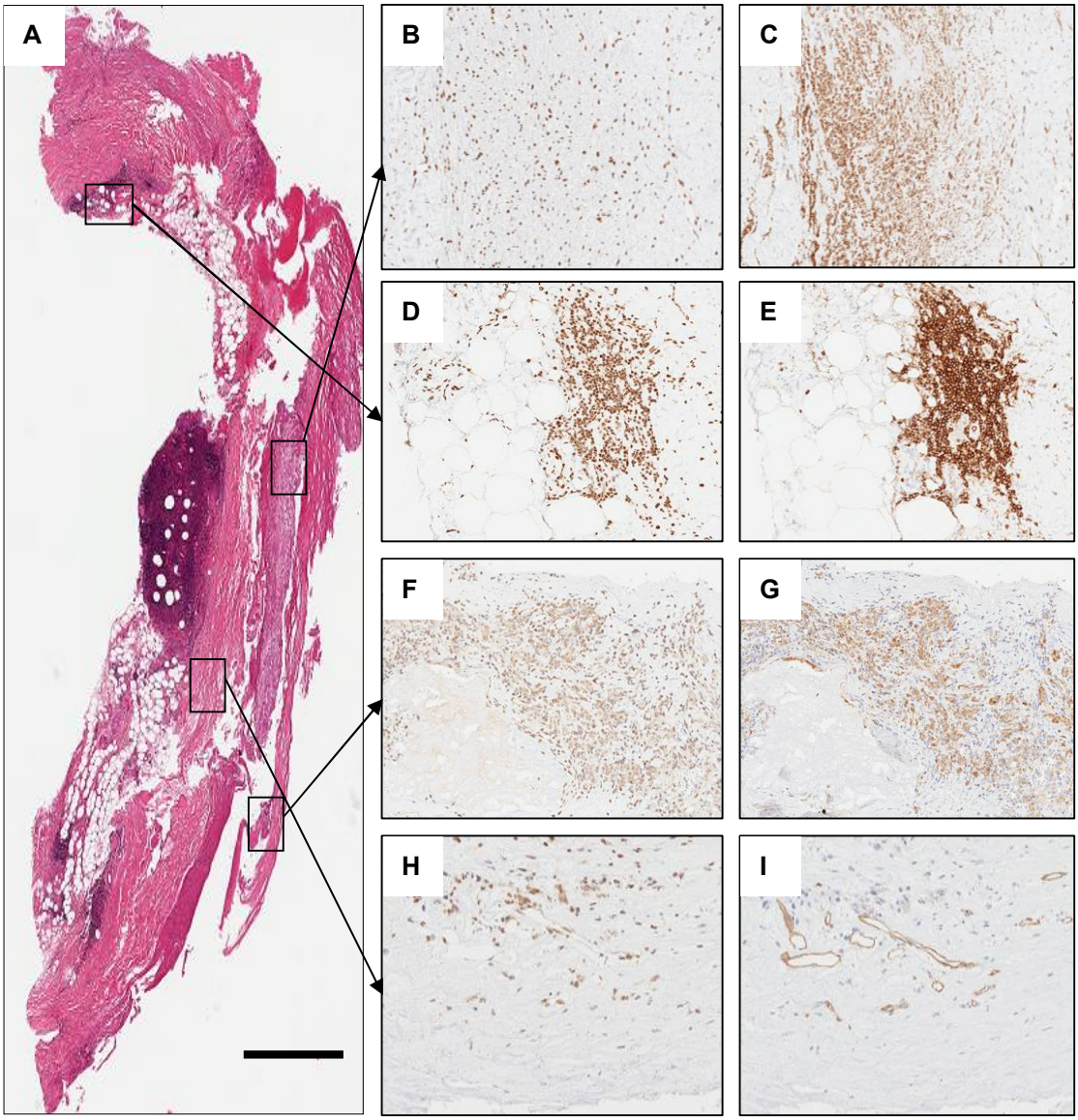

Figure 32. Selected AAA example of IHC for cellular localization and acetylation of H3K18 by consecutive staining. (A) Overview of selected AAA tissue by HE staining (scale bar represents 1 mm). (B, C) acetylated H3K18 and SMC staining; (D, E) acetylated H3K18 and CD45 staining; (F, G) acetylated H3K18 and CD68 staining; (H, I) acetylated H3K18 and CD34 staining. B-I: original magnification x 20.

3.4.3 IHC analysis for histone acetyltransferases in control group

In contrast to AAA tissue samples, no expression at protein level was detected for KAT2B, KAT3B and KAT6B in the healthy aortic tissue samples. Therefore, the images of these results are not provided in this study.

3.5 Expression analysis of KATs at protein level

The results from qRT-PCR clearly demonstrated significant increase in expression of all KATs analyzed in this study at mRNA level in AAA compared with the control healthy aorta, with the exception TFIIIC. To confirm these results also at protein level,

western blot (WB) analysis of the corresponding acetyltransferases was therefore performed. Furthermore, because western blot is a cost- and time-intensive procedure and because these experiments should serve to conform the results of RT-PCRs, fresh tissues from 8 healthy aortas and 24 AAA samples were selected for analysis.

3.5.1 Western blot for KATs

Generally, the sensitivity of protein detection by WB is markedly lower than that of PCR at mRNA level. For this reason and as already mentioned above for IHC, only KATs with a high expression at mRNA level were used for expression analysis at protein level: KAT2B, KAT3A and B, KAT6B. The RT-PCR results for KAT2A, KAT5, KAT6A, KAT7, KAT8 and TAF1 at mRNA level were very low achieving only <1% of the expression of GAPDH, therefore these acetyltransferases were not analyzed by Western blot, not expecting that the protein level of these transferases would be detectable. Furthermore, no suitable antibody against KAT3A for WB analysis was available. Therefore the analysis of protein expression of KAT3A could not be performed.

3.5.2 Immunoblot for GAPDH

After quantification of the intensity of protein bands, as described in section Methods, the results were normalized to the expression of GAPDH, a housekeeping gene protein, from the same samples. As expected according the protein size, the clear bands were visible in the range of approximately 36 kDa (**Figure 33**).

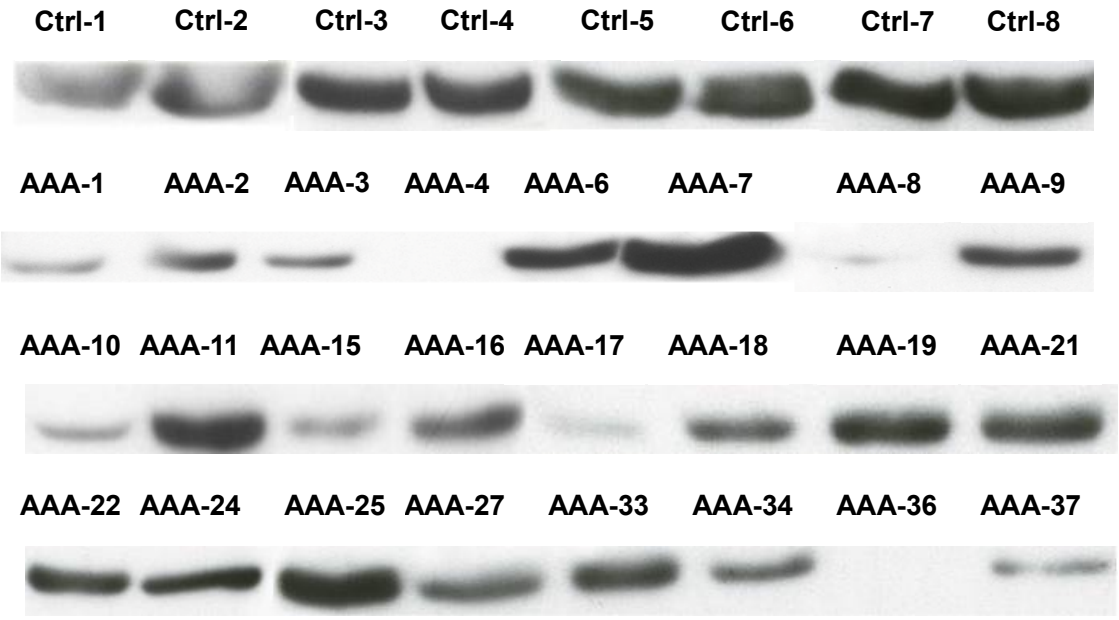

Figure 33. Expression of GAPDH at the protein level in all AAA tissue samples and all healthy aorta tissue samples used in western blot analysis.

3.5.3 Immunoblot for KAT2B

The representative blot bands for KAT2B are shown in **Figure 34**. As expected according the protein size, the bands appeared in the range of approximately 93 kDa. Quantification of the protein bands, normalized to GAPDH is demonstrated in **Figure 35**. The expression of KAT2B at protein level was significantly higher in AAA group than control aortic tissue (P<0.001).

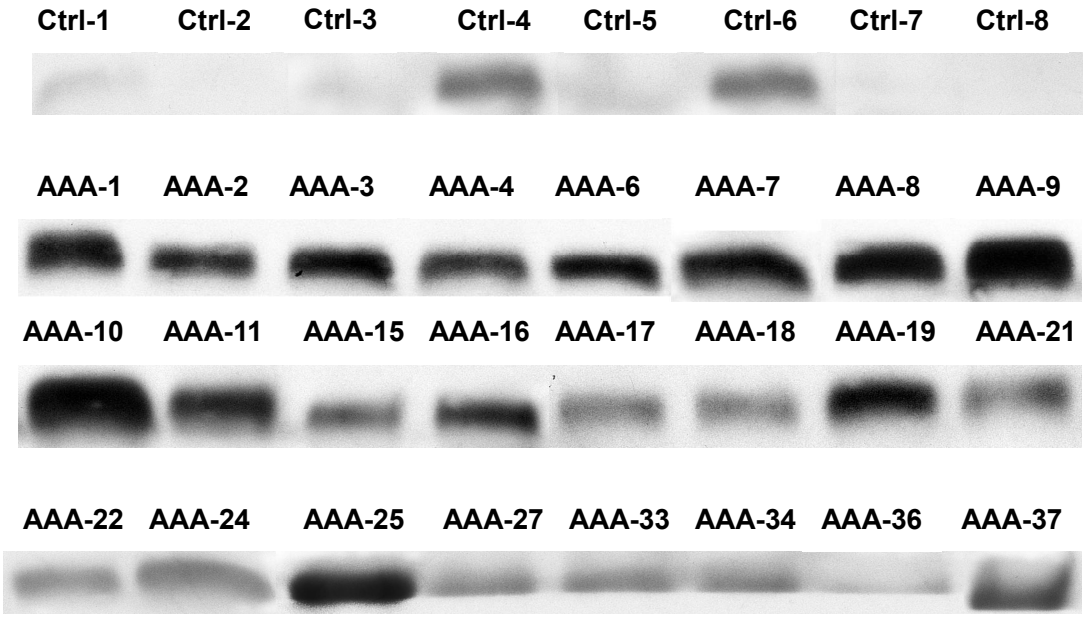

Figure 34. Expression of KAT2B at the protein level in all AAA tissue and all healthy aorta tissue samples analyzed by western blot.

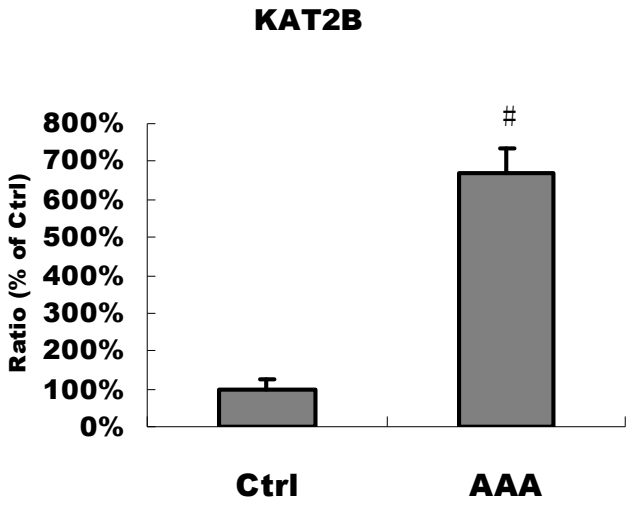

Figure 35. Quantitative densitometric analysis of KAT2B protein expression in AAA tissues samples (n=24) and control aorta (n=8). The data were plotted as mean ± SE. **#** = P < 0.001.

3.5.4 Immunoblot for KAT3B

The representative blot bands for KAT3B are shown on **Figure 36**. According to the expected protein size, the bands appeared in the range of approximately 290 kDa. The level of expression of KAT3B normalized to the expression of GAPDH was significantly higher in AAA group than control group (P<0.001) (**Figure 37)**.

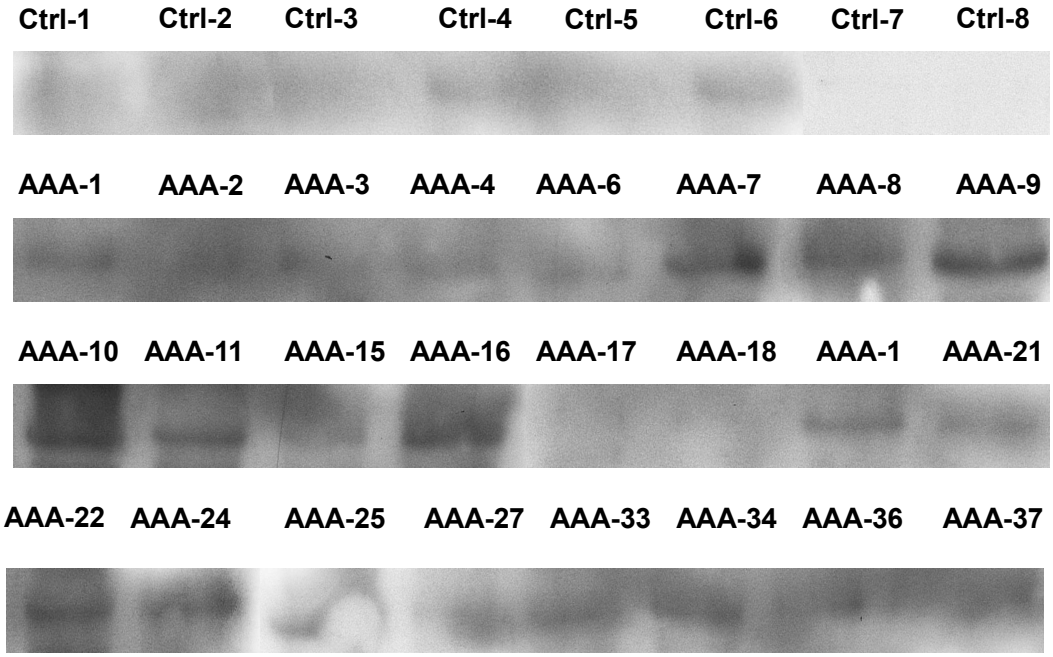

Figure 36. Expression of KAT3B at the protein level in all AAA tissue and all healthy aorta tissue samples, analyzed by western blot.

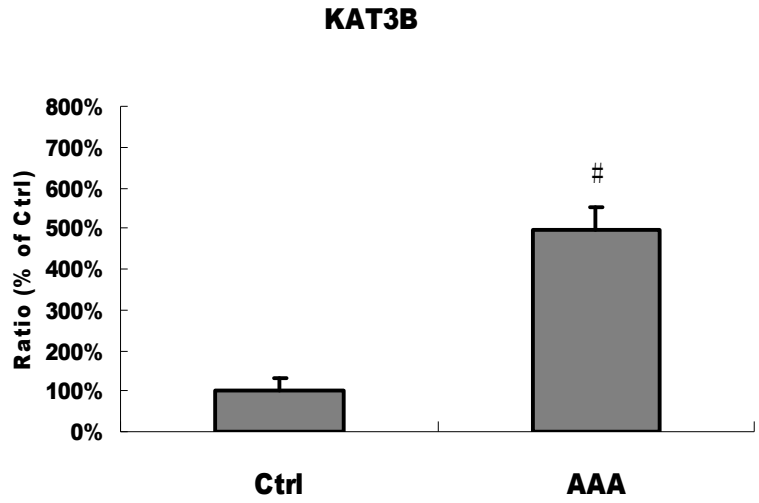

Figure 37. Quantitative densitometric analysis of KAT3B protein expression in AAA tissues samples (n=24) and control aorta (n=8). The data were plotted as mean ± SE. **#** = P < 0.001.

3.5.5 Immunoblot for KAT6B

The representative blot bands for KAT6B are shown in **Figure 38**. According to the expected protein size, the bands were found in the range of approximately 231 kDa. The level of expression of KAT6B, again normalize for the expression of GAPDH in the same tissue samples was significantly higher in AAA group compared to the group of control healthy aorta (P<0.001) (**Figure 39)**.

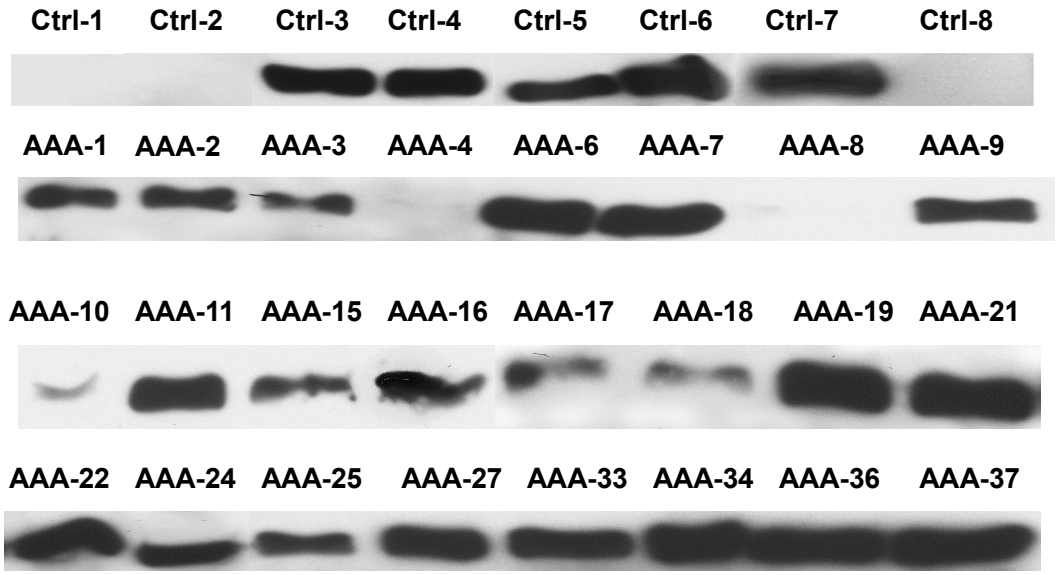

Figure 38. Expression of KAT6B at the protein level in all AAA tissue and all healthy aorta tissue samples, analyzed by western blot.

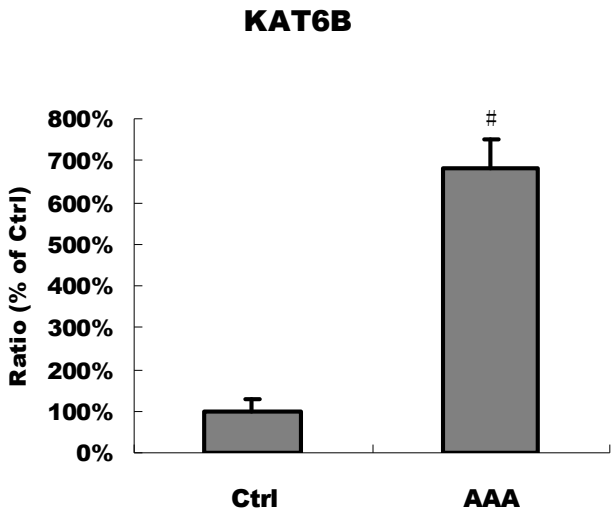

Figure 40. Quantitative densitometric analysis of KAT6B protein expression in AAA tissues samples (n=24) and control aorta (n=8). The data were plotted as mean ± SE. **#** = P < 0.001.

4. DISCUSSION

Epigenetic regulation through histone modification plays a key role in gene expression, its activation or silencing [137]. This is due to the fact that modifying histone residues can markedly influence the structure of chromatin, which may result either in restriction of transcription mediated by RNA polymerase II or in facilitating of this polymerase to bind DNA. In other words, the dynamics of chromatin structure through various histone modifications effectively regulate gene expression by influencing accession of RNA polymerase and transcription factors to DNA [207].

The N-terminal tails of histone are the target of most histone modifications, including methylation, acetylation, sumoylation, and ubiquitinylation. Herein, such specific histone modifications are frequently associated with repressed gene and others with active gene [208]. Nevertheless, the molecular biological mechanisms by which histone acetylation regulates transcription still remain unascertained [209]. Histone acetylation is mediated by the activities of histone acetyltransferases (HATs, also called KAT for is substrate specificity, which is mainly lysine residue [K]). As acetylation is a histone mark for active transcription, HATs have been associated with active gene [210]. So far there is no knowledge about such modifications in aneurysm. Thus, the goal of this study pursued the purpose to get a better insight into the epigenetics and its role in human AAA. The results presented in this thesis clearly confirmed epigenetic changes in AAA referring to histone acetylation. Not only significant increase in acetylation was observed in AAA tissue samples compared to healthy aorta, but the expression of many KATs was significantly higher in the diseased aortic tissue at both mRNA and protein level. Thus, these results confirmed a potential role of histone acetyltransferases and the corresponding acetylation of histones in AAAs.

It is widely accepted that genetic alterations in the genes encoding HATs, leading to aberrant forms of many regulatory proteins, have been linked with various human diseases, including congenital developmental disorders and various forms of cancer [211]. Consequently, scientists raised a hypothesis that several diseases could be associated with e.g. hyperacetylation of chromosomal regions that are usually silenced or deacetylation of chromosomal regions that are actively transcribed. The alteration in the expression of HATs at the genomic level disturbs the balance of the histone acetylation status, which in turn may play an important role in regulating their gene expression [212].

4.1 Gene expression of KATs

4.1.1 Over-expression of KATs in AAA

Acetylation of histone is accomplished by histone acetyltransferases (HATs). The expression analysis in this study showed that the mRNA levels of HATs including GNAT, CBP, and MYST family were significantly increased in AAA patients than to individual with healthy aorta.

Up to date, no information about the role of KATs in AAA is available. However, many previous studies have confirmed the evidence that hyperacetylated core histones are associated with transcriptionally active chromatin in other tissue or animal model [213,214]. The hyperacetylation status was described to be mediated especially by histone acetyltransferases such as GNAT, CBP/p300 and MYST family.

The KAT2A (GCN5) expression was described e.g. to potentiate lung cancer growth by directly promoting the expression of E2F1, cyclin D1, and cyclin E1 [215]. However, there is so far no data linking KAT2A expression to cardiovascular disease or atherosclerosis, not to mention AAA. Interestingly, in this study, KAT2A was over-expressed in AAA wall compared to healthy aorta. The proliferation of vascular smooth muscle cells (VSMCs) is mediated by E2F activity and expression of its target genes, including E2F1, E2F2, cyclin A [216]. The over-expression of KAT2A may thus play a key role in proliferation of VSMCs and pathogenesis of AAA by E2F1 gene activation. This might explain the results of the current study. In addition, other study identified a large molecular coactivator complex including GCN5 and other subunits, which is necessary for the estrogen receptor alpha (ER-α) transactivation [217]. On the other hand, ER-α mediates inflammation in atherosclerotic lesions. In this manner, KAT2A expression might contribute to the progression of AAA by facilitating proinflammatory processes via ER-α.

Histone acetylating activity of P/CAF is essential for NF-κB-mediated gene transcription [218] and lead to upregulation of inflammatory genes [219]. AAA is well characterized by vascular inflammation and leucocyte infiltration throughout the media and adventitia of the vessel wall. The expression analysis in this study showed that KAT2B (P/CAF) increased in AAA not only at mRNA level but also at protein level. Meanwhile, immunohistological analysis of inflammatory cells showed an increasing acetylation of H3K9ac, H3K14ac and H3K18ac within AAA tissue. Thus, the formation of AAA might increase the recruitment of acetyltransferases such as e.g. KAT2B (P/CAF) to the promoter regions of inflammatory genes, lead to the acetylation of nucleosomal factors histone H3 and consequently promote inflammation in AAA wall.

Furthermore, enhancement of MMP-9 promoter activity requires the HATs activity of P/CAF but not that of CBP/p300. Thus, P/CAF is activating MMP-9 promoter activity either independently or in a synergistic manner [220]. MMP-9 has already been suggested as the key mediators of the degradation of the structural proteins in the aneurysmal aortic wall. In this way the over-expression of KAT2B could also contribute to the development and progression of AAA toward rupture, not only facilitating inflammation but also promoting degradation of extracellular matrix component within the aortic wall.

Another family of KATs named CBP/p300 can stimulate diverse functions of specific transcriptional regulatory proteins [221,222]. The activated CBP may acetylate not only histones but also other transcription factors, such as e.g. p53 to facilitate their binding to DNA [223]. P300 and estrogen receptor (ER) function cooperatively to increase the efficiency of productive transcription initiation [224]. Furthermore, mutations in the p300 binding sites results in a reduction in ligand-induced transactivation functions of both ER-α and ER-β [225]. In this study, p300 was upregulated in AAA not only at the mRNA level but also at the protein level. Although there is no evidence to support that p300 mediated ER gene is associate with aneurismal formation, methylation of ER gene play an important role with ageing and atherosclerosis in the cardiovascular system [226].

In addition, several studies suggested that p53 and HDM2 (human homolog of mouse doubles minute 2) complex interacts relatively weakly with CBP/p300 under absence of genotoxic stress. However, in response to DNA damage, p53 becomes activated by phosphorylation at multiple sites, resulting in release of HDM2, enhanced recruitment of CBP/p300 and acetylation of the C-terminal regulatory domain of p53. Finally, these changes lead to enhancement of p53 transcriptional activity [227,228,229]. Such physiopathologic progress might also contribute to AAA formation. The SMC apoptosis and increased production of p53 associate with medial SMC density are significantly decreased in human AAA tissues, a potential mediator of cell cycle arrest and programmed cell death [230].

Kim et al. suggested that KAT5 (Tip 60) is not only a transcription factor that recognizes specific DNA sequences, it also requires a selective function of transcription factors to regulate the expression of specific target genes [231]. KAT5 (Tip60) has a coactivator function in the NF-κB signaling pathway like other histone acetyltransferases, such as p300/CBP, PCAF [231]. They also found that NF-κB production, as well as its stimulation of the expression of IL-6 and IL-8, is increased by Tip60 overexpression. For AAAs, over-expressed KAT5 was also detected in this study. The reason is seemingly that endothelial NF-κB activation by Tip60 up-regulates expression of various adhesion molecules, which in turn may trigger macrophage infiltration and promote inflammation in the adventitia and media of the

aortic wall [232]. In addition, the fact that in general inflammation in AAA is dominated by profound activation of NF-κB and hyperexpression of IL-6 and IL-8 has already been confirmed [233]. Thus, KAT5 over-expression in AAA might promote inflammatory processes in AAA wall and consequently contribute to progression of this aortic disease.

KAT6A (MOZ)
With regard to KAT6A, few studies suggested that this histone acetyltransferase interacts with NF-κB and enhances expression of NF-κB dependent promoters [234]. Furthermore, another study demonstrated that MOZ (KAT6A) controls p53 acetylation and its transcriptional activity [235]. So far, there are still limited data linking KAT6A expression and disease, with the exception of leukemia. The expression analysis in this study showed that KAT6A was increased with AAAs in comparison to healthy aorta. How far, these circumstances might contribute to AAA development and progression has to be elucidated in future studies.

4.1.2 Low-expression of KATs

Interestingly, all KATs analyzed in our study were detected in AAA tissue samples with the exception of the TF-related family of acetyltransferases. KAT12 (TFIIIC90) was expressed neither in AAA nor in healthy aortic wall. Furthermore, KAT4 (TAF1) expression was significantly lower in AAA group than in the control samples. These results suggest that this family of KATs does not seem to play any important role in aortic wall and does not contribute to AAA.

Only very few studies to date have investigated KAT4 (TAF1) alterations in human nervous system disease. Makino et al. suggested that the reduced neuron-specific expression of the TAF1 gene is associated with X-linked dystonia-parkinsonism [236]. How can a ubiquitous gene such as TAF1 cause formation of AAAs? A mechanism could be hypothesized that the decreased expression of the probably other TAF1 isoforms may result in transcriptional dysregulation of many aneurysmal genes. There is reason to believe that the present findings in AAAs support the concept of “transcription syndromes”, which include congenital cataracts facial dysmorphism neuropathy syndrome, caused by a partial deficiency of RNA polymerase II [237].

4.1.3 Summary

Histone acetylation has been shown to be associated with increased gene transcription [238], which may results in AAA related gene over-expression. Acetylated histone proteins improve the accessibility of the DNA template to the transcriptional machinery for AAA related gene expression. These modifications generally occur in the promoter region, determining the genotype trait. A high degree of acetylation of the promoter region indicates that the gene is in an activated state [239]. These

circumstances increase the expression of various inflammatory cytokines and proteolytic enzymes, which in turn further contribute to the accumulation of inflammatory cells within AAA and improve vessel wall remodeling. In this way, epigenetic changes may contribute to AAA progression toward rupture.

4.2 Correlation between individual KATs

Regarding the inter-relationship of individual KATs, determined by correlation analyses, all these correlations were positive in this study. Consequently, the expression of KATs might be regulated in the way that over-expression of some KATs might contribute to the expression of other acetyltransferases, working in a kind cluster.

4.2.1 KAT3A and KAT3B

Although no closely relation between KAT3A and KAT3B within AAA group was detected in this study, their correlation is widely acknowledged as one of the most closely in the HATs [240]. There are some reasons to illuminate this correlation. On the one hand, KAT3A (CBP) and KAT3B (p300) encode highly related protein acetyltransferases that possess several conserved protein-binding domains e.g., RID, CH1 (TAZ1), KIX, Bromodomain, PHD, HAT, ZZ, CH3 (TAZ2), and IBiD (NCBD)] that bind a variety of transcriptional regulators and other proteins [241] (**Figure 41**). On the other hand, KAT3A-KAT3B interactome includes 400 interacting protein partners. Therefore, they are acting as hubs in gene regulatory networks [242].

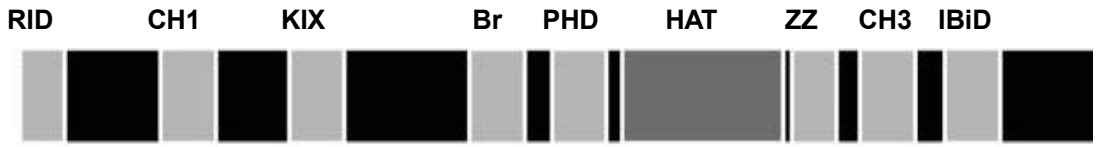

Figure 41. KAT3A (CBP) and KAT3B (p300) are closely related HATs that possess unique protein binding domains. Principal protein-binding domains of CBP and p300: nuclear receptor interaction domain (RID), the Cys/His-rich region 1 (CH1), the CREB-binding domain (KIX), bromodomain (Br), plant homeodomain (PHD), histone acetyltransferase domain (HAT), zinc-binding domain near the dystrophin WW domain (ZZ), the Cys/His-rich region 3 (CH3), and the interferon response factor-binding domain (IBiD). Adapted from Bedford et al. [240].

4.2.2 KAT6A and KAT6B

The mRNA level of KAT6A (MOZ) and of KAT6B (MORF) was significantly correlated in AAAs. There are some reasons to explain this correlation. First, MOZ and MORF are highly homologous, shared the same lysine substrate H3K14ac. Secondly, MOZ and MORF are promiscuous transcriptional co-activators. Indeed, they are involved in regulating transcriptional activation mediated by Runx2 and

Runx2 is an interaction partner of MOZ and MORF [243]. More recently, many studies have proposed a third mechanism by which MOZ and MORF fusion results in catalytic subunits of quartet complexes. Like HAT1, Gcn5, P/CAF and many other HATs, MOZ and MORF are catalytic components of protein complexes. Different from MOZ and MORF, ING5 (inhibitor of growth 5)-MOZ/MORF complexes acetylate e.g. only histone H3 at lysine 14 [244]. The mechanisms by which MOZ and MORF fusions appear to play a critical role in AAAs have yet to be elucidated. It can be hypothesized that the fusion of MOZ and MORF transcripts deregulate histone acetyltransferase activity, which presumably allows an altered transcriptional regulation that again may result in formation of AAA.

4.2.3 KAT5, KAT7 and KAT8

In this study, a significant positive correlation was found between the mRNA level of KAT5 (Tip60) and KAT7 (HBO1) and between KAT5 (Tip60) and KAT8 (HMOF) in AAAs. The reasons for such relationships might be as follows: First, they belong to the same family of KATs (MYST) and thus show high homology. Secondly, all three KATs share the same substrate specificity, acetylating especially histone H4 [142,143]. However, little is known about the epigenetic modifications on the histone H4 N-terminal tail. Last but not least, the NuA4 complex is a histone H4/H2A acetyltransferase involved in transcription and DNA repair. While most nuclear HATs target mainly nucleosomal histone H3, the NuA4 histone acetyltransferase complex acetylates lysine residues in the histone H4 tail (as well as H2A) [245]. Utley and co-worker suggested H4 phosphoserine 1 regulates chromatin acetylation by the NuA4 complex and that this process is important for normal gene expression and DNA repair [246]. In this context, MYST-family of KATs might also be involved in these processes.

4.3 The role of strong expressed KATs

The results of mRNA expression demonstrated that especially the expressions of KAT2B, KAT3A, KAT3B and KAT6B were strong among the KATs in AAA. Therefore, these KATs were analyzed in more details. As already mentioned in section Methods no suitable antibody against KAT3A was commercial available for FFPE tissue samples, therefore more detailed analysis of this acetyltransferase was not possible.

4.3.1 KAT2B

Recently, Bastiaansen et al. demonstrated that KAT2B (P/CAF) acts as master switch in the inflammatory processes required for effective arteriogenesis [247]. The present study also found relationship between inflammatory cells, especially macrophages, and the expression of KAT2B in AAA. The staining of the luminal ECs and

neovessels for KAT2B was positive and correlation of expression at mRNA level showed positive results (r=0.486) for VCAM-1 as a marker of angiogenesis/ arteriogenesis. However, not all cells seemed to express this acetyltransferase, for instance SMCs. There are several reasons to explain these circumstances. Two important cell cycle regulators, E2F1 and p53, can interact with KAT2B [248,249]. Transcription factor E2F induces S-phase specific gene expression and is involved in promoting S-phase-entry. In contrast, p53 acts by inhibiting cell cycle progression and S-phase entry. Induction of p53 usually leads to posttranslational modifications of the protein. Acetylation by P/CAF has three functional consequences on E2F1 activity: increased DNA-binding ability, activation potential and protein half-life [250]. For endothelial cells, acetylation associated with VEGF (vascular endothelial growth factor) signaling appears to be predominantly mediated by KAT2B (P/CAF) and depletion of histone acetyltransferases disrupted the formation of angiogenic tubules. This result suggests a novel role for E2F1 and acetylation in the angiogenic process [251]. It seems to be the conceivable reason for increased neovascularization and growth of these neovessels in AAA mediated by KAT2B. In addition, acetylation of p53 region is observed after DNA damage in vivo, leading to cell cycle arrest or apoptosis; therefore, over expression of KAT2B can cause growth arrest [252]. It seems to be the other reason that might support evidence to AAA formation, especially SMCs apoptosis.

In summary, KAT2B can be involved in two opposing states to attribute to formation of AAAs, which are promoting of cell cycle progression by activating E2F, e.g. in inflammatory cells, and cell cycle arresting by activating p53, which might be fatal for SMCs.

4.3.2 KAT3B

In this work, inflammatory cells were strongly positive for KAT3B (p300), particularly T- cells. However, the result of correlation analysis showed that there was only a weak relationship between KAT3B and markers for inflammatory cells. In contrast, medial SMCs and neovessel were negative for KAT3B by IHC analysis.

KAT3B and estrogen receptor (ER) function cooperatively to increase the efficiency of productive transcription initiation [224]. There is so far no evidence to support the reason that KAT3B is playing any key role in the cardiovascular disease. However, the involvement of DNA methylation in cardiovascular diseases by observing estrogen receptor-α (ER-α) promoter methylation to be increased in atherosclerotic lesions compared to normal proximal aortas specimens and a similar promoter methylation was found also in VSMCs obtained from the atheroma [253]. This inference might provide some hint that ER-α promoter acetylation by KAT3B may contribute to formation of AAAs.

4.3.3 KAT6B

The results of the quantitative RT-PCR analysis in this study showed strong positive correlation between the expression of KAT6B and the markers for inflammatory cells e.g. CD45 and CD3.

KAT6B (MORF) is ubiquitously expressed in adult human tissues. Distinguishingly, KAT6B is a histone acetyltransferase that contains multiple functional domains and may be involved in both positive and negative regulation of transcription. Precisely, KAT6B possesses a potent transcriptional activation domain located at its C terminus. On the other hand, KAT6B contains a strong transcriptional repression domain located at its N terminus [172].

4.4 The role of the other KATs

In this work, it is also found that the amount of MYH10, a marker of synthetic phenotype of SMCs tended to positively correlate with mRNA level of KAT6A (MOZ). In addition, a strong negative correlation was detected between expression of KAT7 and expression of MYH11, a marker of the contractile phenotype of SMCs. There is so far no data linking expression of KAT6A or KAT7 with the specific phenotype of vascular smooth muscle cells.

4.5 Possible role for KATs in AAAs

Histone acetyltransferases have been shown to be able to regulate several processes that play a key role in the development of AAAs, such as inflammation, proliferation of smooth muscle cells (SMCs), and remodeling of extracellular matrix.

4.5.1 Inflammatory and HATs

Many KATs, such as KAT3B (p300), KAT3A (CBP) and KAT2B (P/CAF), have been implicated in the modulation of NF-κB activity as already mentioned above. In the field of cardiovascular disease, recent study suggested that these KATs are required to coactivate p65-dependent transcription and have been shown to directly activate the transcription of several NF-κB-regulated inflammatory genes known to be involved in cardiovascular disease, such as eotaxin, GM-CSF (granulocyte-macrophage colony-stimulating factor) and TNFα (**Figure 41**) [254]. The p300 and P/CAF are acetylating lysines 122 and 123 of p65 and p300 in addition acetylate lysine residues 310, 314 and 315 [255]. In this study positive correlation was observed between inflammatory cell infiltration and KAT3B, KAT3A and KAT2B in AAAs. The relationships between p65 mRNA or protein level and corresponding KATs are nevertheless still not elucidated. Independent of the results of the present study, direct evidence of KAT expression and AAA is still lacking, the current data allow only a

speculation about the role of acetylation in AAA.

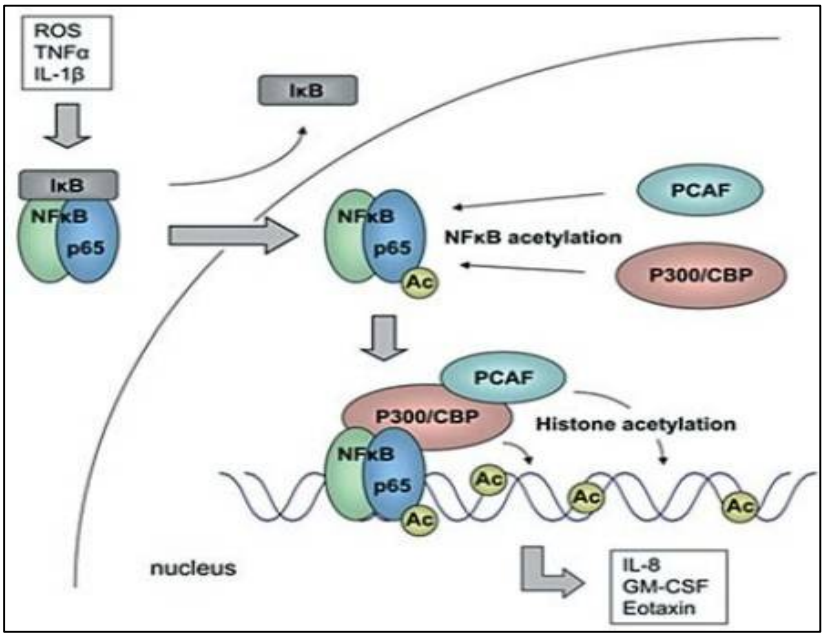

Figure 41. The figure illustrates the dual role of p300, CBP and PCAF in the activation of NF-κB-mediated transcription upon stimulation of N-FκB by e.g. reactive oxygen species (ROS), TNFα or IL-1β. These coactivators act as histone acetyltransferases (HATs/KATs) at the site of NFκB-regulated genes. They acetylate the p65 subunit of NF-κB, increasing its DNA binding and causing transcriptional activation. Adapted from Pons et al. [256].

4.5.2 MMP and HATs

Histone acetylation has also been shown to play a role in the regulation of expression of various matrix metalloproteinases (MMPs), critical mediators in vascular remodeling. CBP and p300 e.g. can provide a platform for formation of multiple protein complexes and bridge interactions between transcription factors and transcriptional machinery such as the RNA polymerase II complex, which may explain their coactivator roles in MMP-9 expression [257].

4.5.3 Smooth muscle cells and HATs

Using IHC, in this work, smooth muscle cells in AAA wall were positive (even if often weak) for KAT2B, KAT3B and KAT6B. Cell culture and animal model studies in atherosclerosis suggests that changes in DNA methylation are an early initiation factor in atherosclerosis, involving both global hypo- and local gene specific hyper-methylation. Furthermore in advanced stages of the disease, the hyper-proliferation of VSMCs results in the global DNA hypomethylation due to the loss of methyl groups in rapidly proliferating VSMCs [258]. Thus, beside the positive results found in this study with regard to histone acetylation in activation or

modifying the phenotype of these cells, DNA methylation is another relevant mechanism of epigenetics, being able to affect the faction and fate of VSMCs in AAA.

4.6 Histone substrates

By staining of consecutive slices it was possible to connect the presence of smooth muscle cells in AAAs tissue, which showed only weak acetylation of H3K9 within SMCs of AAA. Regarding histone H3K14ac and H3K18ac, VSMCs in AAAs tissue were weakly positive, and were almost all negative in control group. In addition, consecutive staining sections from the investigated samples were stained for CD45, CD68 and H3 lysine 9, lysine 14, and lysine 18, and matching area were compared. It was observed that almost all CD45 and CD68- positive cells were slightly positive for H3K9ac, H3K14ac and H3K18ac in AAAs. This study showed that H3K9ac, H3K14ac, and H3K18ac co-occur with other active histone modification in AAAs. Thus, it seems that at these sites all these “active” histone modifications are deposited by the corresponding activities sequentially, or at the same time, to act in a coordinated way.

With regard to the histone substrates analyzed in this study for the corresponding KATs, especially the deletion of KAT2A/KAT2B in AAA specifically and dramatically reduces acetylation on histone H3K9 (H3K9ac) while KAT3A/KAT3B specifically reduces acetylation on H3K18 and H3K27 (H3K18/27ac) [259]. Furthermore, The HAT domain of KAT6A/KAT6B is preceded by a tandem of plant homeodomain (PHD) fingers. Recently, Ali et al. demonstrated that the tandem PHD1/2 fingers of KAT6B (MORF) recognize the N-terminal tail of histone H3 [260]. Acetylation of Lys9 (H3K9ac) or Lys14 (H3K14ac) enhances binding of KAT6B PHD1/2 to unmodified H3 peptides two to three fold [260]. They suggested that the PHD1/2 fingers play a role in KAT6A/KAT6B association with the chromatic regions enriched in acetylated marks.

In general, H3K9 can also be methylated, which are three distinctive methylation states of histone H3K9, e.g., mono-, di-, and tri-methylation [261]. Acetylation of Lysine 9 of histone H3 (H3K9) correlates with gene activation, whereas enrichment of H3K9 methylation is associated with gene silencing [262].

4.7 Future perspectives

The current work outlines that histone acetylation and the expression of the corresponding histone acetyltransferases might markedly contribute to the progression of AAA. Further studies are however necessary, to gain a deeper insight into the mechanism of such epigenetic changes in cardiovascular diseases to be able to used

these knowledge in clinical everyday life and to find cost-effective diagnostic approaches and efficient therapeutic techniques [263]. It is already known that the influence of the environment in early childhood is able to induce epigenetic variations, which affects various metabolic pathways. Understanding the epigenetic aspects of AAA will aid in more exact predicting of patients at higher risk of AAA rupture, also proposing better lifestyle and dietary habits which could prevent AAA incidence in future generations. Further studies using various animal models of AAA will be useful in elucidating the role of epigenetics in AAA. It is still too early to say that treatments with e.g. inhibitors of histone deacetylases (HDACi) might be beneficial in AAA patients, since along with suppressing unfavorable gene expression, there is the possibility to reactivate unfavorable genes, resulting in unwanted complications.

In conclusion, epigenetic changes, histone acetylation particularly, take a significant turn in the aortic wall of AAA patients. These changes may play a pivotal role in activation of pathological immune responses, affecting the phenotype and survival of SMCs and negative remodeling of extracellular matrix of the vessel wall. Thus, this study has revealed not yet well known pathophysiologal changes in AAA, which has to be further investigated and might provide a solid basis for novel and more efficient diagnostic and therapeutic strategies.

5. SUMMARY

The exact mechanism of abdominal aortic aneurysm (AAA) is still unknown. Better understanding of pathophysiologic processes leading to AAA wall destabilization till rupture is indispensable for timely recognition of patients at risk. Epigenetics is a powerful tool to activate or silence gene transcription by changing chromatin structure. So far, no sufficient data are available about the potential contribution of epigenetic mechanism to the pathogenesis of AAA. This current doctoral thesis aimed therefore to investigate selected epigenetic modifications playing an important role in chromatin remodeling such as histone acetylation and expression of corresponding enzymes histone acetyltransferases (HAT, also named KAT for acetylation of lysine [K] residue) in the development and progression of AAA.

In the present study, 37 AAA patients (age 66.8 ± 11.4 years, max. diameter 62.8 ± 16.7 mm), who underwent open surgical procedure and 12 healthy aortic tissues were included (age 59.2 ± 19.4 years, $P = 0.111$). Following excision, AAA samples as well as control aortas were characterized by means of histology and immunohistochemistry (IHC). A comparative expression analysis of GNAT (KAT2A, KAT2B), CBP/P300 (KAT3A, KAT3B), MYST (KAT5, KAT6A, KAT6B, KAT7, KAT8), and TF-related family of HATs was performed at the mRNA level using RT-PCR and at protein level using western blot between AAA and healthy aortic group. The extent of acetylation of the individual cells within AAA wall was evaluated by IHC. Cellular association of HATs was performed by expression analysis using surface markers of the cells in AAA: CD45 for leukocytes, CD3 for T-cells, MSR1 for macrophages, SMTN and MYH11 for the contractile phenotype of smooth muscle cells (SMCs), MYH10 and collagen I for the synthetic phenotype of SMCs, and VCAM1 as a marker of endothelial cells (ECs). Statistical analysis was performed using *t*-test or ANOVA for normal distributed samples, Mann-Whitney-U-test or Kruskal-Wallis for non-parametric data. For categorical variables Chi-quadrate (χ^2) test was applied. Correlations were quantified using Spearman's rank correlation coefficient.

The expression of GNAT, CBP/P300, and MYST family of acetyltransferases analyzed in the present study at mRNA level was significantly higher in AAA than in control group ($P<0.01$). The expression of HATs was either significant lower in healthy aorta than in AAA (KAT2B, KAT3B, KAT6A, KAT6B) or was not detected (KAT2A, KAT3A, KAT5, KAT7, KAT8). In contrast, the expression of TF-related family of HATs was either increased in the control group (KAT4, $P=0.002$), or was detected neither in AAA nor in healthy aorta (KAT12). The highest expression among the HATs analyzed was observed in AAA for KAT2B (2.5-fold higher in AAA compared to control aorta, $P<0.001$), KAT3A (not expressed in healthy aorta), KAT3B (3.9-fold, $P=0.007$), and KAT6B (2.8-fold, $P<0.003$). These results were also

confirmed at protein level. Furthermore, the expression of KAT2B was significantly correlated with KAT3A, KAT3B and KAT6B (r=0.705; P<0.001, r=0.564; P=0.001 and r=0.528; P=0.007, respectively), KAT5 with KAT8 (r=0.443, P=0.001), and KAT6B with KAT3A, KAT3B and KAT6A (r=0.407, r=0.500 and r=0.531; P<0.05 in all cases). With regard to the cellular allocation, KAT3B seemed to be associated with inflammatory cells, correlating with CD45, CD3, and MSR1 (r=0.339, P=0.039; r=0.361, P=0.028 and r=0.351, P=0.032, respectively). Furthermore, strong correlation was seen between KAT6B and CD45 or CD3 (r=0.609, P<0.001 and r=0.553, P<0.001, respectively). In addition, negative correlation was detected between expression of KAT2A and expression of collagen I (r= -0.528, P<0.001). Furthermore, KAT6A was associated with the expression of VCAM-1 (r=0.541, P<0.001). Concluding from the IHC data, KAT2B, KAT3B, and KAT6B were expressed mainly in inflammatory cells. In contrast, SMCs, ECs and neovessels were only weak positive for the staining (KAT2B), or negative (KAT3B, KAT6A). Furthermore, KAT3B was detected particularly in T-cells. Referred to the substrate specificity of the strongly expressed HATs in AAA, H3K9, K14 and K18, they all followed the same pattern and seemed to be acetylated mainly in inflammatory leukocytes and macrophages.

In conclusion, epigenetic changes such as histone acetylation appear to undergo significant changes in the aortic wall of AAA patients compared to healthy aorta. Subsequently, aberrant expression of epigenetic modifier may be involved in the pathogenesis of AAA. These changes may play a pivotal role especially in activation of pathological immune responses, affecting the phenotype and survival of SMCs and contributing to negative remodeling of extracellular matrix of the aortic wall. Thus, the data of the current study provide important clues for better understanding of the pathobiology of AAA and might contribute to the development of novel diagnostic and therapeutic strategies.

6. REFERENCES

1 Moll FL, Powell JT, Fraedrich G, Verzini F, Haulon S, Waltham M, van Herwaarden JA, Holt PJ, van Keulen JW, Rantner B, Schlösser FJ, Setacci F, Ricco JB. Management of abdominal aortic aneurysms clinical practice guidelines of the European Society for Vascular Surgery. *Eur J endovasc Surg.* 2011;41:s1-s58.

2 Scott RA, Wilson NM, Ashton HA, Kay DN. Influence of screening on the incidence of ruptured abdominal aortic aneurysm: 5-year results of a randomised controlled study. *Br J Surg.* 1995;82:1066-70.

3 Lederle FA, Johnson GR, Wilson SE, Chute EP, Littooy FN, Bandyk D, Krupski WC, Barone GW, Acher CW, Ballard DJ. Prevalence and associations of abdominal aortic aneurysm detected through screening. Aneurysm Detection and Management (ADAM) Veterans Affairs Cooperative Study Group. *Ann Intern Med.* 1997;126:441-9.

4 Levin DC, Rao VM, Frangos AJ, Sunshine JH. Endovascular repair vs open surgical repair of abdominal aortic aneurysms: comparative utilization trends from 2001 to 2006. *J Am Coll Radiol.* 2009;6:506-9.

5 Vardulaki KA, Walker NM, Day NE, Duffy SW, Ashton HA, Scott RA. Quantifying the risks of hypertension, age, sex and smoking in patients with abdominal aortic aneurysm. *Br J Surg.* 2000;87:195-200.

6 Wilmink TB, Quick CR, Day NE. The association between cigarette smoking and abdominal aortic aneurysms. *J Vasc Surg.* 1999;30:1099-105.

7 Singh K, Bonaa KH, Jacobsen BK, Bjork L, Solberg S. Prevalence and risk factors for abdominal aortic aneurysms in a population-based study: the Tromsø Study. *Am J Epidemiol.* 2001;154:236-44.

8 Scott RA, Bridgewater SG, Ashton HA. Randomised clinical trial of screening for abdominal aortic aneurysm in women. *Br J Surg.* 2002;89:283-5.

9 Larsson E, Granath F, Swedenborg J, Hultgren R. A populationbased case-control study of the familial risk of abdominal aortic aneurysm. *J Vasc Surg.* 2009;49:47-50.

10 van Vlijmen-van Keulen CJ, Pals G, Rauwerda JA. Familial abdominal aortic aneurysm: a systematic review of a genetic background. *Eur J Vasc Endovasc Surg.* 2002;24:105-16.

11 Graham LM, Zelenock GB, Whitehouse Jr WM, Erlandson EE, Dent TL, Lindenauer SM, Stanley JC. Clinical significance of arteriosclerotic femoral artery aneurysms. *Arch Surg.* 1980;115:502-7.

12 Shapira OM, Pasik S, Wassermann JP, Barzilai N, Mashiah A. Ultrasound screening for abdominal aortic aneurysms in patients with atherosclerotic peripheral vascular disease. *J Cardiovasc Surg (Torino)*. 1990;31:170-2.

13 Sakalihasan N, Limet R, Defawe OD. Abdominal Aortic Aneurysm. *Lancet.* 2005;365: 1577-89.

14 Sofi F, Marcucci R, Giusti B, Pratesi G, Lari B, Sestini I, Lo Sapio P, Pulli R, Pratesi C, Abbate R, Gensini GF. High levels of homocysteine, lipoprotein (a) and plasminogen activator inhibitor-1 are present in patients with abdominal aortic aneurysm. *Thromb Haemost*. 2005;94:1094-8.

15 Salem MK, Rayt HS, Hussey G, Rafelt S, Nelson CP, Sayers RD, Naylor AR, Nasim A. Should Asian men be included in abdominal aortic aneurysm screening programmes? *Eur J Vasc Endovasc Surg.* 2009;38:748-9.

16 Yii MK. Epidemiology of abdominal aortic aneurysm in an Asian population. *ANZ J Surg.* 2003;73:393-5.

17 Hallin A, Bergqvist D, Holmberg L. Literature review of surgical management of abdominal aortic aneurysm. *Eur J Vasc Endovasc Surg*. 2001;22:197-204.

18 Watanabe Y, Shigematsu H, Obitsu Y, Koizumi N, Saiki N, Iwahashi T. Growth rates of abdominal aortic aneurysms in Japanese patients observed in one institute. *Int Angiol.* 2012;31:181-6.

19 Brady AR, Thompson SG, Fowkes FG, Greenhalgh RM, Powell JT. Abdominal aortic aneurysm expansion: risk factors and time intervals for surveillance. *Circulation*. 2004; 110:16-21.

20 Brady AR, Thompson SG, Greenhalgh RM, Powell JT. Cardiovascular risk factors and abdominal aortic aneurysm expansion: only smoking counts. US small aneurysm trial participants. *Br J Surg*. 2003;90:491-2.

21 Vega de CM, Gomez R, Estallo L, Rodriguez L, Baquer M, Barba A. Growth rate and associated factors in small abdominal aortic aneurysms. *Eur J Vasc Endovasc Surg.* 2006;31:231-6.

22 Kontopodis N, Metaxa E, Papaharilaou Y, Georgakarakos E, Tsetis D, Ioannou CV. Value of volume measurements in evaluating abdominal aortic aneurysms growth rate and need for surgical treatment. *Eur J Radiol.* 2014;83:1051-6.

23 Schouten O, van Laanen JH, Boersma E, Vidakovic R, Feringa HH, Dunkelgrun M, Bax JJ, Koning J, van Urk H, Poldermans D. Statins are associated with a reduced infrarenal abdominal aortic aneurysm growth. *Eur J Vasc Endovasc Surg*. 2006;32:21-6.

24 Sukhija R, Aronow WS, Sandhu R, Kakar P, Babu S. Mortality and size of abdominal aortic aneurysm at long-term follow-up of patients not treated surgically and treated with and without statins. *Am J Cardiol*. 2006;97:279-80.

25 Periard D, Guessous I, Mazzolai L, Haesler E, Monney P, Hayoz D. Reduction of small infrarenal abdominal aortic aneurysm expansion rate by statins. *Vasa*. 2012;41:35-42.

26 Vega de Céniga M, Gómez R, Estallo L, Rodríguez L, Baquer M, Barba A. Growth rate and associated factors in small abdominal aortic aneurysms. *Eur J Vasc Endovasc Surg*. 2006;31:231-6.

27 Leach SD, Toole AL, Stem H, DeNatale RW, Tilson MD. Effect of beta-adrenergic blockade on the growth rate of abdominal aortic aneurysms. *Arch Surg*. 1988;123:606-9.

28 Scott RA, Tisi PV, Ashton HA, Allen DR. Abdominal aortic aneurysm rupture rates: a 7-year follow-up of the entire abdominal aortic aneurysm population detected by screening. *J Vasc Surg*. 1998;28:124-8.

29 Limet R, Sakalihassan N, Albert A. Determination of the expansion rate and incidence of rupture of abdominal aortic aneurysms. *J Vasc Surg*. 1991;14:540-8.

30 Stenbaek J, Kalin B, Swedenborg J. Growth of thrombus may be a better predictor of rupture than diameter in patients with abdominal aortic aneurysms. *Eur J Vasc Endovasc Surg*. 2000;20:466-9.

31 Bengtsson H, Bergqvist D. Ruptured abdominal aortic aneurysm: a population-based study. *J Vasc Surg*. 1993;18:74-80.

32 Schumacher H, Eckstein HH, Kallinowski F, Allenberg JR. Morphometry and classification in abdominal aortic aneurysms: patient selection for endovascular and open surgery. *J Endovasc Surg*. 1997;4:39-44.

33 Kiell CS, Ernst CB. Advances in management of abdominal aortic aneurysm. *Adv Surg*. 1993;26:73-98.

34 Muluk SC, Gertler JP, Brewster DC, Cambria RP, LaMuraglia GM, Moncure AC, Darling RC, Abbott WM. Presentation and patterns of aortic aneurysms in young patients. *J Vasc Surg*. 1994;20:880-6.

35 Lederle FA, Simel DL. The rational clinical examination. Does this patient have abdominal aortic aneurysm? JAMA. 1999;281:77-82.

36 Lederle FA, Walker JM, Reinke DB. Selective screening for abdominal aortic aneurysms with physical examination and ultrasound. *Arch Intern Med*. 1988;148:1753-6.

37 May AG, DeWeese JA, Frank I, Mahoney EB, Rob CG. Surgical treatment of abdominal aortic aneurysms. *Surgery*. 1968;63:711-21.

38 Lindholt JS, Vammen S, Juul S, Henneberg EW, Fasting H. The validity of ultrasonographic scanning as screening method for abdominal aortic aneurysm. *Eur J Vasc Endovasc Surg*. 1999;17:472-5.

39 Sparks AR, Johnson PL, Meyer MC. Imaging of abdominal aortic aneurysms. *Am Fam Physician*. 2002; 65:1565-70.

40 Jaakkola P, Hippeläinen M, Farin P, Rytkönen H, Kainulainen S, Partanen K. Interobserver variability in measuring the dimensions of the abdominal aorta: comparison of ultrasound and computed tomography. *Eur J Vasc Endovasc Surg*. 1996;12:230-7.

41 Papanicolaou N, Wittenberg J, Ferrucci JT Jr, Stauffer AE, Waltman AC, Simeone JF, Mueller PR, Brewster DC, Darling RC. Preoperative evaluation of abdominal aortic aneurysms by computed tomography. *AJR Am J Roentgenol*. 1986;146:711-5.

42 Armon MP, Yusuf SW, Latief K, Whitaker SC, Gregson RH, Wenham PW, Hopkinson BR. Anatomical suitability of abdominal aortic aneurysms for endovascular repair. *Br J Surg*. 1997;84:178-80.

43 Balm R, Eikelboom BC, van Leeuwen MS, Noordzij J. Spiral CT-angiography of the aorta. *Eur J Vasc Surg*. 1994;8:544-51.

44 van Essen JA, Gussenhoven EJ, van der Lugt A, Huijsman PC, van Muiswinkel JM, van Sambeek MR, van Dijk LC, van Urk H. Accurate assessment of abdominal aortic aneurysm with intravascular ultrasound scanning: validation with computed tomographic angiography. *J Vasc Surg*. 1999;29:631-8.

45 Errington ML, Ferguson JM, Gillespie IN, Connell HM, Ruckley CV, Wright AR. Complete pre-operative imaging assessment of abdominal aortic aneurysm with spiral CT angiography. *Clin Radiol*. 1997;52:369-77.

46 Smoking, lung function and the prognosis of abdominal aortic aneurysm. The UK small aneurysm trial participants. *Eur J Vasc Endovasc Surg*. 2000;19:636-42.

47 Nakahashi TK, Hoshina K, Tsao PS, Sho E, Sho M, Karwowski JK, Yeh C, Yang RB, Topper JN, Dalman RL. Flow loading induces macrophage antioxidative gene expression in experimental aneurysms. *Arterioscler Thromb Vasc Biol*. 2002;22:2017-22.

48 Myers JN, White JJ, Narasimhan B, Dalman RL. Effects of exercise training in patients with abdominal aortic aneurysm: preliminary results from a randomized trial. *J Cardiopulm Rehabil Prev*. 2010;30:374-83.

49 Lindholt JS, Henneberg EW, Juul S, Fasting H. Impaired results of a randomized double blinded clinical trial of propranolol versus placebo on the expansion rate of small abdominal aortic aneurysms. *Int Angiol*. 1999;18:52-7.

50 Propanolol Aneurysm Trial Investigators. Propranolol for small abdominal aortic aneurysms: results of a randomized trial. *J Vasc Surg*. 2002;35:72-9.

51 Brady AR, Gibbs JS, Greenhalgh RM, Powell JT, Sydes MR. Perioperative beta-blockade (pobble) for patients undergoing infrarenal vascular surgery: results of a randomised doubleblind controlled trial. *J Vasc Surg*. 2005;41:602-9.

52 Yang H, Raymer K, Butler R, Parlow J, Roberts R. The effects of perioperative beta-blockade: results of the Metoprolol after Vascular Surgery (MaVS) study, a randomised controlled trial. *Am Heart J*. 2006;152:983-90.

53 Poldermans D, Bax JJ, Kertai MD, Krenning B, Westerhout CM, Schinkel AF, Thomson IR, Lansberg PJ, Fleisher LA, Klein J, van Urk H, Roelandt JR,Boersma E. Statins are associated with a reduced incidence of perioperative mortality in patients undergoing major noncardiac vascular surgery. *Circulation*. 2003;107: 1848-51.

54 Leurs LJ, Visser P, Laheij RJ, Buth J, Harris PL, Blankensteijn JD. Statin use is associated with reduced all-cause mortality after endovascular abdominal aortic aneurysm repair. *Vascular*. 2006;14:1-8.

55 Mosorin M, Niemelä E, Heikkinen J, Lahtinen J, Tiozzo V, Satta J, Juvonen T, Biancari F. The use of statins and fate of small abdominal aortic aneurysms. *Interact Cardiovasc Thorac Surg*. 2008;7:578-81.

56 Karrowni W, Dughman S, Hajj GP, Miller FJ Jr. Statin therapy reduces growth of abdominal aortic aneurysms. *J Investig Med*. 2011;59:1239-43.

57 Ferguson CD, Clancy P, Bourke B, Walker PJ, Dear A, Buckenham T, Norman P, Golledge J. Association of statin prescription with small abdominal aortic aneurysm progression. *Am Heart J*. 2010;159:307-13.

58 Hackam DG, Thiruchelvam D, Redelmeier DA. Angiotensin-converting enzyme inhibitors and aortic rupture: A population-based case-control study. *Lancet*. 2006;368:659-65.

59 Thompson A, Cooper JA, Fabricius M, Humphries SE, Ashton HA, Hafez H. An analysis of drug modulation of abdominal aortic aneurysm growth through 25 years of surveillance. *J Vasc Surg*. 2010;52:55-61.

60 Sweeting MJ, Thompson SG, Brown LC, Greenhalgh RM, Powell JT. Use of angiotensin converting enzyme inhibitors is associated with increased growth rate of abdominal aortic aneurysms. *J Vasc Surg*. 2010;52:1-4.

61 Baxter BT, Pearce WH, Waltke EA, Littooy FN, Hallett JW Jr, Kent KC, Upchurch GR Jr, Chaikof EL, Mills JL, Fleckten B, Longo GM, Lee JK, Thompson RW. Prolonged administration of doxycycline in patients with small asymptomatic abdominal aortic aneurysms: Report of a prospective (Phase II) multicenter study. *J Vasc Surg.* 2002;36: 1-12.

62 Abdul-Hussien H, Hanemaaijer R, Verheijen JH, van Bockel JH, Geelkerken RH, Lindeman JH. Doxycycline therapy for abdominal aneurysm: Improved proteolytic balance through reduced neutrophil content. *J Vasc Surg.* 2009;49:741-9.

63 Hirsch AT, Haskal ZJ, Hertzer NR, Bakal CW, Creager MA, Halperin JL, Hiratzka LF, Murphy WR, Olin JW, Puschett JB, Rosenfield KA, Sacks D, Stanley JC,Taylor LM Jr, White CJ, White J, White RA, Antman EM, Smith SC Jr, Adams CD, Anderson JL, Faxon DP, Fuster V, Gibbons RJ, Hunt SA, Jacobs AK, Nishimura R, Ornato JP, Page RL, Riegel B. ACC/AHA 2005 Practice Guidelines for the management of patients with peripheral arterial disease (lower extremity, renal, mesenteric, and abdominal aortic): a collaborative report from the American Association for Vascular Surgery/Society for Vascular Surgery, Society for Cardiovascular Angiography and Interventions, Society for Vascular Medicine and Biology, Society of Interventional Radiology, and the ACC/AHA Task Force on Practice Guidelines (Writing Committee to Develop Guidelines for the Management of Patients With Peripheral Arterial Disease): endorsed by the American Association of Cardiovascular and Pulmonary Rehabilitation; National Heart, Lung, and Blood Institute; Society for Vascular Nursing; TransAtlantic Inter-Society Consensus; and Vascular Disease Foundation. *Circulation.* 2006;113:463–654.

64 Ernst CB. Current therapy for infrarenal aortic aneurysms. *N Engl J Med.* 1997;336:59-60.

65 Prager MR, Hoblaj T, Nanobashvili J, Sporn E, Polterauer P, Wagner O, Böhmig HJ, Teufelsbauer H, Ploner M, Huk I. Collagen- versus gelatine-coated Dacron versus stretch PTFE bifurcation grafts for aortoiliac occlusive disease: long-term results of a prospective, randomized multicenter trial. *Surgery.* 2003;134:80-5.

66 Parodi JC, Palmaz JC, Barone HD. Transfemoral intraluminal graft implantation for abdominal aortic aneurysms. *Ann Vasc Surg.* 1991;5:491-9.

67 Teufelsbauer H1, Prusa AM, Wolff K, Polterauer P, Nanobashvili J, Prager M, Hölzenbein T, Thurnher S, Lammer J, Schemper J, Schemper M, Kretschmer G, Huk I. Endovascular stent grafting versus open surgical operation in patients with infrarenal aortic aneurysms: apropensity score-adjusted analysis. *Circulation.* 2002;106:782-7.

68 Arko FR, Hill BB, Reeves TR, Olcott C, Harris EJ, Fogarty TJ, Zarins CK. Early and late functional outcome assessments following endovascular and open aneurysm repair. *J Endovasc Ther.* 2003;10:2-9.

69 Sicard GA, Zwolak RM, Sidawy AN, White RA, Siami FS. Endovascular abdominal aortic aneurysm repair: long-term outcome measures in patients at high-risk for open surgery. *J Vasc Surg.* 2006;44:229-36.

70 Hua HT, Cambria RP, Chuang SK, Stoner MC, Kwolek CJ, Rowell KS, Khuri SF, Henderson WG, Brewster DC, Abbott WM. Early outcomes of endovascular versus open abdominal aortic aneurysm repair in the National Surgical Quality Improvement Program-Private Sector (NSQIP-PS). *J Vasc Surg.* 2005;41:382-9.

71 Becquemin JP, Pillet JC, Lescalie F, Sapoval M, Goueffic Y, Lermusiaux P Steinmetz E, Marzelle J; ACE trialists. ACE trialists. A randomized controlled trial of endovascular aneurysm repair versus open surgery for abdominal aortic aneurysms in low-to moderate-risk patients. *J Vasc Surg.* 2011;53:1167-73.

72 Mani K, Bjrck M, Lundkvist J, Wanhainen A. Improved long-term survival after abdominal aortic aneurysm repair. *Circulation.* 2009;120:201-11.

73 De Bruin JL, Baas AF, Buth J, Prinssen M, Verhoeven EL, Cuypers PW, van Sambeek MR, Balm R, Grobbee DE, Blankensteijn JD; DREAM Study Group. DREAM Study Group. Long-term outcome of open or endovascular repair of abdominal aortic aneurysm. *N Engl J Med.* 2010;362:1881-9.

74 United Kingdom EVAR Trial Investigators, Greenhalgh RM, Brown LC, Powell JT, Thompson SG, Epstein D, Sculpher MJ. Endovascular versus open repair of abdominal aortic aneurysm. *N Engl J Med.* 2010;362:1863-71.

75 Schermerhorn ML, O'Malley AJ, Jhaveri A, Cotterill P, Pomposelli F, Landon BE. Endovascular vs. open repair of abdominal aortic aneurysms in the Medicare population. *N Engl J Med.* 2008;358:464-74.

76 Sakalihasan N, Limet R, Defawe OD. Abdominal aortic aneurysm. *Lancet.* 2005;365: 1577-89.

77 Han YS, Zhang J, Xia Q, Liu ZM, Zhang XY, Wu XY, Lun Y, Xin SJ, Duan ZQ, Xu K. A comparative study on the medium-long term results of endovascular repair and open surgical repair in the management of ruptured abdominal aortic aneurysms. *Chin Med J (Engl).* 2013;126:4771-9.

78 Powell JT, Bashir A, Dawson S, Vine N, Henney AM, Humphries SE, Greenhalgh RM. Genetic variation on chromosome 16 is associated with abdominal aortic aneurysm. *Clin Sci (Lond).* 1990;78:13-6.

79 Schuld J, Kollmar O, Schuld S, Schommer K, Richter S. Impact of meteorological conditions on abdominal aortic aneurysm rupture: evaluation of an 18-year period and review of the literature. *Vasc Endovascular Surg.* 2013;47:524-31.

80 Wang DH, Makaroun M, Webster MW, Vorp DA. Mechanical properties and microstructure of intraluminal thrombus from abdominal aortic aneurysm. *J Biomech Eng.* 2001;123:536-9.

81 Dobrin PB, Mrkvicka R. Failure of elastin or collagen as possible critical connective tissue alteration underlying aneurysmal dilatation. *Cardiovasc Surg.* 1994;2:484-8.

82 Zhang J, Schmidt J, Ryschich E, Schumacher H, Allenberg JR. Increased apoptosis and decreased density of medial smooth muscle cells in human abdominal aortic aneurysms. *Chin Med J (Engl).* 2003;116:1549-52.

83 López-Candales A, Holmes DR, Liao S, Scott MJ, Wickline SA, Thompson RW. Decreased vascular smooth muscle cell density in medial degeneration of human abdominal aortic aneurysms. *Am J Pathol.* 1997;150: 993-1007.

84 Henderson EL, Geng YJ, Sukhova GK, Whittemore AD, Knox J, Libby P. Death of smooth muscle cells and expression of mediators of apoptosis by T lymphocytes in human abdominal aortic aneurysms. *Circulation.* 1999;99:96-104.

85 Geng YJ, Henderson LE, Levesque EB, Muszynski M, Libby P. Fas is expressed in human atherosclerotic intima and promotes apoptosis of cytokine-primed human vascular smooth muscle cells. *Arterioscler Thromb Vasc Biol.* 1997;17:2200-8.

86 Geng YJ, Wu Q, Muszynski M, Hansson GK, Libby P. Apoptosis of vascular smooth muscle cells induced by in vitro stimulation with interferon-gamma, tumor necrosis factor-alpha, and interleukin-1 beta. *Arterioscler Thromb Vasc Biol.* 1996;16:19-27.

87 Pearce WH, Koch AE. Cellular components and features of immune response in abdominal aortic aneurysms. *Ann N Y Acad Sci.* 1996; 800:175-85.

88 Juvonen J, Surcel HM, Satta J, Teppo AM, Bloigu A, Syrjälä H, Airaksinen J, Leinonen M, Saikku P, Juvonen T. Elevated circulating levels of inflammatory cytokines in patients with abdominal aortic aneurysm. *Arterioscler Thromb Vasc Biol.* 1997;17:2843-7.

89 Newman KM, Jean-Claude J, Li H, Ramey WG, Tilson MD. Cytokines that activate proteolysis are increased in abdominal aortic aneurysms. *Circulation.* 1994;90:II224-7.

90 Tanaka S, Toh Y, Mori R, Komori K, Okadome K, Sugimachi K. Possible role of cytomegalovirus in the pathogenesis of inflammatory aortic diseases: a preliminary report. *J Vasc Surg.* 1992;16:274-9.

91 McCormick ML, Gavrila D, Weintraub NL. Role of oxidative stress in the pathogenesis of abdominal aortic aneurysms. *Arterioscler Thromb Vasc Biol.* 2007;27:461-9.

92 Freestone T, Turner RJ, Coady A, Higman DJ, Greenhalgh RM, Powell JT. Inflammation and and matrix metalloproteinases in the enlarging abdominal aortic aneurysm. *Arterioscler Thromb Vasc Biol.* 1995;15:1145-51.

93 Hirose H, Tilson MD. Abdominal aortic aneurysm as an autoimmune disease. *Ann N Y Acad Sci.* 2001;947:416-8.

94 Jagadesham VP, Scott DJ, Carding SR. Abdominal aortic aneurysms: an autoimmune disease? *Trends Mol Med.* 2008;1:522-9.

95 Zhang J, Böckler D, Ryschich E, Klemm K, Schumacher H, Schmidt J, Allenberg JR. Impaired Fas-induced apoptosis of T lymphocytesin patients with abdominal aortic aneurysms. *J Vasc Surg.* 2007:45:1039-46.

96 Yin M, Zhang J, Wang Y, Wang S, Böckler D, Duan Z, Xin S. Deficient CD4+CD25+ T regulatory cell function in patients with abdominal aortic aneurysms. *Arterioscler Thromb Vasc Biol.* 2010;30:1825-31.

97 Vine N, Powell JT. Metalloproteinases in degenerative aortic disease. *Clin Sci.* 1991;81: 233-9.

98 Newman KM, Ogata Y, Malon AM, Irizarry E, Gandhi RH, Nagase H, Tilson MD. Identification of matrix metalloproteinases 3 (stromelysin-1) and 9 (gelatinase B) in abdominal aortic aneurysm. *Arterioscler Thromb.* 1994;14:1315-20.

99 Knox JB, Sukhova GK, Whittemore AD, Libby P. Evidence for altered balance between matrixmetalloproteinases and their inhibitors in human aortic disease. *Circulation.* 1997; 95:205-12.

100 Thompson RW, Holmes DR, Mertens RA, Liao S, Botney MD, Mecham RP, Welgus HG, Parks WC. Production and localization of 92-kilodalton gelatinase in abdominal aortic aneurysms: an elastolytic metalloproteinase expressed by aneurysm-infiltrating macrophages. *J Clin Invest.* 1995;96:318-26.

101 McMillan WD, Pearce WH. Increased plasma levels of metalloproteinase-9 are associated with abdominal aortic aneurysms. *J Vasc Surg.* 1999;29:122-7.

102 McMillan WD, Tamarina NA, Cipollone M, Johnson DA, Parker MA, Pearce WH. Size matters: the relationship between MMP-9 expression and aortic diameter. *Circulation.* 1997;96:2228-32.

103 Pyo R, Lee JK, Shipley JM, Curci JA, Mao D, Ziporin SJ, Ennis TL, Shapiro SD, Senior RM, Thompson RW. Targeted gene disruption of matrix metalloproteinase-9 (gelatinase B) suppresses development of experimental abdominal aortic aneurysms. *J Clin Invest.* 2000;105:1641-9.

104 Ferry G., Goonesekera SD, Feig LA. Activation of MMP-9 by neutrophil elastase in an in vivo model of acute lung injury. *FEBS Lett.* 1997;402:111-5.

105 Mazzieri R, Masiero L, Zanetta L, Monea S, Onisto M, Garbisa S, Mignatti P. Control of type IV collagenase activity by components of the urokinase-plasmin system: a regulatory mechanism with cell-bound reactants. *EMBO J.* 1997;16:2319-32.

106 Davis V, Persidskaia R, Baca-Regen L, Itoh Y, Nagase H, Persidsky Y, Ghorpade A, Baxter BT. Matrix metalloproteinase-2 production and its binding to the matrix are increased in abdominal aortic aneurysms. *Arterioscler Thromb Vasc Biol.* 1998;18: 1625-33.

107 Longo GM, Xiong W, Greiner TC, Zhao Y, Fiotti N, Baxter BT. Matrix metalloproteinase 2 and 9 work in concert to produce aortic aneurysms. *J Clin Invest.* 2002;110:625-32.

108 Longo GM, Buda SJ, Fiotta N, Xiong W, Griener T, Shapiro S, Baxter BT. MMP-12 has a role in abdominal aortic aneurysms in mice. *Surgery.* 2005;137:457-62.

109 Curci JA, Liao S, Huffman MD, Shapiro SD, Thompson RW. Expression and localization of macrophage elastase (matrix metalloproteinase-12) in abdominal aortic aneurysms. *J Clin Invest.* 1998;102:1900-10.

110 Kurosawa K, Matsumura JS, Yamanouchi D. Current status of medical treatment for abdominal aortic aneurysm. *Circ J.* 2013;77:2860-6.

111 Larsson E, Granath F, Swedenborg J, Hultgren R. A population-based case-control study of the familial risk of abdominal aortic aneurysm. *J Vasc Surg.* 2009;49:47-50.

112 Kuivaniemi H, Ryer EJ, Elmore JR, Hinterseher I, Smelser DT, Tromp G. Update on Abdominal Aortic Aneurysm Research: From Clinical to Genetic Studies. *Scientifica (Cairo).* 2014;2014:564734.

113 Elmore JR, Obmann MA, Kuivaniemi H, Tromp G, Gerhard GS, Franklin DP, Boddy AM, Carey DJ. Identification of a genetic variant associated with abdominal aortic aneurysms on chromosome 3p12.3 by genome wide association. *J Vasc Surgery.* 2009; 49:1525-31.

114 Helgadottir A, Thorleifsson G, Magnusson KP, Grétarsdottir S, Steinthorsdottir V, Manolescu A, Jones GT, Rinkel GJ, Blankensteijn JD, Ronkainen A, et al. The same sequence variant on 9p21 associates with myocardial infarction, abdominal aortic aneurysm and intracranial aneurysm. *Nat Genet.* 2008;40:217-24.

115 Gretarsdottir S, Baas AF, Thorleifsson G, Holm H, den Heijer M, de Vries JP, Kranendonk SE, Zeebregts CJ, van Sterkenburg SM, Geelkerken RH, et al.

Genomewide association study identifies a sequence variant within the DAB2IP gene conferring susceptibility to abdominal aortic aneurysm. *Nat Genet.* 2010;42: 692-7.

116 Bown MJ1, Jones GT, Harrison SC, Wright BJ, Bumpstead S, Baas AF, Gretarsdottir S, Badger SA, Bradley DT, Burnand K, et al. Abdominal aortic aneurysm is associated with a variant in low-density lipoprotein receptor-related protein 1. *Am J Hum Genet.* 2011;89:619-27.

117 Bradley DT, Hughes AE, Badger SA, Jones GT, Harrison SC, Wright BJ, Bumpstead S, Baas AF, Grétarsdóttir S, Burnand K, et al. A variant in LDLR is associated with abdominal aortic aneurysm. *Circ Cardiovasc Genet.* 2013;6:498-504.

118 Berger SL, Kouzarides T, Shiekhattar R, Shilatifard A. An operational definition of epigenetics. *Genes Dev.* 2009;23:781-3.

119 Goldberg AD, Allis CD, Bernstein E. Epigenetics: a landscape takes shape. *Cell.* 2007;128:635-8.

120 Waggoner D. Mechanisms of disease: Epigenesis. *Semin Pediatr Neurol.* 2007;14:7-14.

121 Komberg RD. Chromatin structure: a repeating unit of histones and DNA. *Science.* 1974;184:868-71.

122 Matouk CC, Marsden PA. Epigenetic regulation of vascular endothelial gene expression. *Circ Res.* 2008;102:873-87.

123 Sabeti PC, Schaffner SF, Fry B, Lohmueller J, Varilly P, Shamovsky O, Palma A, Mikkelsen TS, Altshuler D, Lander ES. Positive natural selection in the human lineage. *Science.* 2006;312:1614-20

124 Krebs JR. The gourmet ape: evolution and human food preferences. *Am J Clin Nutr.* 2009;90:707S-711S.

125 Kelley JL, Swanson WJ. Positive selection in the human genome: from genome scans to biological significance. *Annu Rev Genomics Hum Genet.* 2008;9:143-60.

126 Mirbahai L, Chipman JK. Epigenetic memory of environmental organisms: a reflection of lifetime stressor exposures. *Mutat Res Genet Toxicol Environ Mutagen.* 2014;764-765: 10-7.

127 Tazi J, Bird A. Alternative chromatin structure at CpG islands. *Cell.* 1990:60:909-20.

128 Miranda TB, Jones PA. DNA methylation: the nuts and bolts of repression. *J Cell Physiol.* 2007;213:384-90.

129 Turunen MP, Aavik E, Ylä-Herttuala S. Epigenetics and atherosclerosis. *Acta Bioch Bioph SIN.* 2009;1790:886–891.

130 Ling C, Groop L. Epigenetics: a molecular link between environmental factors and type 2 diabetes. *Diabetes.* 2009;58:2718-25.

131 Friso S, Pizzolo F, Choi SW, Guarini P, Castagna A, Ravagnani V, Carletto A, Pattini P, Corrocher R, Olivieri O. Epigenetic control of 11 beta-hydroxysteroid dehydrogenase 2 gene promoter is related to human hypertension. *Atherosclerosis.* 2008;199:323-7.

132 Kouzarides T. Chromatin modifications and their function. *Cell.* 2007;128:693-705.

133 Rice JC, Allis CD. Histone methylation versus histone acetylation: new insights into epigenetic regulation. *Curr Opin Cell Biol.* 2001;13:263-73.

134 Allfery VG, Faulkner R, Mirsky AE. Acetylation and methylation of histones and their possible role in the regulation of RNA synthesis. *Proc Natl Acad Sci USA.* 1964;51: 786-94.

135 Marks PA, Miller T, Richon VM. Histone deacetylases. *Curr Opin Pharmacol.* 2003;3: 344-51.

136 Kelly WK, O'Connor OA, Marks PA. Histone deacetylase inhibitors: from target to clinical trials. *Expert Opin Investig Drugs.* 2002;11:1695-713.

137 Khan SN, Khan AU. Role of histone acetylation in cell physiology and diseases: An update. *Clin Chim Acta.* 2010;411:1401-11.

138 Doyon Y, Selleck W, Lane WS, Tan S, Côté J. Structural and functional conservation of the NuA4 histone acetyltransferase complex from yeast to humans. *Mol Cell Biol.* 2004;24:1884-96.

139 Smith ER, Cayrou C, Huang R, Lane WS, Côté J, Lucchesi JC. A human protein complex homologous to the Drosophila MSL complex is responsible for the majority of histone H4 acetylation at lysine 16.*Mol Cell Biol.* 2005;25:9175-88.

140 Valor LM, Viosca J, Lopez-Atalaya JP, Barco A. Lysine acetyltransferases CBP and p300 as therapeutic targets in cognitive and neurodegenerative disorders. *Curr Pharm Des.* 2013;19:5051-64.

141 Allis CD, Berger SL, Cote J, Dent S, Jenuwien T, Kouzarides T, Pillus L, Reinberg D, Shi Y, Shiekhattar R, Shilatifard A, Workman J, Zhang Y. New nomenclature for chromatin- modifying enzymes. *Cell.* 2007;131:633-6.

142 Santos-Rosa H, Caldas C. Chromatin modifier enzymes, the histone code and cancer. *Eur J Cancer.* 2005;41:2381-402.

143 Furdas SD, Kannan S, Sippl W, Jung M. Small molecule inhibitors of histone acetyltransferases as epigenetic tools and drug candidates. *Arch Pharm (Weinheim).* 2012;345:7-21.

144 Brownell JE, Zhou J, Ranalli T, Kobayashi R, Edmondson DG, Roth SY, Allis CD. Tetrahymena histone acetyltransferase A: a homolog to yeast Gcn5p linking histone acetylation to geneactivation. *Cell.* 1996;84:843-51.

145 Nagy Z, Tora L. Distinct GCN5/PCAF-containing complexes function as co-activators and are involved in transcription factor and global histone acetylation. *Oncogene.* 2007;26:5341-57.

146 Yanagisawa J, Kitagawa H, Yanagida M, Wada O, Ogawa S, Nakagomi M, Oishi H, Yamamoto Y, Nagasawa H, McMahon SB, Cole MD, Tora L, Takahashi Nekton. Nuclear receptor function requires a TFTC-type histone acetyl transferases complex. *Mol Cell.* 2002;9:553-62.

147 Yang XJ, Ogryzko VV, Nishikawa J, Howard BH, Nakatani Y. A p300/CBP-associated factor that competes with the adenoviral oncoprotein E1A. *Nature.* 1996;382:319-24.

148 Sartorelli V, Puri PL, Hamamori Y, Ogryzko V, Chung G, Nakatani Y, Wang JY, Kedes L. Acetylation of MyoD directed by PCAF is necessary for the execution of the muscle program. *Mol Cell.* 1999;4:725-34.

149 Pons D, Trompet S, de Craen AJ, Thijssen PE, Quax PH, de Vries MR, Wierda RJ, van den Elsen PJ, Monraats PS, Ewing MM, Heijmans BT, Slagboom PE, Zwinderman AH, Doevendans PA, Tio RA, de Winter RJ, de Maat MP, Iakoubova OA, Sattar N, Shepherd J, Westendorp RG, Jukema JW. Genetic variation in PCAF, a key mediator in epigenetics, is associated with reduced vascular morbidity and mortality: evidence for a new concept from three independent prospective studies. *Heart.* 2011;97:143-50.

150 Roth SY, Denu JM, Allis CD. Histone acetyltransferases. *Annu Rev Biochem.* 2001;70: 81-120.

151 Timmermann S, Lehrmann H, Polesskaya A, Harel-Bellan A. Histone acetylation and disease. *Cell Mol Life Sci.* 2001;58:728-36.

152 Chrivia JC, Kwok RP, Lamb N, Hagiwara M, Montminy MR, Goodman RH. Phosphorylated CREB binds specifically to the nuclear protein CBP. *Nature.* 1993;365: 855-9.

153 Bannister AJ, Oehler T, Wilhelm D, Angel P, Kouzarides T. Stimulation of c-Jun activity

by CBP: c-Jun residues Ser63/73 are required for CBP induced stimulation in vivo and CBP binding in vitro. *Oncogene.* 1995;11:2509-14.

154 Janknecht R, Hunter T. Versatile molecular glue. Transcriptional control. *Curr Biol.* 1996;6:951-4.

155 Whyte P, Williamson NM, Harlow E. Cellular targets for transformation by the adenovirus E1A proteins. *Cell.* 1989;56:67-75.

156 Bedford DC, Kasper LH, Fukuyama T, Brindle PK. Target gene context influences the transcriptional requirement for the KAT3 family of CBP and p300 histone acetyltransferases. *Epigenetics.* 2010;5:9-15.

157 Wu C, Miloslavskaya I, Demontis S, Maestro R, Galaktionov K. Regulation of cellular response to oncogenic and oxidative stress by Seladin-1. *Nature.* 2004;432:640-5.

158 Bousiges O, Vasconcelos AP, Neidl R, Cosquer B, Herbeaux K, Panteleeva I, Loeffler JP, Cassel JC, Boutillier AL. Spatial memory consolidation is associated with induction of several lysineacetyltransferase (histone acetyltransferase) expression levels and H2B/H4 acetylation-dependent transcriptional events in the rat hippocampus. *Neuropsychopharmacology.* 2010;35:2521-37.

159 Chan HM, La Thangue NB. p300/CBP proteins: HATs for transcriptional bridges and scaffolds. *J Cell Sci.* 2001;114:2363-73.

160 Shikama N. The p300/CBP family: integrating signals with transcription factors and chromatin. *Trends Cell Biol.* 1997;7:230-6.

161 Voss AK, Thomas T. MYST family histone acetyltransferases take center stage in stem cells and development. *Bioessays.* 2009;31:1050-61.

162 Kamine J, Elangovan B, Subramanian T, Coleman D, Chinnadurai G. Identification of a cellular protein that specifically interacts with the essential cysteine region of the HIV-1 Tat transactivator. *Virology.* 1996;216:357-66.

163 Brady ME, Ozanne DM, Gaughan L, Waite I, Cook S, Neal DE, Robson CN. Tip60 is a nuclear hormone receptor co-activator. *J Biol Chem.* 1999;274:17599-604.

164 Baek SH, Ohgi KA, Rose DW, Koo EH, Glass CK, Rosenfeld MG. Exchange of N-CoR corepressor and Tip60 co-activator complexes links gene expression by NF-kappaB and beta-amyloid precursor protein. *Cell.* 2002;110:55–67.

165 Frank SR, Parisi T, Taubert S, Fernandez P, Fuchs M, Chan HM, Livingston DM, Amati B. MYC recruits the TIP60 histone acetyltransferase complex to chromatin. *EMBO Rep.* 2003;4:575-80.

166 Berns K, Hijmans EM, Mullenders J, Brummelkamp TR, Velds A, Heimerikx M, Kerkhoven RM, Madiredjo M, Nijkamp W, Weigelt B, Agami R, Ge W, Cavet G,Linsley PS, Beijersbergen RL, Bernards R. A large-scale RNAi screen in human cells identifies new components of the p53 pathway. *Nature.* 2004;428:431-7.

167 Champagne N, Pelletier N, Yang XJ. The monocytic leukemia zinc finger protein MOZ is a histone acetyltransferase. *Oncogene.* 2001;20:404-9.

168 Kitabayashi I, Aikawa Y, Nguyen LA, Yokoyama A, Ohki M. Activation of AML1-mediated transcription by MOZ and inhibition by the MOZ–CBP fusion protein. *Embo J.* 2001;20:7184-96.

169 Pelletier N, Champagne N, Stifani S, Yang XJ. MOZ and MORF histone acetyltransferases interact with the Runt-domain transcription factor Runx2. *Oncogene.* 2002;21:2729-40.

170 Chan EM, Chan RJ, Comer EM, Goulet RJ 3rd, Crean CD, Brown ZD, Fruehwald AM, Yang Z, Boswell HS, Nakshatri H, Gabig TG.. MOZ and MOZ–CBP cooperate with NF-kappaB to activate transcription from NF-kappaB-dependent promoters. *Exp Hematol.* 2007;35:1782-92.

171 Yang XJ, Ullah M. MOZ and MORF, two large MYSTic HATs in normal and cancer stem cells. *Oncogene.* 2007;26:5408-19.

172 Champagne N, Bertos NR, Pelletier N, Wang AH, Vezmar M, Yang Y, Heng HH, Yang XJ. Identification of a human histone acetyltransferase related to monocytic leukemia zinc finger protein. *J Biol Chem.* 1999;274:28528-36.

173 Panagopoulos I, Fioretos T, Isaksson M, Samuelsson U, Billström R, Strömbeck B, Mitelman F, Johansson B. Fusion of the MORF and CBP genes in acute myeloid leukemia with the t(10;16) (q22; p13). *Hum Mol Genet.* 2001;10:395-404.

174 Moore SD, Herrick SR, Ince TA, Kleinman MS, Dal Cin P, Morton CC, Quade BJ. Uterine leiomyomata with t(10;17) disrupt the histone acetyltransferase MORF. *Cancer Res.* 2004;64:5570-7.

175 Iizuka M., Stillman B. Histone acetyltransferase HBO1 interacts with the ORC1 subunit of the human initiator protein. *J Biol Chem.* 1999;274:23027-34.

176 DePamphilis ML. The 'ORC cycle': a novel pathway for regulating eukaryotic DNA replication. *Gene.* 2003;310:1-15.

177 Iizuka M, Matsui T, Takisawa H, Smith MM. Regulation of replication licensing by acetyltransferase Hbo1. *Mol Cell Biol.* 2006;26:1098-108.

178 Rea S, Xouri G and Akhtar A. Males absent on the first (MOF): from flies to humans. *Oncogene.* 2007;26:5385-94.

179 Sykes SM, Mellert HS, Holbert MA, Li K, Marmorstein R, Lane WS, McMahon SB. Acetylation of the p53 DNA-binding domain regulates apoptosis induction. *Mol Cell.* 2006;24:841-51.

180 Hilfiker A, Hilfiker-Kleiner D, Pannuti A, Lucchesi JC. Mof, a putative acetyl transferases gene related to Tip60 and MOZ human genes and to the SAS gene of yeast, is required for dosage compensation in Drosophila. *EMBO J.* 1997;16:2054-60.

181 Sharma GG, So S, Gupta A, Kumar R, Cayrou C, Avvakumov N, Bhadra U, Pandita RK, Porteus MH, Chen DJ, Cote J, Pandita TK. MOF and histone H4 acetylation at lysine 16 are critical for DNA damage response and double-strand break repair. *Mol Cell Biol.* 2010;30:3582-95.

182 Gupta A, Guerin-Peyrou TG, Sharma GG, Sharma GG, Park C, Agarwal M, Ganju RK, Pandita S, Choi K, Sukumar S, Pandita RK, Ludwig T, Pandita TK. The mammalian ortholog of Drosophla MOF that acetylates histone H4 lysine 16 is essential for embryogenesis and oncogenesis. *Mol Cell Biol.* 2008;28:397-409.

183 Pfister S, Rea S, Taipale M, Mendrzyk F, Straub B, Ittrich C, Thuerigen O, Sinn HP, Akhtar A, Lichter P. The histone acetyltransferase hMOF is frequently downregulated in primary breast carcinoma and medulloblastoma and constitutes a biomarker for clinical outcome in medulloblastoma. *Int J Cancer.* 2008;122:1207-13.

184 Roeder R. The role of general initiation factors in transcription by RNA polymerase II. *Trends Biochem Sci.* 1996;21:327-35.

185 Mizzen CA, Yang XJ, Kokubo T, Brownell JE, Bannister AJ, Owen-Hughes T, Workman J, Wang L, Berger SL, Kouzarides T, Nakatani Y, Allis CD. The TAF(II)250 subunit of TFIID has histone acetyltransferase activity. *Cell.*1996;87:1261-70.

186 Dikstein R, Ruppert S, Tjian R. TAFII250 is a bipartite protein kinase that phosphorylates the base transcription factor RAP74. *Cell.* 1996;84:781-90.

187 Lively TN, Ferguson HA, Galasinski SK, Seto AG, Goodrich JA. c-Jun binds the N terminus of human TAFII 250 to derepress RNA polymerase II transcription in vitro. *J Biol Chem.* 2001;276:25582-8.

188 Tavassoli P, Wafa LA, Cheng H, Zoubeidi A, Fazli L, Gleave M, Snoek R, Rennie PS. TAF1 differentially enhances androgen receptor transcriptional activity via its N-terminal kinase and ubiquitin-activating and -conjugating domains. *Mol Endocrinol.* 2010;24:696-708.

189 Willis IM. RNA polymerase III. Genes, factors and transcriptional specificity. *Eur J Biochem*. 1993;212:1-11.

190 Kundu TK, Wang Z, Roeder RG. Human TFIIIC relieves chromatin-mediated repression of RNA polymerase III transcription and contains an intrinsic histone acetyltransferase activity. *Mol Cell Biol.* 1999;19:1605-15.

191 Lassar AB, Martin PL, Roeder RG. Transcription of class III genes: formation of preinitiation complexes. *Science.* 1983;222:740-8.

192 Wang Z, Roeder RG. Three human RNA polymerase III specific subunits form a subcomplex with a selective function in specific transcription initiation. *Genes Dev.* 1997;11:1315-26.

193 Gray SG, Ekstrom TJ. The human histone deacetylse family. *Exp Cell Res.* 2006;262: 75-83.

194 Grozinger CM, Schreiber SL. Deacetylase enzymes: biological functions and the use of small-molecule inhibitors. *Chem Biol.* 2002;9:3-16.

195 Li Z, Zhu WG. Targeting Histone Deacetylases for Cancer Therapy: From Molecular Mechanisms to Clinical Implications. *Int J Biol Sci.* 2014;10:757-70.

196 Turunen MP, Aavik E, Ylä-Herttuala S. Epigenetics and atherosclerosis. *Biochim Biophys Acta.* 2009;1790:886–891.

197 Sharma P, Kumar J, Garg G, Kumar A, Patowary A, Karthikeyan G, Ramakrishnan L, Brahmachari V, Sengupta S. Detection of altered global DNA methylation in coronary artery disease patients. *DNA Cell Biol.* 2008;27:357-65.

198 Krishna SM, Dear AE, Norman PE, Golledge J. Genetic and epigenetic mechanisms and their possible role in abdominal aortic aneurysm. *Atherosclerosis.* 2010;212:16-29.

199 World Medical Association Declaration of Helsinki. Recommendations guiding physicians in biomedical research involving human subjects. *Cardiovasc Res.* 1997;35: 2-3.

200 Reeps C, Pelisek J, Seidl S, Schuster T, Zimmermann A, Kuehnl A, Eckstein HH. Inflammatory infiltrates and neovessels are relevant sources of MMPs in abdominal aortic aneurysm wall. *Pathobiology.* 2009;76:243-52.

201 ImageJ[http://rsb.info.nih.gov/ij/]

202 Warnke RA, Gatter KC, Falini B, Hildreth P, Woolston R-E, Pulford K, Cordell JL, Cohen B, De Wolf-Peeters C, Mason DY. Diagnosis of human lymphoma with

monoclonal antileukocyte antibodies. *N Engl J Med*. 1983;309:1275-81.

203 Shimizu K, Mitchell RN, Libby P. Inflammation and cellular immune responses in abdominal aortic aneurysms. *Arterioscler Thromb Vasc Biol.* 2006;26:987-94.

204 Holness CL, Simmons DL. Molecular cloning of CD68, a human macrophage marker related to lysosomal glycoproteins. *Blood.* 1993;81:1607-13.

205 Schlingemann RO, Rietveld FJ, de Waal RM, Bradley NJ, Skene AI, Davies AJ, Greaves MF, Denekamp J, Ruiter DJ. Leukocyte antigen CD34 is expressed by a subset of cultured endothelial cells and on endothelial abluminal microprocesses in the tumor stroma. *Lab Invest.* 1990;62:690-6.

206 Rensen SS, Doevendans PA, van Eys GJ. Regulation and characteristics of vascular smooth muscle cell phenotypic diversity. *Neth Heart J.* 2007;15:100-8.

207 Li B, Carey M, Workman JL. The role of chromatin during transcription. *Cell.* 2007;128: 707-19.

208 Jenuwein T, Allis CD. Translating the histone code. *Science.* 2001;293:1074-80.

209 Georghiou S, Ababneh AM. Maintenance of open DNA base pairs through histone acetylated lysine-purine interaction leading to transcriptional activation: a proposed mechanism. *Int J Mol Med.* 2005;16:911-7.

210 Wang Z, Zang C, Cui K, Schones DE, Barski A, Peng W, Zhao K. Genome-wide mapping of HATs and HDACs reveals distinct functions in active and inactive genes. *Cell.* 2009;138:1019-31.

211 Van Beekum O, Kalkhoven E. Aberrant forms of histone acetyltransferases in human disease. *Subcell Biochem.* 2007;41:233-62.

212 Khan SN, Khan AU. Role of histone acetylation in cell physiology and diseases: An update. *Clin Chim Acta.* 2010;411:1401-11.

213 Hebbes TR, Clayton AL, Thorne AW, Crane-Robinson C. Core histone hyperacetylation co-maps with generalized DNase I sensitivity in the chicken beta-globin chromosomal domain. *EMBO J.* 1994;13:1823-30.

214 Vettese-Dadey M, Grant PA, Hebbes TR, Crane-Robinson C, Allis CD, Workman JL. Acetylation of histone H4 plays a primary role in enhancing transcription factor binding to nucleosomal DNA in vitro. *EMBO J.* 1996;15:2508–18.

215 Chen L, Wei T, Si X, Wang Q, Li Y, Leng Y, Deng A, Chen J, Wang G, Zhu S, Kang J. Lysine acetyltransferase GCN5 potentiates the growth of non-small cell lung cancer via

promotion of E2F1, cyclin D1, and cyclin E1 expression. *J Biol Chem.* 2013;288: 14510-21.

216 Kim MJ, Park KG, Lee KM, Kim HS, Kim SY, Kim CS, Lee SL, Chang YC, Park JY, Lee KU, Lee IK. Cilostazol inhibits vascular smooth muscle cell growth by downregulation of the transcription factor E2F. Hypertension. 2005;45:552-6.

217 Yanagisawa J, Kitagawa H, Yanagida M, Wada O, Ogawa S, Nakagomi M, Oishi H, Yamamoto Y, Nagasawa H, McMahon SB, Cole MD, Tora L, Takahashi Nekton. Nuclear receptor function requires a TFTC-type histone acetyl transferase complex. *Mol Cell.* 2002;9:553-62.

218 Sheppard KA, Rose DW, Haque ZK, Kurokawa R, McInerney E, Westin S, Thanos D, Rosenfeld MG, Glass CK, Collins T. Transcriptional activation by NF-kappaB requires multiple coactivators. *Mol Cell Biol.* 1999;19:6367-78.

219 Miao F, Gonzalo IG, Lanting L, Natarajan R. In vivo chromatin remodeling events leading to inflammatory gene transcription under diabetic conditions. *J Biol Chem.* 2004; 279:18091-7.

220 Zhao X, Benveniste EN. Transcriptional activation of human matrix metalloproteinase-9 gene expression by multiple co-activators. *J Mol Biol.* 2008;383:945-56.

221 Goodman RH, Smolik S. CBP/p300 in cell growth, transformation, and development. *Genes Dev.* 2000;14:1553-77.

222 Chan HM, La Thangue NB. P300/CBP proteins: HATs for transcriptional bridges and scaffolds. *J Cell Sci.* 2001;114:2363-73.

223 Gu W, Shi XL, Roeder RG. Synergistic activation of transcription by CBP and p53. *Nature.* 1997;387:819-23.

224 Kraus WL, Kadonaga JT. p300 and estrogen receptor cooperatively activate transcription via differential enhancement of initiation and reinitiation. *Genes Dev.* 1998;12:331-42.

225 Kobayashi Y, Kitamoto T, Masuhiro Y, Watanabe M, Kase T, Metzger D, Yanagisawa J, Kato S. p300 mediates functional synergism between AF-1 and AF-2 of estrogen receptor alpha and beta by interacting directly with the N-terminal A/B domains. *J Biol Chem.* 2000;275:15645-51.

226 Post WS, Goldschmidt-Clermont PJ, Wilhide CC, Heldman AW, Sussman MS, Ouyang P, Milliken EE, Issa JP. Methylation of the estrogen receptor gene is associated with aging and atherosclerosis in the cardiovascular system. *Cardiovasc Res.* 1999;43: 985-91.

227 Ferreon JC, Lee CW, Arai M, Martinez-Yamout MA, Dyson HJ, Wright PE. Cooperative regulation of p53 by modulation of ternary complex formation with CBP/p300 and HDM2. *Proc Natl Acad Sci USA*. 2009;106:6591-6.

228 Xu Y. Regulation of p53 responses by post-translational modifications. *Cell Death Differ.* 2003;10:400-3.

229 Bode AM, Dong Z. Post-translational modification of p53 in tumorigenesis. *Nat Rev Cancer.* 2004;4:793–805.

230 López-Candales A, Holmes DR, Liao S, Scott MJ, Wickline SA, Thompson RW. Decreased vascular smooth muscle cell density in medial degeneration of human abdominal aortic aneurysms. *Am J Pathol.* 1997;150:993-1007.

231 Kim JW, Jang SM, Kim CH, An JH, Kang EJ, Choi KH. New molecular bridge between RelA/p65 and NF-κB target genes via histone acetyltransferase TIP60 cofactor. *J Biol Chem.* 2012;287:7780-91.

232 Saito T, Hasegawa Y, Ishigaki Y, Yamada T, Gao J, Imai J, Uno K, Kaneko K, Ogihara T, Shimosawa T, Asano T, Fujita T, Oka Y, Katagiri H. Importance of endothelial NF-κB signalling in vascular remodelling and aortic aneurysm formation. *Cardiovasc Res.* 2013; 97:106-14.

233 Abdul-Hussien H, Hanemaaijer R, Kleemann R, Verhaaren BF, van Bockel JH, Lindeman JH. The pathophysiology of abdominal aortic aneurysm growth: corresponding and discordant inflammatory and proteolytic processes in abdominal aortic and popliteal artery aneurysms. *J Vasc Surg.* 2010;51:1479-87.

234 Chan EM, Chan RJ, Comer EM, Goulet RJ 3rd, Crean CD, Brown ZD, Fruehwald AM, Yang Z, Boswell HS, Nakshatri H, Gabig TG. MOZ and MOZ–CBP cooperate with NF-kappaB to activate transcription from NF-kappaB-dependent promoters. *Exp Hematol.* 2007;35:1782-92.

235 Rokudai S, Laptenko O, Arnal SM, Taya Y, Kitabayashi I, Prives C. MOZ increases p53 acetylation and premature senescence through its complex formation with PML. *Proc Natl Acad Sci USA.* 2013;110:3895-900.

236 Makino S, Kaji R, Ando S, Tomizawa M, Yasuno K, Goto S, Matsumoto S, Tabuena MD, Maranon E, Dantes M, Lee LV, Ogasawara K, Tooyama I, Akatsu H,Nishimura M, Tamiya G. Reduced neuron-specific expression of the TAF1gene as associated with X-linked dystonia-parkinsonism. *Am J Hum Genet.* 2007;80:393-406.

237 Varon R, Gooding R, Steglich C, Marns L, Tang H, Angelicheva D, Yong KK, Ambrugger P, Reinhold A, Morar B, Baas F, Kwa M, Tournev I, Guerguelcheva V,Kremensky I, Lochmüller H, Müllner-Eidenböck A, Merlini L, Neumann L, Bürger

J, Walter M, Swoboda K, Thomas PK, von Moers A, Risch N, Kalaydjieva L. Partial deficiency of the C-terminal-domain phosphatase of RNA polymerase II is associated with congenital cataracts facial dysmorphism neuropathy syndrome. *Nat Genet.* 2003;35:185-9.

238 Struhl K. Histone acetylation and transcriptional regulatory mechanisms. *Genes Dev.* 1998;12:599-606.

239 Dieker J, Muller S. Epigenetic Histone Code and Autoimmunity. *Clin Rev Allerg Immu.* 2010;39:78-84.

240 Bedford DC, Kasper LH, Fukuyama T, Brindle PK. Target gene context influences the transcriptional requirement for the KAT3 family of CBP and p300 histone acetyltransferases. *Epigenetics*. 2010;5:9-15.

241 Dyson HJ, Wright PE. Intrinsically unstructured proteins and their functions. *Nat Rev Mol Cell Biol.* 2005;6:197-208.

242 Jeong H, Mason SP, Barabasi AL, Oltvai ZN. Lethality and centrality in protein networks. *Nature.* 2001;411:41-2.

243 Pelletier N, Champagne N, Stifani S, Yang XJ. MOZ and MORF histone acetyltransferases interact with the Runt-domain transcription factor Runx2. *Oncogene.* 2002;21:2729-40.

244 Doyon Y, Cayrou C, Ullah M, Landry AJ, Cote V, Selleck W Lane WS, Tan S, Yang XJ, Côté J. ING tumor suppressors are critical regulators of chromatin acetylation required for genome expression and perpetuation. *Mol Cell.* 2006;21:51-64.

245 Doyon Y, Côté J. The highly conserved and multifunctional NuA4 HAT complex. *Curr Opin Genet Dev.* 2004;14:147-54.

246 Utley RT, Lacoste N, Jobin-Robitaille O, Allard S, Côté J. Regulation of NuA4 histone acetyltransferase activity in transcription and DNA repair by phosphorylation of histone H4. *Mol Cell Biol.* 2005;25:8179-90.

247 Bastiaansen AJ, Ewing MM, de Boer HC, van der Pouw Kraan TC, de Vries MR, Peters EA, Welten SM, Arens R, Moore SM, Faber JE, Jukema JW, Hamming JF, Nossent AY, Quax PH. Lysine acetyltransferase PCAF is a key regulator of arteriogenesis. *Arterioscler Thromb Vasc Biol.* 2013;33:1902-10.

248 Hupp TR, Meek DW, Midgley CA, Lane DP. Regulation of the specific DNA binding function of p53. *Cell.* 1992;71:875-86.

249 Grossman SR. p300/CBP/p53 interaction and regulation of the p53 response. *Eur J Biochem.* 2001;268:2773–8.

250 Martinez-Balbas MA, Bauer UM, Nielsen SJ, Brehm A, Kouzarides T. Regulation of E2F1 activity by acetylation. *EMBO J.* 2000;19:662-71.

251 Pillai S, Kovacs M, Chellappan S. Regulation of vascular endothelial growth factor receptors by Rb and E2F1: role of acetylation. *Cancer Res.* 2010;70:4931-40.

252 Gu W, Roeder RG. Activation of p53 sequence specific DNA binding by acetylation of the p53 C-terminal domain. *Cell.* 1997;90:595-606.

253 Ying AK, Hassanain HH, Roos CM, Smiraglia DJ, Issa JJ, Michler RE, Caligiuri M, Plass C, Goldschmidt-Clermont PJ. Methylation of the estrogen receptoralpha gene promoter is selectively increased in proliferating human aortic smooth muscle cells. *Cardiovasc Res.* 2000;46:172-9.

254 Kiernan R, Brès V, Ng RW, Coudart MP, El Messaoudi S, Sardet C, Jin DY, Emiliani S, Benkirane M. Post-activation turn-off of NF-kappa B-dependent transcription is regulated by acetylation of p65. *J Biol Chem.* 2003;278:2758-66.

255 Buerki C, Rothgiesser KM, Valovka T, Owen HR, Rehrauer H, Fey M, Lane WS, Hottiger MO. Functional relevance of novel p300-mediated lysine 314 and 315 acetylation of RelA/p65. *Nucleic Acids Res.* 2008;36:1665-80.

256 Pons D, de Vries FR, van den Elsen PJ, Heijmans BT, Quax PH, Jukema JW. Epigenetic histone acetylation modifiers in vascular remodelling: new targets for therapy in cardiovascular disease. *Eur Heart J.* 2009;30:266-77.

257 Chan HM, La Thangue NB. p300/CBP proteins: HATs for transcriptional bridges and scaffolds. *J. Cell Sci.* 2001;114:2363-73.

258 Zaina S, Lindholm MW, Lund G. Nutrition and aberrant DNA methylation patterns in atherosclerosis: more than just hyperhomocysteinemia? *J Nutr.* 2005;135:5-8.

259 Jin Q, Yu LR, Wang L, Zhang Z, Kasper LH, Lee JE, Wang C, Brindle PK, Dent SY, Ge K. Distinct roles of GCN5/PCAF-mediated H3K9ac and CBP/p300-mediated H3K18/27ac in nuclear receptor transactivation. *EMBO J.* 2011;30:249-62.

260 Ali M, Yan K, Lalonde ME, Degerny C, Rothbart SB, Strahl BD, Côté J, Yang XJ, Kutateladze TG. Tandem PHD fingers of MORF/MOZ acetyltransferases display selectivity for acetylated histone H3 and are required for the association with chromatin. *J Mol Biol.* 2012;424:328-38.

261 Bannister AJ, Kouzarides T. Histone methylation: recognizing the methyl mark. *Methods Enzymol.* 2004;376:269-88.

262 Jenuwein T, Allis CD. Translating the histone code. *Science.* 2001;293:1074-80.

263 Sipido KR, Tedgui A, Kristensen SD, Pasterkamp G, Schunkert H, Wehling M, Steg PG, Eisert W, Rademakers F, Casadei B, Fuster V, Cerbai E, Hasenfuss G, Fernandez-Aviles F, Garcia-Dorado D, Vidal M, Hallen M, Dambrauskaite V. Identifying needs and opportunities for advancing translational research in cardiovascular disease. *Cardiovasc Res.* 2009;83:425-35.

7. APPENDIX

7.1 Abbreviations

AAA	abdominal aortic aneurysm
ACC	American college of cardiology
ACE-I	angiotensin converting enzyme inhibitor
AHA	American heart association
AML	acute myelocytic leukemia
ASA	acetyl salicilic acid
CAD	coronary artery disease
cDNA	complementary deoxyribonucleic acid
CREB	cAMP responsive element binding
CT	computed tomography
CTA	computed tomography angiography
Ctrl	control healthy aorta group
DNMTs	DNA methyltransferases
DREAM trial	Dutch randomized endovascular aneurysm management trial
DSA	digital substraction angiography
dsDNA	double stranded DNA
ECM	extracellular matrix
ECs	endothelial cells
ER-α	estrogen receptor α
ESVS	European society for vascular surgery
EVAR	endovascular repair
EvG	elastica van gieson
FFPE	formalin fixed paraffin-embedded
GAPDH	glyceraldehyde-3-phosphate dehydrogenase
GWAS	genome-wide association studies
HATs	histone acetyl transferases
HDACs	histone deacetylases
HE	haematoxylin-eosin
HMTs	histone methyltransferases
HRP	horse reddish peroxidase
hsCRP	high sensitivity C reactive protein
IFN-γ	interferon-gamma
IHC	immunological histological chemistry
IL-1β	interleukin 1 beta
IL-6	interleukin 6

IVUS	intravascular ultrasound
KAT12	TFIIIC90, transcription factor IIIC
KAT2A	GCN5, general control nonderepressible 5
KAT2B	P/CAF, p300/CBP-associated factor
KAT3A	CBP, CREB-binding protein
KAT3B	300-kDa protein
KAT4	TAF1, TBP-associated factors 1
KAT5	Tip60, HIV Tat-interacting protein of 60 kDa
KAT6A	MOZ, monocytic leukemia zinc finger protein
KAT6B	MORF, monocytic leukemia zinc finger protein-related factor
KAT7	HBO1, HAT bound to ORC1
KAT8	hMOF, males-absent on the first
K-S test	Kolmogorov-Smirnov test
LCA	leukocyte common antigen
LSAB	Labeled Streptavidin Biotin
MCH	mean corpuscular hemoglobin
MCHC	mean corpuscular hemoglobin concentration
MCV	mean corpuscular volume
MHCII	Myosin heavy chain 11
MMPs	matrix metalloproteinases
mRNA	Messenger ribonucleic acid
OR	odds ratio
OSR	open surgery repair
PAGE	preparation polyacrylamide gel electrophoresis
PHD	plant homeodomain
PTFE	polytetrafluoroethylene
PVDF	polyvinylidene fluoride
qPCR	quantitative polymerase chain reaction
rAAA	ruptured abdominal aortic aneurysm
ROS	reactive oxygen species
RT-PCR	real-time polymerase chain reaction
SDS	sodium dodecyl sulfonate
SMCs	smooth muscle cells
SMTN	smoothelin
TBP	TATA box binding protein
TEMED	N,N,N',N'-Tetra-methylethylenediamene
TIMP-1	tissue inhibitor of metalloproteinase 1
TNF-α	tumor necrosis factor-alpha
uPA	urokinase-type plasminogen activator
VCAM-1	vascular cell adhesion molecule-1

7.2 Publications

7.2.1 Original publications

Han YS, Zhang J, Xia Q, Liu ZM, Zhang XY, Wu XY, Lun Y, Xin SJ, Duan ZQ, Xu K. A comparative study on the medium-long term results of endovascular repair and open surgical repair in the management of ruptured abdominal aortic aneurysms. Chin Med J (Engl). 2013;126(24):4771-9. PMID: 24342327.

Han Y, Zhang J, Wu X, Jiang H, Gang Q, Shen S, Xin S, Duan Z. A comparative study on medium-long term results of conventional and eversion endarterectomy in management of carotid artery stenosis: a meta-analysis. Natl Med J China. 2014;94(7):510-6. [Article in Chinese] PMID: 24767293.

Wu X, Jiang B, Lun Y, Xia Q, Han Y, Liu Z, Zhang X, Gang Q, Jiang H, Xin S, Duan Z, Zhang J. Venous occlusion due to cystic adventitial degeneration of the common femoral vein. Vasa. 2013;42(6):461-4. PMID: 24220125.

Yanshuo H, Fadwa T, Reeps C, Jian Z, Eckstein HH, Pelisek J, Zernecke A. Histone acetylation and expression of corresponding histone acetyl transferases in human abdominal aortic aneurysm, in preparation.

7.2.2 Oral presentations

Yanshuo H. Jian Z. A comparative study on the medium-long term results of endovascular repair and open surgical repair in the management of ruptured abdominal aortic aneurysms. 2011 Asian Chapter Congress of the International Union of Angiology, 8th International Congress on Vascular and Endovascular Surgery, the 5th Chinese Conference of Vascular Surgery and Tissue Engineering.

7.3 Acknowledgments

The work for this thesis was undertaken at the Department of Vascular and Endovascular Surgery, in close collaboration with the Department of Pathology and Orthopaedics, at Klinikum rechts der Isar der Technische Universität München.

I wish to express my gratitude to all enthusiastic friends and colleagues, with whom I have had the privilege of working. Especially, I would like to thank some people of special importance to me:

First and foremost, I would like to thank my supervisor, Priv.-Doz. Dr. rer. nat. Jaroslav Pelisek. His patience, knowledge and judgment guided me throughout the entire time. At the beginning, I knew little about the laboratory work concerning my project and Dr. Pelisek inducted me patiently in all techniques necessary to fulfil my thesis. He was all still very understanding and patient with me. I appreciate him not only for his excellent technical help, but also for being good listener and supporter.

I am also very thankful to Prof. Dr. med. Alma Zernecke for giving me the opportunity to pursue my doctoral education at TUM. Thanks for her valuable comments and advice.

In addition, I want to thank also Prof. Dr. Hans-Henning Eckstein, head of the Department of Vascular and Endovascular Surgery, for allowing me to join his research team.

An equally important person was Prof. Dr. Jian Zhang, my Master's supervisor, from the Department of Vascular and Thyroid Surgery, the first affiliate Hospital of China Medical University. He has recommended me to go abroad at TUM without reservation.

I gratefully acknowledge the skillful technical assistance of PhD candidate Fadwa Tanios. She shared the deepest thoughts and concerns of my thesis and encouraged me during the whole steps of this work.

I would also like to thank the members of working group for their support of my project: Renate Hegenloh and Almut Glinzer. Their scientific guidance and willingness to share perspective have been critical for my research. I especially want to extend my gratitude to Renate for here technical support in IHC.

This dissertation is dedicated to my parents Mr. Zelun Han and Mrs. Juan Du, who have provided me with constant support throughout all my life. Without their encouragement, I wouldn’t have been able to achieve my goals.

My deepest and loving thanks go to Yeni Li, my fiancée. She was standing by my side through good and bad times during my study in Germany and without her strong support, this thesis would never have been finished.